DEVELOPMENT OF NEW STATIONARY PHASES AND THEIR APPLICATIONS

IN HIGH PERFORMANCE LIQUID CHROMATOGRAPHY

by

HAIXIAO QIU

Presented to the Faculty of the Graduate School of

The University of Texas at Arlington in Partial Fulfillment

of the Requirements

for the Degree of

DOCTOR OF PHILOSOPHY

THE UNIVERSITY OF TEXAS AT ARLINGTON

AUGUST 2013

Acknowledgements

It is with great pleasure I convey my sincere appreciation to all who made my doctoral degree a success. First and foremost, I would like to express my gratitude to my research advisor, Dr. Daniel W. Armstrong, for his support, encouragement, patience and guidance during my graduate studies. I will never forget what I have learned from him and I look forward to our future endeavors. I consider myself extremely fortunate to have the opportunity to work under his supervision. I would also like to thank Dr. Frederick MacDonnell, Dr. Martin Pomerantz and Dr. Junha Jeon for their help and serving on my research committee.

I am indebted to Dr. Yongjia Shen, who is my M.S. advisor at East China University of Science and Technology, for encouraging and inspiring me to pursue my doctoral studies in United States. I am also indebted to Dr. Max (Qiqing) Zhong, who is my internship mentor at Genentech, for broadening my understanding of separation science and sponsoring my industrial training.

I greatly appreciate the assistance of all faculty and staff in the Department of Chemistry and Biochemistry at the University of Texas at Arlington, especially Barbara J. Smith for taking care of my orders and paperwork, Brian Edwards for helping me to maintain HPLC instruments and training me in the use of other instrumentation, and Maciej Kukula for assistanting me in using ICP-OES in the Shimadzu center. I also thank my fellow group members and other colleagues in the Chemistry Department (Dr. Ping Sun, Dr. Chunlei Wang, Dr. Zachary S. Breitcach, Dr. Xiaotong Zhang, Dr. Alain Berthod, Dr. John Lang, Dr. Eranda Wanigasekara, Dr. Ying Zhang , Dr. Yasith, Qing, Sirantha, Jonathan, Edra, Nilusha, Jason, Ross, Choyce, Lily, Howard, Suzen, Milan, Tharanga) for their help and friendship.

Last but not least, I would especially like to thank my parents, mother Lingfeng Shen and father Zijian Qiu, for their unconditional love and support during my life.

July 12, 2013

Abstract

DEVELOPMENT OF NEW STATIONARY PHASES AND THEIR APPLICATIONS

IN HIGH PERFORMANCE LIQUID CHROMATOGRAPHY

Haixiao Qiu, PhD

The University of Texas at Arlington, 2013

Supervising Professor: Daniel W. Armstrong

High performance liquid chromatography (HPLC) has proven to be the most widely applicable and versatile technique in separation science. Hydrophilic interaction liquid chromatography (HILIC) has attracted considerable interest and has become a viable option for the separation of polar compounds. Chirality is another major concern in the modern pharmaceutical industry for two reasons: 1). the majority of bio-organic molecules are chiral; 2). enantiomers of a racemic drug may often exhibit different biological activities, pharmacokinetics, and toxicities. The field of enantiomeric separations has reached a clear level of maturity after approximately 30 years of development. However, with the continued emphasis on stereochemistry in drug design and development, chiral separations are in ever increasing demand. The development of new, more effective methods is still challenging and demanding experimentally.

This dissertation discusses new research in three areas:

1). Development and application of new HILIC stationary phases for the separation of polar organic compounds. Two types of new HILIC stationary phases have been successfully synthesized and evaluted. One is based on native cyclofructan 6 and another one is a zwitterionic stationary phase based on 3-P,P-diphenylphosphonium-

propylsulfonate. Their performance and retention mechanisms in the HILIC mode will be discussed in this dissertation.

2). Development and evaluation of new chiral stationary phases. R-naphthylethyl-carbamate cyclofructan 6 (RN-CF6) and dimethylphenyl-carbamate cyclofructan 7 (DMP-CF7) were successfully synthesized and provide enantioselectivity toward a broad range of chiral compounds. They were found to be the best aromatic-functionalized cyclofructan chiral stationary phases and provide enantiomeric separations complementary to the isopropyl-carbamate cyclofructan 6 based chiral stationary phase. This dissertation also describes method development of enantiomeric impurities quantification in chiral reagents. Three macrocyclic chiral stationary phases, including cyclodextrins, macrocyclic glycopeptides and cyclofructans, have been used to determine enantiomeric impurities in new chiral catalysts, auxiliaries and synthons used in asymmetric syntheses. It was found that many of the newer chiral reagents are highly enantiopure, probably due to continual improvements in asymmetric syntheses and purification in the manufacturing process.

3). Development and application of new stationary phases based on a resin substrate instead of silica gel. This dissertation describes methods for binding cyclofructan 6 to resin via "click" chemistry. It was found that these resin based stationary phases appear to have potential in HILIC separations (native cyclofructan 6 bonded to resin as stationary phases) and enantiomeric separations (isopropyl-carbamated cyclofructan 6 bonded to resin).

Table of Contents

List of Illustrations

List of Tables

Chapter 1

Introduction

High performance liquid chromatography (HPLC, including UHPLC) is one of the most powerful separation techniques capable of providing analysis difficult or impossible with other separation approaches [1]. From the 1980s to the present time, reversed phase liquid chromatography (RPLC) has been the dominant HPLC technology its ability to separate a broad range of analytical solutes, which are important in the fields of life science separating proteomics, metabolomics, pharmacology, agrochemistry and so on. Polar compounds, including peptides, glycopeptides, oligonucleotides, saccharides, carboxylic acids, amino acids, highly polar natural products and many drug components have been found to be of great relevance in these fields [2]. The most useful drugs often have been found to have polarities in a region that allows them to be well-separated from most naturally occurring substances in blood plasma [3].

One problem that has been the focus of separation scientiests is how to create retention in RPLC for polar compounds with inadequate affinity for nonpolar stationary phases. Another major concern is the separation of chiral compounds for the modern pharmaceutical industry, since most bioorganic compounds are chiral and enantiomers of a racemate have different biological activities, pharmacokinetics and toxicities. Hydrophilic interaction liquid chromatography (HILIC) offers a means of addressing the former problem and the well established chiral stationary phases (CSPs) have provided the best alternative for addressing the latter.

1.1 HILIC separations

Hydrophilic interaction liquid chromatography (HILIC) is an alternative
chromatographic mode for efficiently separating polar compounds. This chromatographic
mode has been applied to the separation of polar compounds for more than 60 years by
using polar stationary phases with hydro-organic mobile phases [4]. Typically, the use of
a mobile phase containing some water and a higher percentage of a water miscible
organic solvent is the defining characteristic of HILIC. As early as the 1950s, this special
LC mode was used in separating a mixture of fructose, glucose, and mannose on ion
exchange stationary phases [5]. Linden and co-workers [6] used this mode to separate
carbohydrates on an amino-silica phase in a mixture of acetonitrile and water (75:25 *v/v*).
Also, Armstrong and co-workers separated saccharides and sugar alcohols on
cyclodextrin stationary phases in the 1980s [4, 7, 8]. The acronym HILIC, first coined by
Alpert in 1990 [9], was applied in the analysis of hydrophilic substances, such as
peptides and nucleic acids. Recently, HILIC has emerged as a viable option to RPLC
because of its ability to retain and separate polar and hydrophilic analytes, which often
have insufficient retention and resolution in RPLC. Figure 1−1 shows the number of HILIC
related articles published in the period of 1990-2013. It illustrates that HILIC has emerged
as an increasingly popular and viable chromatographic mode since 2004.
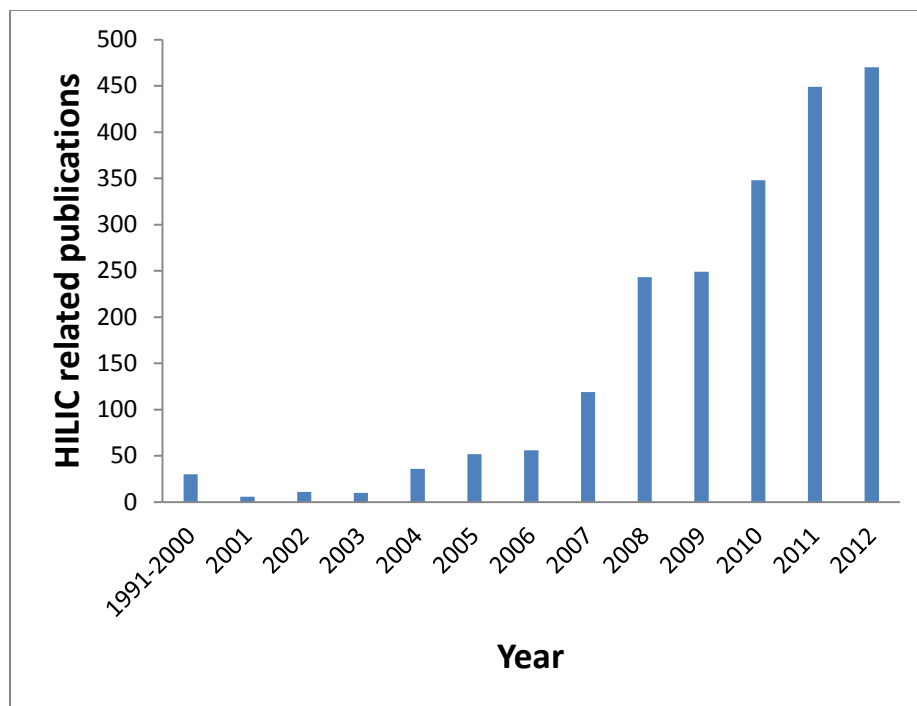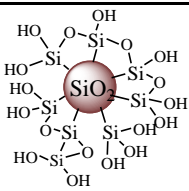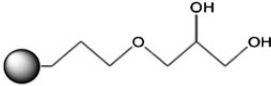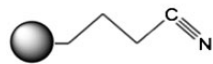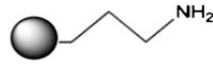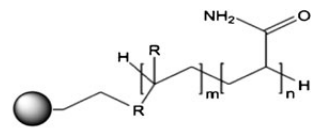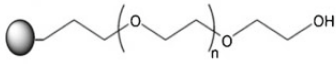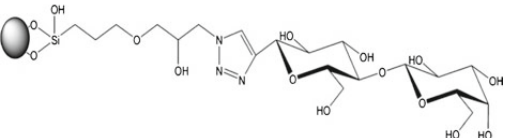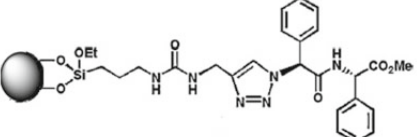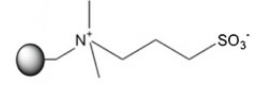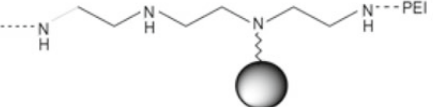
Figure 1-1 SciFinder Scholar search results documenting the continuously growing research area of HILIC, based on the number of publications per year.

Historically, it has been reported that HILIC is a variant of normal phase liquid chromatography (NPLC), since both use polar stationary phases. Table 1-1 lists typical stationary phases used in HILIC. However, the separations achieved using HILIC are more complicated than that in NPLC, as they have multiple mechanisms of interaction.

Table 1-1 Selected stationary phases used in HILIC separation and dominant interactions

with analytes

Packing materials	Structure of represented stationary phase	Dominant interactions
Bare silica gel		Partitioning Electrostatic interactions
Diol bonded phases		Partitioning Hydrogen bonding interactions
Cyano bonded phases		Partitioning
Amino bonded phases		Partitioning Hydrogen bonding interactions
Amide bonded phases		Partitioning Hydrogen bonding interactions
Polyethylene glycol bonded phases		Partitioning Hydrogen bonding interactions
Saccharides bonded phases		Partitioning Hydrogen bonding interactions
Peptides bonded phases		Partitioning Hydrogen bonding interactions
Zwitterionic bonded phases		Partitioning Electrostatic interactions
Cation/anion exchanger bonded phases		Partitioning Electrostatic interactions

The mechanism of HILIC separations remains open to question, largely due to the fact that it involves several different types of interactions [3, 4, 10, 11]. One proposition is that there may be a partitioning of polar analytes between the highly organic mobile phase and the hydration layer that surrounds the polar surface of the stationary phase [5, 12-14]. This water enriched layer can have a large influence on the selectivity of the separation in HILIC systems [15]. When the concentration of water in the mobile phase is lower than 20%, water adsorption can be restricted to multilayer having an excess of adsorbed water in comparison with the concentration of water in the eluent (Figure 1-2) [16]. The existence of the water layer has been shown by McCalley and Neue [17], who demonstrated that about 4-13% of the pore volume of a silica phase is occupied by a water layer when there is 75-90% of acetonitrile in the eluent.
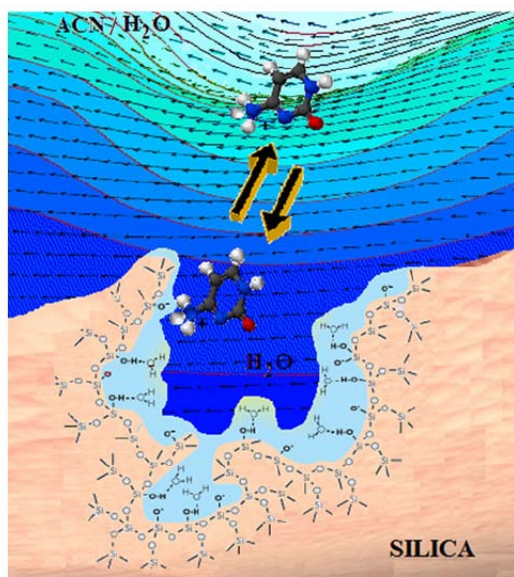
Figure 1-2 Scheme of the partioning mechanism in a HILIC system. Reprinted with permission from reference [16].

Another perspective is that electrostatic interactions play an important role in HILIC separations when ionic groups are present on the surface of solid supports, such as residual silanol groups and zwitterionic functionalites [18]. As described by Alpert [9], the zwitterionic stationary phase exhibits an overall negative charge when using typical HILIC mobile phases due to the dissociation of residual silanol groups. Therefore some electrostatic repulsion interactions might occur between dissociated acidic analytes and the negatively charged stationary phases. Alternatively, some attractive electrostatic interactions might occur for protonated basic compounds in the HILIC mode.

Alternatively, hydrogen bonding interactions [7, 19, 20] provide the predominant impact on HILIC retention and selectivity when using polar stationary phases with abundant hydroxyl groups, such as diol bonded stationary phases, amine/amide bonded stationary phases, polyethylene glycol bonded stationary phases, and saccharide/polysaccharide bonded stationary phases (Table 1-1). Hydrogen bonding interactions drive the HILIC separation not only by the number of hydrogen bonding sites but also by their molecular location and orientation. Armstrong and co-workers used cyclodextrin based stationary phases for the HILIC separation of monosaccharides, which have the same number of hydroxyl groups but different stereochemistry, such as glucose and glactose [21]. Beside the above possibilities, other interactions derived from functionalities on the surface of stationary phases need to be considered as well, such as π-π and/or n-π interactions, and dipole-dipole interactions [22-24].

HILIC has many specific advantages over conventional NPLC and RPLC. As a well-established chromatographic mode, HILIC is used in separations of uncharged highly hydrophilic and amphiphilic compounds, which are too polar or inadequately oleophilic to be well retained in RPLC but have insufficient charge to allow effective electrostatic retention in ion-exchange chromatography (IEC) [25]. The hydro-organic

mobile phase used in HILIC provides excellent dissolving power for polar compounds and overcome the drawbacks of the poor solubility often encountered in NPLC. Furthermore, HILIC can be coupled easily to mass spectrometry (MS), especially in the electrospray ionization (ESI) mode, since the hydro-ogranic mobile phase is compatible with ESI-MS [26]. Additionally, HILIC also can be facilely orthogonal to other chromatographic techniques to address complicated sample matrix [27-29]. To date, HILIC×RPLC has been successfully applied to the analysis and purification of carbohydrates [30, 31], peptides [10, 32, 33] and polar pharmaceuticals [34, 35].

1.2 Enantiomeric separations in HPLC

Since Louis Pasteur first accomplished the enantiomeric separation of sodium ammonium tartrate in 1858, enantiomeric separations have continued to be of great interest and relevance in many areas of science and technology [36-39]. It is well established that enantiomers often exhibit different biological activities, pharmacokinetics, and toxicities [40, 41]. Thalidomide [42] and perhexiline [43, 44] are well-known cases, in which enantiomers were discovered to have dangerously divergent pharmacologies. A world-wide tragedy caused by the use of thalidomide occurred in the late 1950s and early 1960s, when thalidomide was manufactured and sold as a racemate of N-phthalylglutamic acid imide. Unfortunately, it was not clear that the S-(-)-isomer has significant teratogenicity leading to serious fetal malformations [45] (Figure 1-3). It has become a necessity to address stereochemistry in drug development. In 1992, the Food and Drug Administration issued a policy statement concerning the development of new stereoisomeric drugs [46], which resulted in a great demand for improved methods for separating enantiomers.

7
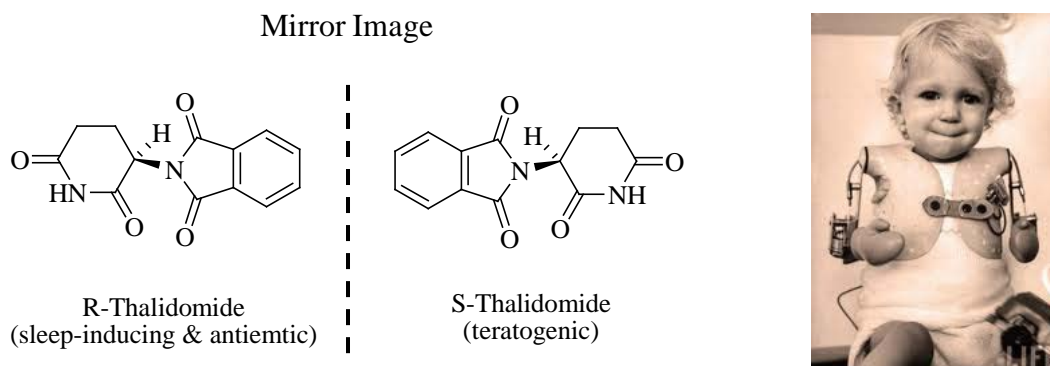
Figure 1-3 Thalidomide tragedy, resulting from S-isomer's teragogenic effect.

Enantiomers remain a challenge to separate due to their identical physical and chemical properties in an achiral environment, and research on specialized separation techniques continues to be developed to resolve individual enantiomers. Many non-chromatographic techniques have been used for enantiomeric analysis, e.g., polarimetry, nuclear magnetic resonance, isotopic dilution, calorimetry, and enzyme techniques. Unfortunately, these techniques require enantiomerically pure samples as standards or references. Chromatographic methods, including gas chromatography (GC), liquid chromatography (LC), supercritical fluid chromatography (SFC), and capillary electrophoresis (CE), are the dominant technologies used to separate and purify mixtures of enantiomers. Enantiomeric separations performed by HPLC remain the workhorse for enantiomeric separations, due to the wide availability of chromatographic instruments, high extent of automation, wide selectivity, good reproducibility, as well as the capability for both analytical and preparative scale separations.

Table 1-2 Chiral stationary phases classified by their structures

Class	Examples	Retention mechanims	Primary interaction
Macrocyclic	Crown ether	Inclusion complexation	Ion (primary amino-group)-dipole
	Glycopeptides	Multiple-bonding sits	Variable
	Cyclodextrin	Inclusion complexation	H-bond
	Cyclofructans	Multiple-bonding sites	Variable
Polymeric	Polysaccharides	Insertion in helical structures	H-bond or dipolar or steric
	Proteins	Multiple-bonding sites	Variable
	Synthetic polymers	Diastereoisomeric selector/analyte complex	H-bond
π-π Association	π-complex selector	Transient 3-point	π-π interaction
Ligand exchange	Hydroxyproline/ Penicillamine	Diastereoisomeric selector/metal ion/analyte	Coulomb or ion-dipole (lone electron pair coordination)
Miscellaneous and hybrid	Cross-linked tartaric acid derivatives		coulomb

Pertinent references for each class and type of chiral selector can be found in refs.[37, 38, 47]

The most challenging aspect of chiral method development in HPLC is the selection of the proper chiral stationary phase (CSP). Currently, there are over a hundred CSPs available commercially. The large number of CSPs can be categorized within several classes listed in Table 1-2. Fortunately, most of the chiral separations can be achieved on relatively few CSPs [47]. Macrocyclic glycopeptides CSPs, cyclodextrin CSPs, cyclofructan CSPs and polysacchareides CSPs are predominant CSPs with well established retention mechanisms and mobile phase starting points. Understanding mechanisms of chiral recognition can help in the selection of potential columns and appropriate mobile phases. However, even with these "mainstay" CSPs, it is not usually an easy task to find the right chromatographic conditions for certain compounds. Some

practical factors also should be considered, including the solubility of analyte in the mobile phase, analysis run time, column cost, column robustness, and column capacity.

1.3 Research objectives and organization of the dissertation

This dissertation is centered on the development of new stationary phases and their applications in HPLC separations. The first portion (Chapters 2-4) of the dissertation focuses on the development new HILIC stationary phases and evaluation of their performance in the HILIC mode. Specifically, Chapter 2 describes the development of cyclofructan 6 based stationary phases, which appear to have exceptionally broad applicability for polar compounds separations in the HILIC mode. Chapter 3 discusses the development of a new zwitterionic HILIC stationary phase based on 3-P,P-diphenylphosphonium-propylsulfonate. Chapter 4 describes the thermodynamic studies performed on HILIC stationary phases and demonstrates that the phase ratio is not constant in the HILIC mode.

The second portion (Chapters 5-6) of this dissertation discusses new chiral stationary phases and enantiomeric separations. Chapter 5 investigates the enantioselectivity of aromatic-derivatized cyclofructan 6 and 7 as new chiral selectors. It also offers useful information on method development for specific chiral analytes and a better knowledge of the enantiomeric separation mechanism. Chapter 6 describes methods for the determination of enantiomeric impurities in chiral catalysts, auxiliaries and synthons used in asymmetric syntheses. It emphasizes the importance of using proper chiral stationary phases with suitable mobile phase conditions in separating specific enantimers.

The last portion of the dissertation describes an extention of the work to the synthesis and evaluation of a different family of stationary phases. Chapter 7 relates

results from stationary phases composed of native/derivatized cyclofructan 6 bound to resin in both HILIC and chiral separations. Lastly, a general summary will be presented in Chapter 8.

Chapter 2

Cyclofructan 6 based stationary phases for hydrophilic interaction liquid

chromatrography

Abstract

New stationary phases for hydrophilic interaction liquid chromatography (HILIC) were synthesized by covalently attaching native cyclofructan 6 (CF6) to silica gel. The chromatographic characteristics of the new stationary phases were evaluated and compared to three different types of commercial HILIC columns. The CF6 columns produced considerably different retention and selectivity patterns for various classes of polar analytes, including nucleic acid compounds, xanthines, β-blockers, salicylic acid and its derivatives, and maltooligosaccharides. Univariate optimization approaches were examined including organic modifier (acetonitrile) contents, buffer pH, and salt concentration. The thermodynamic characteristic of the CF6 stationary phase was investigated by considering the effect of column temperature on retention and utilizing van't Hoff plots. CF6 based stationary phases appear to have exceptionally broad applicability for HILIC mode separations.

2.1 Introduction

Among various separation modes in liquid chromatography, reversed phase liquid chromatography (RPLC) is by far the most frequently used. However, RPLC has limitations in the analysis of very polar compounds like sugars, amino acids, nucleosides, sulfonated compounds, etc [4]. Such solutes typically have insufficient interactions with the hydrophobic surface of reversed phase materials and thus elute with poor retention and are often not separated from other polar compounds [11]. Over the last several years,

hydrophilic interaction liquid chromatography (HILIC) has emerged as a viable alternative to RPLC for many applications. It has been steadily gaining popularity for the separation of polar and hydrophilic analytes, including carbohydrates [30, 31], peptides [10], and polar pharmaceuticals [35, 48].

Alpert first coined the name HILIC in 1990 [9], although this specific separation mode has been used in polar analyte separations for many years [6, 49-53]. In this chromatographic technique, the polar analytes interact with a hydrophilic stationary phase often via hydrogen bonding interactions, dipolar interactions or columbic interactions. They are eluted with a binary eluent, which consists mainly of a large amount of acetonitrile (usually > 60%) and a smaller amount of aqueous solvent. There are several commercially available columns dedicated to HILIC separations [3]. These stationary phases can be classified by their chemistry into several categories, including underivatized silica [54, 55], aminopropyl silica [56], amide silica [57], diol silica [58, 59], cyclodextrin-bonded silica [7, 53], sulfonated polystyrene-divinylbenzene resin [60, 61], and sulfoalkylbetaine silica [62]. Nevertheless, it is of great importance to explore new stationary phases in order to expand and hopefully improve this technique.

In this paper, native cyclofrutan 6 (CF6) based stationary phases have been developed as effective stationary phases for the separation of polar analytes in the HILIC mode.

Cyclofructans are new types of macrocyclic oligosaccharides [63, 64]. They consist of six or more β-(2→1) linked D-fructofuranose units and each unit contains one primary hydroxyl group and two secondary hydroxyl groups, which account for the hydrophilic character of these molecules. Functionalized cyclofructans have proven to be exceptional chiral selectors and broadly useful in enantiomeric separations [65-67]. Although native cyclofructans have very limited capabilities as chiral selectors [65], their

13

unique structures may make it possible for them to be used for achiral separations in the HILIC mode. Among cyclofructans, CF6 has attracted most attention due to its highly defined geometry and its availability in pure form. Therefore, in the present work, CF6 was chosen for development as a new HILIC stationary phase and was compared with three commercial HILIC columns.

2.2 Experimental

2.2.1. Reagents

CF6 was produced via inulin fermentation from various microorganisms (for example, Bacillus circulans OKUMZ 31B and B. circulans MCI-2554) [68-70]. Also, CF6 can be produced by incubation of inulin with the active enzyme cycloinulooligosaccharide fructanotransferase (CFTase) [71]. Consequently, mass produced CF6 could be available at low cost.

Daiso silica of 5 μm spherical diameter with 100 Å pore size and 440 m^2/g surface area was utilized as the supporting material. Anhydrous N, N-dimethylformamide (DMF), anhydrous toluene, anhydrous pyridine, 3-(triethoxysilyl) propylisocyanate, (3-aminopropyl)triethoxysilane, 1,6-diisocyanatohexane, ammonium acetate, acetic acid, and all polar analytes tested in this study were purchased from Sigma-Aldrich (Milwaukee, WI). Acetonitrile of HPLC grade was obtained from EMD (Gibbstown, NJ). Water was purified by a Milli-Q Water Purification System (Millipore, Billerica, MA).

2.2.2. Synthesis of cyclofructan 6 (CF6) based stationary phase

In this work, native CF6 was chemically bonded to silica gel via carbamate linkage by two different methods [65]. Thus far, two stationary phases named the high coverage propyl carbamate CF6 (H-CF6) and the low coverage propyl carbamate CF6 (L-CF6) were produced using the first method (see below), and one stationary phase

named the dicarbamoxyl-hexyl linked CF6 (DCH-CF6) was produced using the second

method (see below). Structures of the newly prepared stationary phases are shown in

Figure 2-1. Elemental analysis was conducted to confirm the successful synthesis of the

CF6 based stationary phases and to determine the cyclofructan coverage. The results

are reported in Table 2-1.
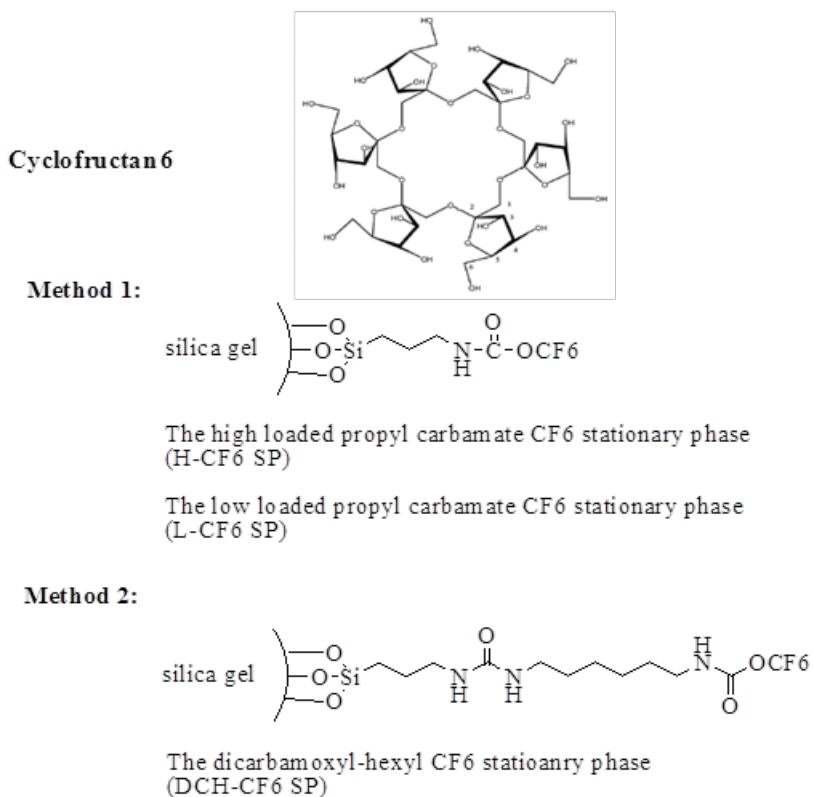
Figure 2-1 Structures of cyclofructan 6 bonded stationary phases prepared via different

methods.

Table 2-1 Elemental analysis results of three native CF6 based stationary phases

	C(%)	H(%)	N(%)
H-CF6	16.0±0.2	2.7±0.1	2.6±0.1
L-CF6	13.2±0.1	2.2±0.1	1.2±0.1
DCH-CF6	14.5±0.1	2.6±0.1	4.3±0.1

Method 1: a slurry of 3.00 g silica gel in 80 mL of anhydrous toluene was refluxed for 2 hours and 10 mL toluene with the residual water was azeotropically removed using a Dean-Stark trap. Simultaneously, 3-(triethoxysilyl)propyl isocyanate (0.76 mL, 3.08 mmol for L-CF6; 2.07 mL, 8.00 mmol for H-CF6) dissolved in 15 mL of pyridine was added drop by drop to a solution of CF6 (1.50 g, 1.54 mmol for L-CF6; 2.02 g, 2.08 mmol for H-CF6) in 60 mL anhydrous DMF over 30 mins. The reaction was carried out with continuous stirring under a nitrogen atmosphere at 70 ^{o}C for 5 hours. After cooling to room temperature, the product was mixed with the dried silica gel. This slurry was heated at 110 ^{o}C for 12 hours to yield the stationary phases. The H-CF6 stationary phase and the L-CF6 stationary phase had 16.0% and 13.2% carbon loading, respectively.

Method 2: In this method, 5.00 g silica gel was suspended in 80 mL of anhydrous toluene and refluxed to remove residual water via the same approach described in Method 1. After cooling to room temperature, (3-aminopropyl) triethoxysilane (2.50 mL, 11.00 mmol) was added and the mixture was heated to reflux for 4 hrs. The reaction was stopped and the modified silica gel was isolated by filtration. After washing with 50 mL portions of toluene, methanol and water, the silica gel was dried at reduced pressure. To a slurry of 3.00 g (3-aminopropyl)-silica gel in 60 mL of dry toluene, 1,6-diisocyanatohexane (2.5 mL, 15.5 mmol) was added with a syringe. The mixture was heated at 70 ^{o}C for 2 hrs. After cooling to room temperature, the liquid phase was

16

removed by suction filtration through an immersion sintered Teflon filter under nitrogen atmosphere. A suspension of cyclofructan 6 in anhydrous DMF (1.45 g, 1.49 mmol) was added to the activated silica and the mixture was heated to 70 ^{o}C for 12 hrs under continuous stirring. After cooling to room temperature, the product (DCH-CF6) was washed with 50 mL portions of DMF, toluene, methanol, water, acetone and dichloromethane, and dried in the vacuum oven, to give 14.5% carbon loading (Table 2-1).

2.2.3. HPLC method

The HPLC column packing system is composed of an air driven fluid pump (HASKEL, DSTV-122), an air compressor, a pressure regulator, a low pressure gauge, two high pressure gauges (70 and 40 MPa, respectively), a slurry chamber, check valves, and tubings. The stainless-steel columns (250×4.6 mm i.d.) were slurry packed with the above mentioned stationary phases.

All experiments were conducted on Agilent HPLC series 1200 systems (Agilent Technologies, Palo Alto, CA), equipped with a quaternary pump, an autosampler, and a multi-wavelength UV-vis detector or a RI detector. For data acquisition and analysis, the Chemstation software version Rev. B.01.03 was used on the system in Microsoft Windows XP environment. The injection volume was 5 µL and the flow rate of the mobile phase 1.0 mL/min. Separations were carried out at room temperature if not otherwise specified. Each sample was analyzed in duplicate. The separations of standard mixtures were carried out in the HILIC mode with a mobile phase composed of 60 - 95% acetonitrile in 20 mM ammonium acetate, pH = 4.1. The ammonium acetate buffer concentration and pH were varied between 0 - 20 mM and pH = 3.0 - 6.5, respectively, as a part of the optimization process. The 20 mM buffer solution was prepared by dissolving 1.54 g ammonium acetate in 200 mL of purified water. The stock solution was transferred

to a 1000 mL volumetric flask which was filled to just below the mark with purified water.

Then the desired pH can be adjusted by using 99.7% acetic acid. Appropriate amounts of

acetonitrile and the buffer solution were mixed thoroughly and degassed by

ultrasonication under vacuum for 5 min before use.
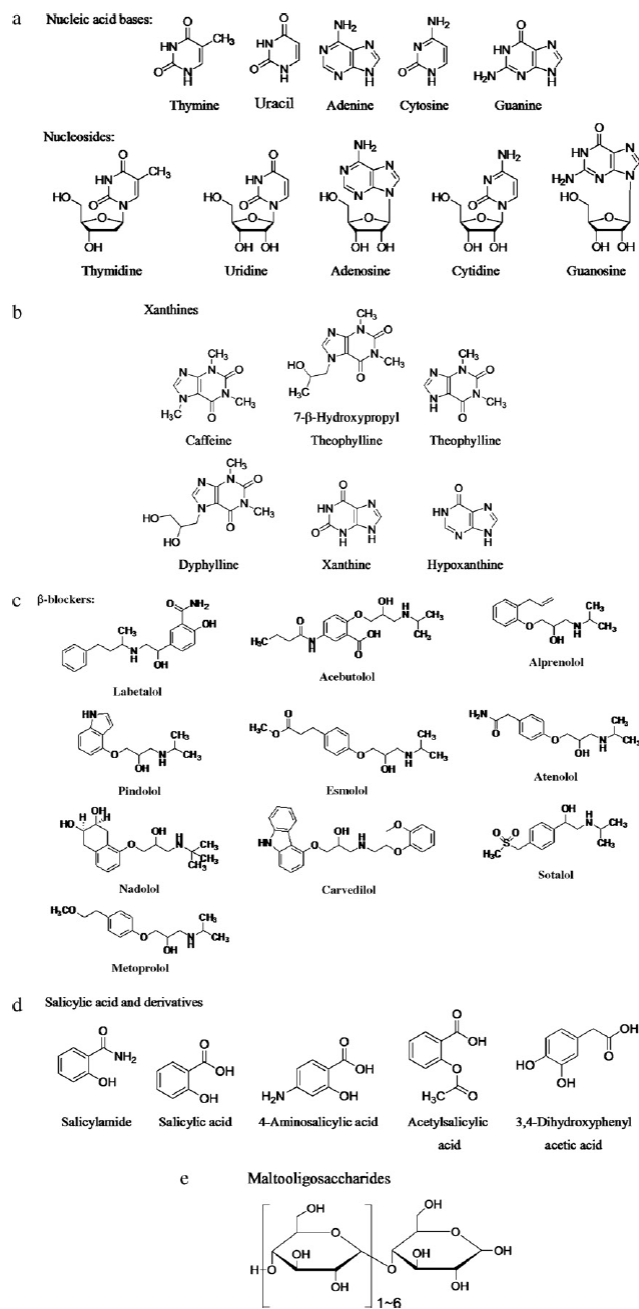
Figure 2-2 Test compounds for chromatographic characterization of the columns in the HILIC mode. (a) Nucleic acid bases and nucleosides; (b) Xanthines; (c) β-blockers; (d) Salicylic acid and derivatives; (e) Maltooligosaccharides.

Several types of polar compounds were used to investigate and compare the separation properties of the newly prepared stationary phases in the HILIC mode (see Figure 2-2). Nucleic acid bases and nucleosides are polar compounds of significant biological and pharmaceutical interests. Uracil is included as it is often employed as a void volume marker in RPLC. Xanthines, β-blockers, salicylic acid and its derivatives, and maltooligosaccharides also were used to examine the potential of the cyclofructan based columns in the HILIC mode and to access the retention mechanism. After more than 1000 injections, the column still gave good selectivity and similar retention for the same analytes. There was no significant deterioration observed for the column after six months of use. It is indicated that these CF6 columns are stable, have good efficiencies and good reproducibility.

Three commercial columns were chosen for comparison, on the basis of differences in their structures, their popularity, and availability of published data on separating polar analytes. The ZIC-HILIC, 250×4.6 mm i.d., 5 μm and 200 Å, was purchased from Merck SeQuant (Darmstadt, Germany). This column is functionalized with a sulfopropylbetaine ligand that overall confers a high capability of binding water and various coulombic interactions with a low contribution of hydrogen bonding interactions [62]. These unique properties play an important role in the HILIC mode separations. Astec Diol HPLC column and Astec Cyclobond I 2000 column, 250×4.6 mm i.d., 5 μm and 100 Å, were obtained from Supelco (Bellefonte, PA). Both the Astec Diol HPLC and Astec Cyclobond I 2000 columns have hydroxyl groups as active functionalities.

For the calculation of chromatographic data, t_0 was determined by the refractive index change caused by the sample solvent or by injecting toluene in the HILIC mode. Column efficiency was evaluated using uracil and cytosine as the test compounds. The

optimized mobile phase consisted of 90/10 (*v/v*) acetonitrile with 20 mM ammonium

acetate buffer pH = 4.1.

Thermodynamic data were obtained using isothermal conditions over a

temperature range of 20 - 70 $^{\circ}$C at 10 $^{\circ}$C intervals, with a mobile phase containing

acetonitrile and 20 mM ammonium acetate, pH = 4.1 (90/10, *v/v*). The precision of the

controlled temperature was ± 0.1 $^{\circ}$C.

2.3 Results and Discussion

The elemental analysis data in Table 2-1 indicate that the H-CF6 stationary

phase has a higher native CF6 loading than does the L-CF6 stationary phase. Table 2-1

also shows that the carbon loading of DCH-CF6 stationary phase is 14.5%. However, this

does not mean that the coverage of CF6 on this column was as high as it was on the L-

CF6 stationary phase. The carbon loading value of the DCH-CF6 stationary phase also

reflects the high amount of C6-aliphatic covalent spacer present. The column efficiency

data in Table 2-2 show that some of the synthesized stationary phases are competitive

with or superior to current commercial stationary phases. The compounds used to

measure column efficiency were selected because they are used to measure the column

efficiency of the commercial ZIC-HILIC column. The L-CF6 column had (90000 plates per

meter for uracil and 65000 plates per meter for cytosine) the highest peak efficiency

among six tested columns, when using a mobile phase containing acetonitrile and 20 mM

ammonium acetate, pH = 4.1 (90/10, *v/v*). The H-CF6 column also shows good peak

symmetry when separating the same analytes with the same mobile phase. However, the

DCH-CF6 column had poorer efficiencies and peak shapes.

Table 2-2 Physical evaluation of the six tested columns.

	H-CF6	L-CF6	DCH-CF6	Astec Diol	Astec Cyclobond I 2000	ZIC-HILIC
k (Uracil)	1.10	1.01	0.63	0.45	0.69	0.72
N/m	61 600	90 000	50 400	58 800	82 800	54 400
Peak symmetry	0.86	0.70	0.63	0.97	1.39	0.75
k (Cytosine)	5.94	5.90	2.13	2.47	3.22	3.21
N/m	43 700	64 800	19 600	55 600	63 800	37 700
Peak symmetry	0.77	0.69	0.52	0.91	1.43	0.75

*Uracil and cytosine were tested as standards under the following conditions: acetonitrile/20mM ammonium acetate pH = 4.1, 90/10 (*v/v*); column temperature: 20 ^{o}C; flow rate: 1.0 mL/min. UV detection: 254nm.

2.3.1. Optimized separation of polar mixtures

Initially, the characterization of these HILIC stationary phases was done using test mixtures of nucleic acid bases and nucleosides, β-blockers, xanthines, salicylic acid and its analogues, and maltooligosaccharides. The structures of these compounds are shown in Figure 2-2.

Figures 2-3~2-7 compare the separation performance of the three newly prepared cyclofructan 6 based stationary phases with three commercially available columns.
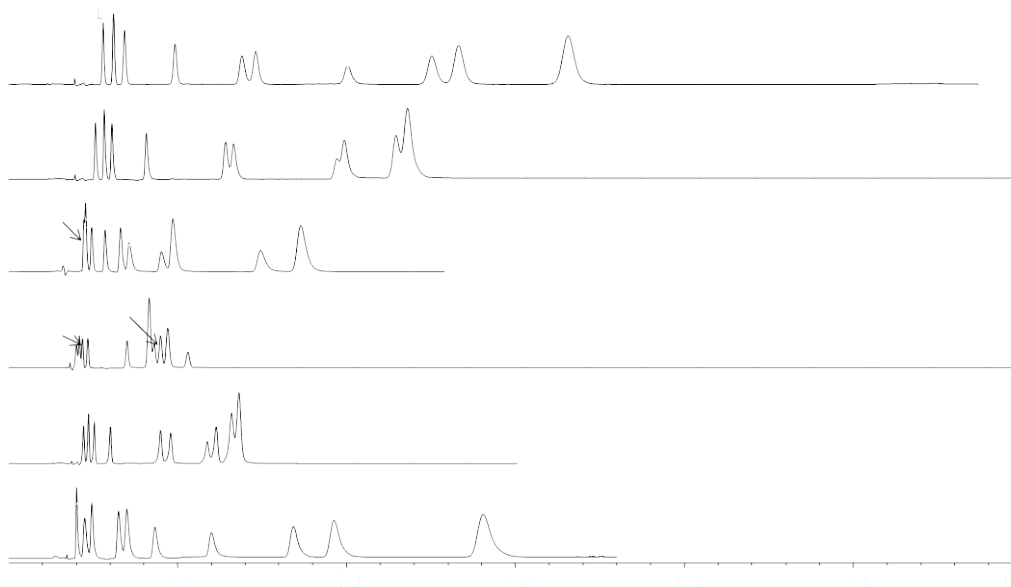
Figure 2-3 Separation of nucleic acid bases and nucleosides on the six compared columns. Mobile phase: acetonitrile/20 mM ammonium acetate, pH = 4.1, 90/10 (*v/v*); flow rate: 1.0 mL/min; UV detection: 254 nm. Compounds: 1. Thymine; 2. Uracil; 3. Thymidine; 4. Uridine; 5. Adenine; 6. Adenosine; 7. Cytosine; 8. Guanine; 9. Cytidine; 10. Guanosine.

Figure 2-3 shows chromatograms of nucleic acid bases and nucleosides obtained on the six columns under the same mobile phase conditions with acetonitrile and 20 mM ammonium acetate, pH = 4.1 (90/10, *v/v*). These 10 analytes have a "separation window" of around 40 min on the H-CF6 column, of around 30 min on the L-CF6 and ZIC-HILIC columns, and of less than 20 min on the other columns. Comparable elution orders were observed on all six columns. The H-CF6 column and the ZIC-HILIC column provided the best performance in separating nucleic acid bases and nucleosides. The selectivity factors ($\alpha > 1.07$) and resolutions ($R_s > 1.4$) of all adjacent peaks were observed for all ten nucleic acid compounds on the H-CF6 column. Except for thymidine

and uracil (α = 1.08; R_s = 1.3) and adenine and adenosine (α = 1.09; R_s = 1.3), the other

adjacent peaks were baseline separated on the ZIC-HILIC column. The L-CF6 column

did not perform as well as the former columns, in terms of selectivity and resolution. For

example, the pairs adenine and adenosine (α = 1.04; R_s = 1.0), cytosine and guanine (α

= 1.02; R_s = 0.7), cytidine and guanosine (α = 1.03; R_s = 0.8) were partially separated on

this column. It is believed that the different coverage of cyclofructan is the main reason

for the reversed elution order of adenine and adenosine, and the different resolutions for

cytosine, guanine, cytidine and guanosine observed on the H-CF6 and the L-CF6

columns. Both the steric interactions and number of available silanol groups would be

somewhat different for these closely related stationary phases. The elution profile on the

DCH-CF6 column showed that there was no selectivity between thymine and uracil and

there were three partial separations - uracil and thymidine, adenosine and adenine,

cytosine and guanine. Three partially separated pairs were obtained on the Astec

Cyclobond I 2000 column and there were four partial separations on the Astec Diol HPLC

column. There are previous reports on the HILIC separation of fewer nucleic acid bases

and nucleosides than reported here [48, 55, 72-75]. In these cases, overlapping analytes

were replaced with unrelated amines, such as theophylline and caffeine. Also thermal or

solvent gradient conditions were used. No other isocratic separations of the ten analytes

in this study (Figure 2-3) have been reported.
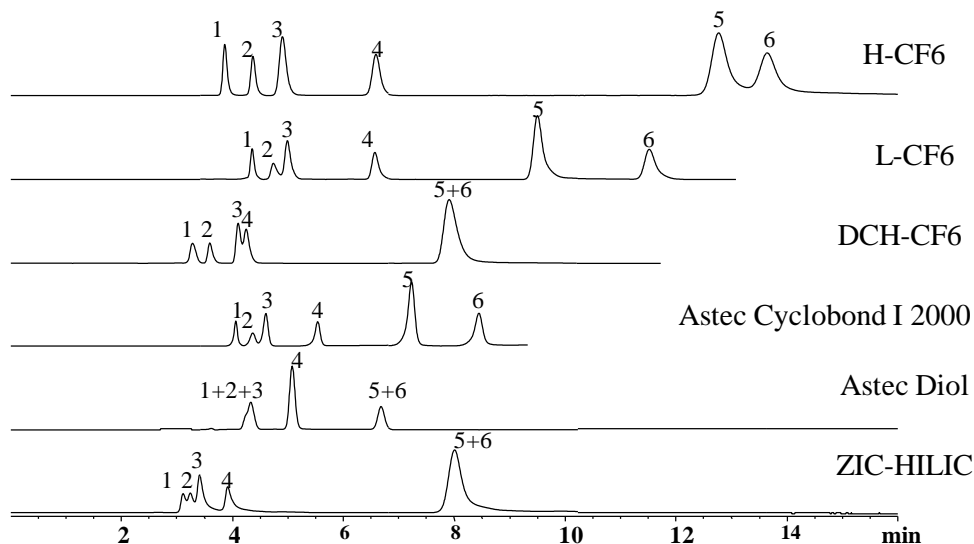
Figure 2-4 Separation of xanthines on the six compared stationary phases. Mobile phase: acetonitrile/20 mM ammonium acetate buffer, pH = 4.1, 90/10 (*v/v*); flow rate: 1.0 mL/min; UV detection: 254 nm. Compounds: 1. Caffiene; 2. 7-β-Hydroxypropyl Theophylline; 3. Theophylline; 4. Dyphilline; 5. Hypoxanthine; 6. Xanthine.

All xanthines were baseline separated on the H-CF6, the L-CF6 and the Astec Cyclobond I 2000 columns, as shown in Figure 2-4. The separation times were less than 15 min for all columns. Under the same mobile phase condition, the DCH-CF6 and the ZIC-HILIC columns were less successful in separating these types of analytes, since two pairs of partially separated peaks were observed on the DCH-CF6 and three on the ZIC-HILIC. Previously, it was proposed that the poor retention of xanthines on the ZIC-HILIC column could be due to the weaker ionic-dipolar interactions or coulombic interactions between these analytes and the stationary phases as xanthines remain neutral in a hydro-organic environment [76]. Thus, differences in the hydrophilic interactions between these analytes and the stationary phases are not significant. The Astec Diol HPLC column also is a poor choice for this separation given the three co-eluting peaks obtained.

25

Additionally, compared with other columns, the H-CF6 column consistently produced higher retention factor values. This result can be related to a greater number of available hydroxyl groups that can enhance hydrogen bonding interactions between the polar solutes and the stationary phase.
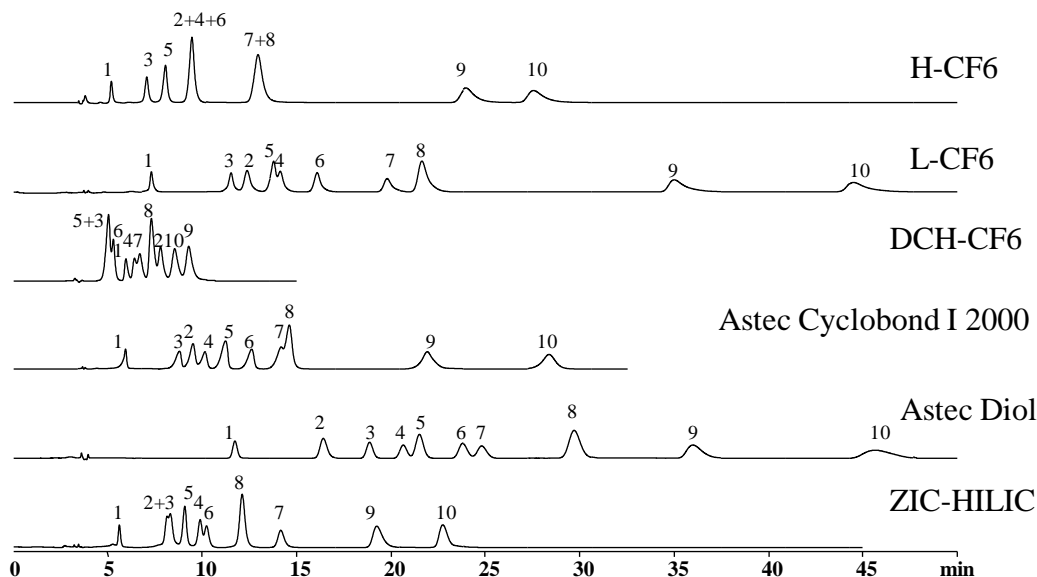
Figure 2-5 Separation of β-blockers on the six compared stationary phases. Mobile phase: acetonitrile/20 mM ammonium acetate buffer, pH = 4.1 90/10 (*v/v*); flow rate: 1.0 mL/min; UV detection: 254 nm. Compounds: 1. Carvedilol; 2. Labetalol; 3. Alprenolol; 4. Pindolol; 5. Esmolol; 6. Metoprolol; 7. Sotalol; 8. Acebutolol; 9. Nadolol; 10. Atenolol.

In the case of the β-blockers, the mobile phase composition was adjusted in order to separate as many analytes as possible. The resolution between adjacent analytes improved with increasing concentrations of acetonitrile. When the mobile phase contained percentages higher than 90% of acetonitrile, nadolol and atenolol did not elute. Figure 2-5 shows the performance of the HILIC columns for the separation of β-blockers. Among the six tested columns, the L-CF6 was most effective and retentive column for

separating this mixture of β-blockers. All ten compounds were almost baseline separated. There were two partially separated pairs: alprenolol and esmolol (α = 1.05, R_s = 1.3) and labetalol and pindolol (α = 1.04, R_s = 1.1) on this column. The Astec Diol HPLC column was the second most effective in terms of selectivity and resolution with eight analytes baseline separated in 42 min. Pindolol and esmolol were partially separated with α = 1.02, R_s = 0.5, and metoprolol and sotalol were partially separated (α = 1.04, R_s = 1.0). However, the H-CF6 and Astec Cyclobond I 2000 columns did not perform as well in separating this mixture of analytes with shorter retention and worse selectivitities. For example, labetalol, pindolol and metoprolol coeluted on the H-CF6 column, as did sotalol and acebutolol. Labetalol and pindolol were partially separated on the Astec Cyclobond I 2000 column and sotalol and acebutolol coeluted. Neither the DCH-CF6 column nor the ZIC-HILIC column was adequate for the separation of such mixtures even under optimum conditions. Longer retention and better selectivities of β-blockers were obtained on the L-CF6 as compared to the H-CF6 column. This likely results from the mixed-mode interactions of the analytes with the stationary phase (hydrogen bonding interaction and silanol group adsorption) [77].
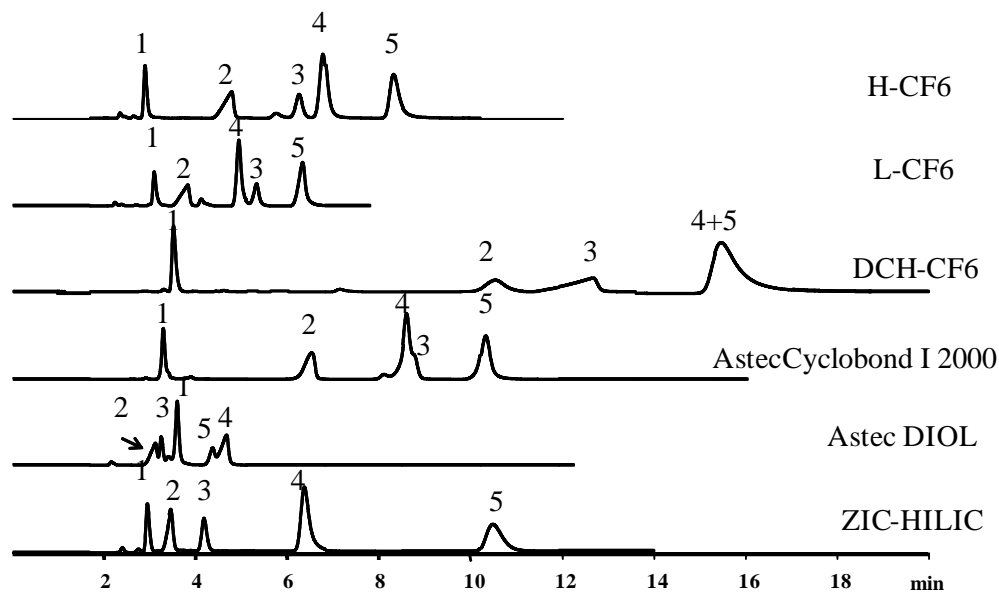
Figure 2-6 Separation of salicylic acid and its derivatives on the six compared stationary phases. Mobile phase: acetonitrile/20 mM ammonium acetate buffer, pH = 4.1, 85/15 (*v/v*).; flow rate: 1.0 mL/min; UV detection at 254 nm. Compounds: 1. Salicylamide 2. Salicylic acid; 3. 4-Aminosalicylic acid; 4. Acetylsalicylic acid; 5. 3,4-Dihydroxyphenylacetic acid.

As shown in Figure 2-6, the H-CF6, the L-CF6 and the ZIC-HILIC columns can separate salicylic acid and its derivatives with good peak shapes and efficiencies. Comparing the retention and selectivities of these acidic analytes on the cyclofructan-based stationary phases, the H-CF6 produced greater retention (around 9 min) for salicylic acid and its analogues than the L-CF6 column (around 7 min). This could be attributed to the higher cyclofructan content of the stationary phase. In comparison, the H-CF6 and ZIC-HILIC columns show similar retentions and selectivities for the first four eluted analytes but the latter column has greater retention (around 11 min) and a more

28

tailing peak for 3,4-dihydroxyphenylacetic acid than does the H-CF6 column. Co-elution

or partial separations occurred on the DCH-CF6, the Astec Cyclobond I 2000 and the

Astec Diol HPLC columns. Comparing a previous report [55, 78] on the separation of

salicylic acid and its analogues on commercial columns, under similar mobile phase

conditions, the performance of the H-CF6 column is better than that of the HILIC silica

(Agilent) column, the ZIC-HILIC column and the YMC Pack NH2 column, but comparable

to that of the TSK-gel Amide-80 column and the Polyhydroxyethyl A column.
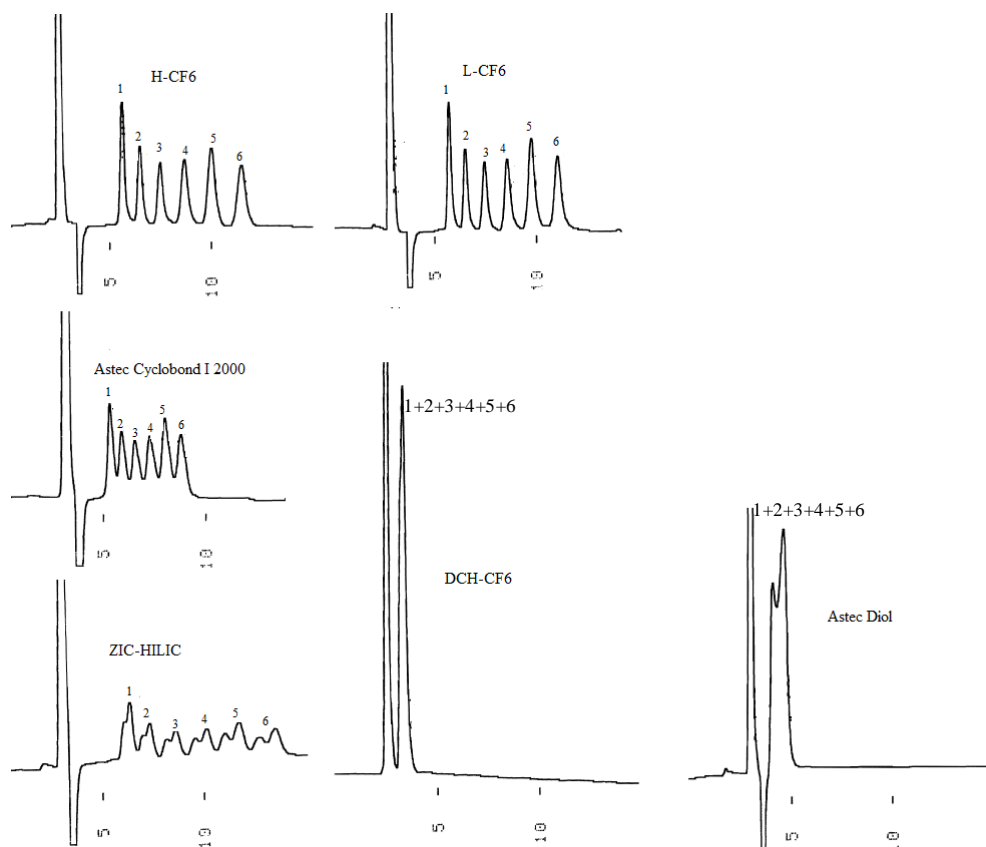
Figure 2-7 Separation of maltooligosaccharides on the six compared columns. Mobile

phase: acetonitrile/water 65/35 (*v/v*); flow rate: 1.0 mL/min; RI detection. Compounds: 1.

Maltose; 2. Maltotriose; 3. Maltotetraose; 4. Maltopentaose; 5. Maltohexaose; 6.

Maltoheptaose.

Native cyclodextrin-based columns are particularly useful for analysis of oligosaccharides due to possible hydrogen bonding interactions of the oligosaccharide hydroxyl groups with those of the cyclodextrin stationary phase [7, 58, 79, 80] in a mobile phase consisting of acetonitrile/water 65/35 (*v/v*). CF6-based columns have somewhat analogous hydrogen bonding capabilities but a different geometry. The separation of maltooligosaccharides (with two to seven glucose units) was conducted on the six columns as shown in Figure 2-7. In this separation environment, the retention times predictably increased with the number of analyte hydroxyl groups, which correspond to the degree of polymerization (dp). Hence, maltoheptaose (dp = 7) tends to be retained more than maltohexaose (dp = 6), and maltose (dp = 2) is always eluted first. With a mobile phase of acetonitrile and water (65/35, *v/v*), baseline separation of all maltooligosaccharides was achieved on both the H-CF6 and the L-CF6 columns but the analytes were more retained on the former column (separation times around 12 min on the H-CF6 column and 11 min on the L-CF6 column). The Cyclobond I 2000 column showed a moderate capability in separating these oligomers with this mobile phase in terms of shorter retentions (running time is around 9 min) and slightly poorer selectivities. Under the same mobile phase condition, peak splitting of all sugars was observed on the ZIC-HILIC column as the anomeric separation occurred. There was no separation of maltooligosaccharides on the DCH-CF6 column and on the Astec Diol HPLC column. For native saccharides, anomeric separations have been probed on the cyclofructan-based column when acetonitrile content in the mobile phase exceeded 80%. Similarly, anomeric separations have been reported on cyclodextrin-bonded columns in acetonitrile rich mobile phases [7, 21, 81]. Clearly, the CF6-based stationary phases are exceptional for sugar/carbohydrate separations in the HILIC mode and do not react with reducing saccharides. Consequently, they are good for quantitative analysis of carbohydrates.

The H-CF6 column produced the best separation for the nucleic acid bases and nucleosides, xanthine analogues, and also afforded better separation of maltooligosaccharides. A better separation of β-blockers was achieved on the L-CF6 column. The H-CF6, ZIC-HILIC, and L-CF6 all separated the polar acidic analytes effectively. The main difference between the H-CF6 and L-CF6 stationary phases is the cyclofructan content on the silica support. The difference in retention and selectivity observed on both columns not only depends on the degree of cyclofructan coverage and binding chemistry but also on the nature of the analyte and mobile phase composition.

2.3.2.   Impact of mobile phase variables on retention and selectivity

Experimental parameters were selected to study their effect on retention and selectivity. These included the nature and amount of organic modifier, salt concentration and buffer pH, and temperature.

2.3.2.1. Nature and amount of organic modifier

In the HILIC mode, acetonitrile is most commonly used as the organic modifier. The optimized separations for polar mixtures (Figure 2-2) were achieved with a large amount of acetonitrile and a smaller amount of the aqueous part of the mobile phase. Acetonitrile is advantageous for the HILIC mode, because it is a poor hydrogen bonding solvent and it is polar and miscible with water in all proportions. Thus, it provides an environment for attractive and discriminative interactions of polar solutes with the hydrophilic stationary phases. Usually, protic solvent, such as methanol, affords insufficient retention and incomplete separation for polar analytes. At higher percentages of acetonitrile in the mobile phase, the retention factor is governed by a contribution of hydrogen bonding, dipolar and hydrophilic interactions between the solute and the stationary phase. The solutes with a higher number of available polar sites, such as the

ribose structural element in nucleosides (which is absent in nucleic acid bases) have stronger interactions with polar stationary phases.
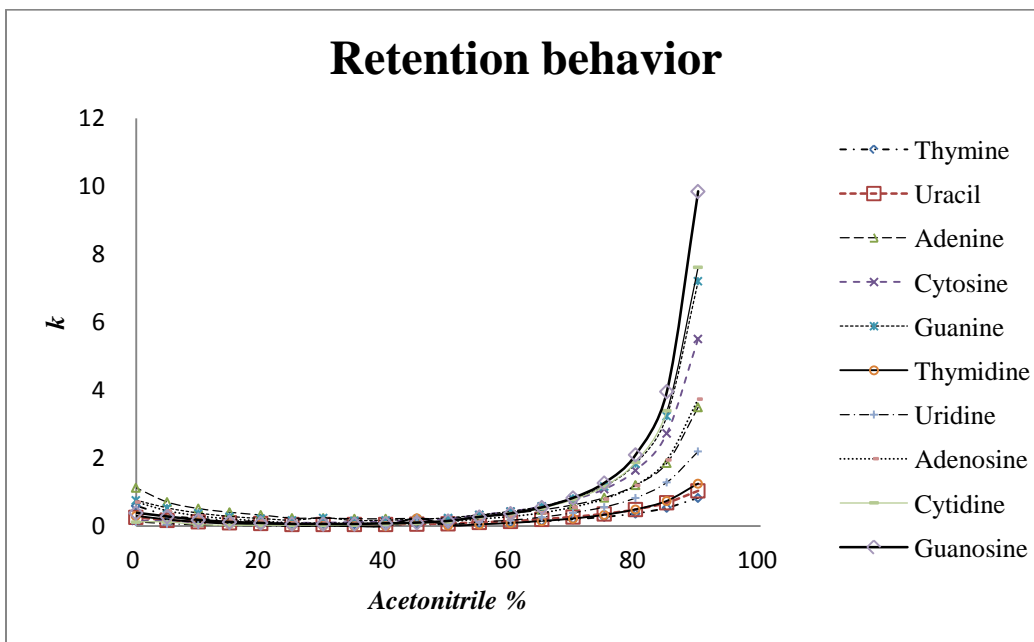
Figure 2-8 Effect of acetonitrile content on the retention (k) of ten tested nucleic acid bases and nucleosides on the H-CF6 column. Mobile phase: acetonitrile and 20 mM ammonium acetate, pH = 4.1. Flow rate: 1.0 mL/min. UV detection at 254 nm.

Figure 2-8 shows a typical dependence of retention factors (k) on acetonitrile content in the mobile phase for five nucleic acid bases and five nucleosides on the H-CF6 column. The retention factor profiles of all analytes are similar in shape. When acetonitrile in the mobile phase is in the range of 20-60%, retention is minimal as all solutes elute near the dead volume. Decreasing the acetonitrile content in the mobile phase (<20%) results in longer retention, which is similar to what is found in RPLC. However, this trend is not substantial, as the cyclofructan-based stationary phase has very high hydrophilic nature [9, 76, 82]. The HILIC separation environment becomes predominant when the acetonitrile amount exceeds ~60% by volume. Then the retention factors increase is

steep for the hydrogen-bonding interaction domain. However, all analytes produced broad peaks or were not eluted if the acetonitrile amount was higher than 95%, often due to the solubility limitations of these compounds. Similar dependences were obtained on the other tested columns.

2.3.2.2. Buffer effects

2.3.2.2.1. Salt concentration

Various salts (e.g. triethylammonium phosphate, or carbonate salts) typically used in RPLC are not suitable for HILIC, as they are poorly soluble in mobile phases containing high amounts of acetonitrile [55]. Initially, triethylammonium acetate and ammonium acetate were used for HILIC separations. In most cases, these columns have better performance when using ammonium acetate buffer. Many researchers also used ammonium formate for separation because they could achieve higher selectivity and better compatibility with MS detection [73]. The effect of the amount of ammonium acetate in the mobile phase also was evaluated. The investigation was carried out by varying the salt concentration of the buffer in the range of 0-20 mM at pH = 4.1 (acetonitrile percentage was kept constant). Generally, the separation of nonionic solutes, such as maltooligosaccharides, did not show significant differences either in terms of retention or selectivity, when changing the salt concentration from 0 mM to 20 mM. For nucleic acid compounds and xanthines, slight differences in the separations were observed when the salt concentration changed. However, there was a substantial influence of ionic strength on β-blockers and salicylic acid analogues, not only on their retention but also on resolution. The obtained data indicated that the retention of β-blockers increased if no buffer was used. The data in Table 2-3 show retention parameters for nadolol and atenolol, as representative β-blockers, at two ammonium acetate concentrations (5 mM and 20 mM, at the same pH) on different HILIC columns.

The results indicate that the retention factors and resolutions increased greatly when the buffer concentration increased from 5 mM to 20 mM but the selectivity changed only slightly. Similar results were observed with salicylic acid and analogues.

Table 2-3 Effect of buffer concentration on retention parameters of nadolol (k_1) and atenolol (k_2).

Column	5mM ammonium acetate, pH = 4.1				20mM ammonium acetate, pH = 4.1			
	k_1	k_2	α	R_s	k_1	k_2	α	R_s
H-CF6	11.24	13.00	1.14	2.28	7.87	9.16	1.15	2.63
L-CF6	19.32	24.48	1.25	4.88	12.28	15.77	1.26	6.16
DCH-CF6	1.00	1.15	1.08	1.00	1.79	2.05	1.09	1.54
ZIC-HILIC	13.95	16.05	1.14	2.79	6.32	7.61	1.18	3.24
Astec Cyclond I 2000	5.95	8.02	1.30	4.10	6.88	9.44	1.33	6.65
Astec Diol	19.05	23.01	1.20	2.86	10.48	13.31	1.25	6.06

Mobile phase: acetonitrile/ammonium acetate, pH = 4.1, 90/10 (*v/v*); flow rate: 1.0 mL/min; UV detection: 254nm.

2.3.2.2.2. Buffer pH

Buffer pH influences the retention behavior of some solutes, since it affects the ionization of solutes and/or stationary phase functional groups. This investigation was carried out by varying the buffer pH from 3.0 to 6.5 at a fixed buffer concentration and acetonitrile content in the mobile phase. For nucleic acid bases, nucleosides, xanthines, only slight retention variations with pH differences were observed. This is consistent with the general observations for HILIC-type commercial columns reported earlier [72, 74, 83]. Thus, little or no pH effect on retention of nonionic solutes, such as maltooligosaccharides, can be expected. On the other hand, the retention of β-blockers is greatly affected by buffer pH. Nadolol and atenolol were again taken as representative

examples to show the effect of buffer pH on the retention in Figures.2- 9(a) and 2-9(b)

with a mobile phase of acetonitrile/20 mM ammonium acetate 90/10 (*v/v*). The retention

factors of nadolol and atenolol increased with the pH on all columns except for the DCH-

CF6. The sharpest increase was observed in the range of 4.0-5.0, which correspond to

the pK_b of these compounds (nadolol, pK_b=4.3; atenolol pK_b=4.4) [75, 84, 85]. The

highest retention resulted from two columns, i.e., the L-CF6 and Astec Diol. However, an

increase in retention does not necessarily translate into improved selectivity, as the

selectivity on all the tested columns for these analytes was the highest at a pH of

approximately 4 (Figure 2-9(c)). The maximum resolution also was observed around pH

= 4 as shown in Figure 2-9(d). Both the selectivity and resolution of β-blockers were best

on the L-CF6 stationary phase. For salicylic acid and analogues compounds, the buffer

pH only appreciably affected the retention of 3,4-dihydroxyphenylacetic acid.
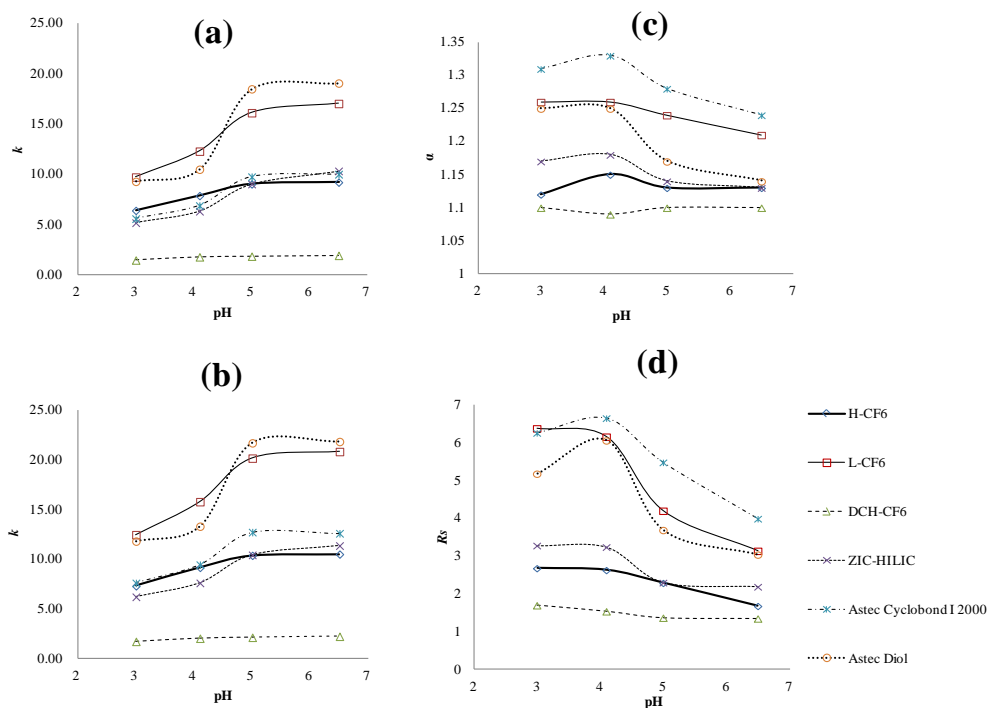
Figure 2-9 Effect of buffer pH on the retention, k, of nadolol (a) and atenolol (b) and on the selectivity, α, (c) and resolution, R_s, (d) of nadolol and atenolol on the six compared stationary phases. Mobile phase: acetonitrile/20 mM ammonium acetate, 90/10 (*v/v*); flow rate: 1.0 mL/min; UV detection at 254 nm.

While the nature and amount of organic modifier in the mobile phase affect the retention and separation of all analytes, the buffer concentration and pH influence some but not others. There was a significant impact of buffer concentration and buffer pH on the retention and resolution of β-blockers but a minor effect on the retention parameters of nucleic acid bases, nucleosides, xanthines, and maltooligosaccharides. As expected, higher buffer concentrations increased the eluting strength of the mobile phase, thus resulting in less retention of anionic components, but it did not affect the retention of

neutral compounds. Buffer pH effects on retention and resolution is directly related to nature of analytes (e.g., pK_a values, solubilities, etc.).

2.3.2.3. Thermodynamic study

There have been numerous studies of temperature effects on solute retention in the HILIC mode [55, 72, 75]. The dependence of the natural logarithms of retention factors (ln k_i) on the inverse of temperature ($1/T$) is routinely used to determine

It is generally accepted that the HILIC mode separation is based on the formation of reversible associates (hydrogen bonding associates for polyhydroxyl stationary phases, coulombic interactions for the zwitterionic stationary phases, e.g., the ZIC-HILIC column) that are created by intermolecular interactions of polar analytes and hydrophilic stationary phase. In this work, thermodynamic data (ΔG_i, ΔH_i, ΔS_i) were calculated according to the Gibbs-Helmholtz equation:

$$\Delta G_i = \Delta H_i - T\Delta S_i = -RT \ln K_i \tag{1}$$

Where ΔG_i is the molar Gibbs energy, ΔH_i is the molar enthalpy, ΔS_i is the molar entropy, K_i is the solute partition coefficient, R is the universal gas constant, and T is the temperature (in K).

The dependence of analyte retention on the temperature can be expressed by the van't Hoff equation:

$$\ln k_i = \frac{-\Delta H_i}{RT} + \frac{\Delta S_i}{R} + \ln \emptyset \tag{2}$$

Where k_i is the retention factor of a solute, ΔH_i is the molar enthalpy of transfer of a solute in the chromatographic system, ΔS_i is the molar entropy, and Φ is the phase ratio of the chromatographic column ($\Phi = V_M/V_S$).
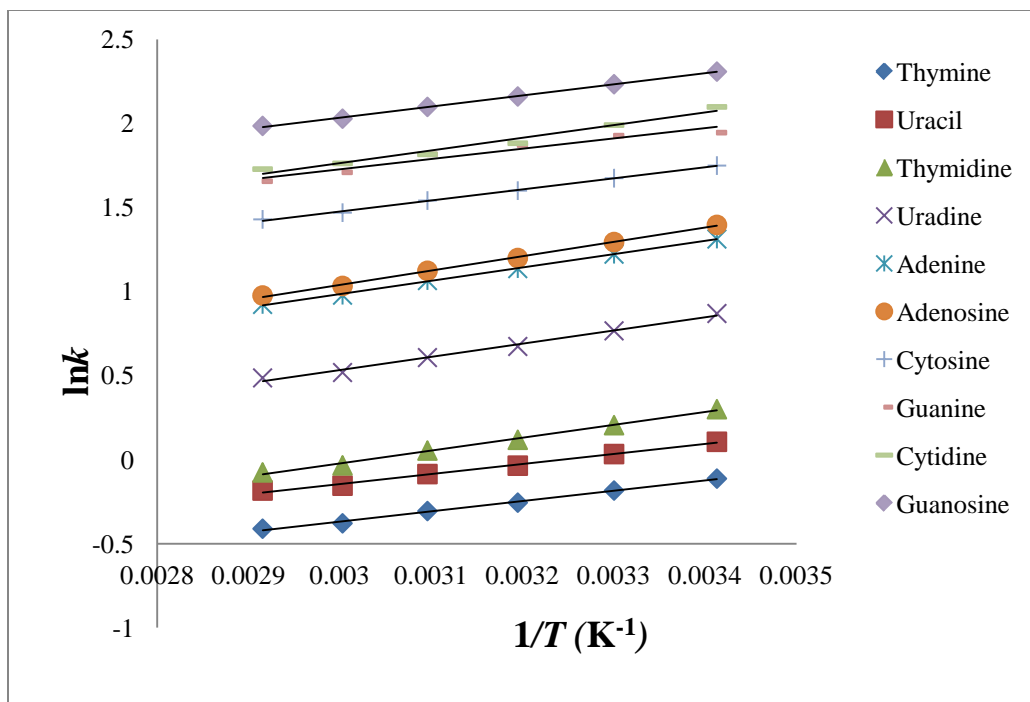
Figure 2-10 Dependences of logarithms of retention factors (ln k) on the inverse of temperature (1/T) for nucleic acid bases and nucleosides using the H-CF6 column. Mobile phase: acetonitrile/20 mM ammonium acetate, pH = 4.1, 90/10 (*v/v*); flow rate: 1.0 mL/min; UV detection at 254 nm.

The van't Hoff plots (dependence of ln k_i on 1/T) were linear within the studied temperature interval for nucleic acid bases and nucleosides using the H-CF6 column, as shown in Figure 2-10. Similar dependencies were obtained for other analytes. Linear dependencies indicate no change of interaction mechanism within the measured temperature range. Table 2-4 lists the thermodynamic data for nucleic acid bases and nucleosides on the tested columns. The ΔH_i values calculated from the slope of the plot of Eq. (2) were negative for all analytes on the H-CF6 column, ranging from -4.94 to -7.08 kJ/mol. The negative sign of ΔH_i indicates an exothermic process. The ΔH_i values

obtained on the L-CF6 column varied from -4.07 to -6.68 kJ/mol. For the Astec

Cyclobond I 2000 column, the ΔH_i values ranged from -5.05 to -7.97 kJ/mol with high

linearity. Comparing with the thermodynamic data obtained from other columns, the ΔH_i

values from the ZIC-HILIC were relatively greater, ranging from 2.71 to -4.06 kJ/mol.

Additionally, there were two positive ΔH_i values calculated from the plots on the ZIC-

HILIC column, including guanine (0.97 kJ/mol) and guanosine (2.71 kJ/mol). The $\Delta S_i'$

values on the ZIC-HILIC were more positive than the values obtained from all other

columns. It was evidence that entropic contributions are more dominant on the ZIC-HILIC

stationary phase. Guanine showed a nonlinear van't Hoff plot on the ZIC-HILIC that was

previously reported by Marrubini [72]. It suggested that guanine's retention was

influenced by mixed retention mechanism, ion-exchange and displacement of waters of

hydration on the stationary phase. In most other cases, correlation coefficients are

greater than 0.99, which indicates that one retention mechanism dominates [85]. For the

polyhydroxyl functionalized stationary phases, hydrogen bonding interactions between

the polar solute and the hydrophilic stationary phases are dominant and enthalpic in

nature. For the ZIC-HILIC column, the influence of columbic interaction must be taken

into consideration.

Table 2-4 The thermodynamic parameters resulting from linear regression (ln$k$ vs.1/T) for nucleic acid bases and nucleosides on the HILIC columns.

analyte	H-CF6			L-CF6			ZIC-HILIC			Astec Cyclobond I 2000		
	ΔH kJ/mol	$\Delta S'$ [a] J/mol K	correlation coefficient	ΔH kJ/mol	$\Delta S'$ [a] J/mol K	correlation coefficient	ΔH kJ/mol	$\Delta S'$ [a] J/mol K	correlation coefficient	ΔH kJ/mol	$\Delta S'$ [a] J/mol K	correlation coefficient
Thymine	-5.09	-11.37	0.9953	-4.07	-8.56	0.9977	-4.06	-14.12	0.9968	-5.05	-14.72	0.9922
Uracil	-4.94	-9.08	0.9944	-4.09	-6.90	0.9979	-2.21	-3.24	0.9918	-5.48	-14.54	0.9879
Thymidine	-6.37	-12.41	0.9957	-5.21	-9.31	0.9699	-3.52	-9.87	0.9971	-6.94	-17.91	0.9855
Uradine	-6.54	-8.22	0.9908	-5.75	-7.24	0.9986	-2.23	5.10	0.9983	-7.35	0.34	0.9857
Adenine	-6.57	-4.56	0.9987	-5.49	-0.63	0.9989	-2.92	-0.83	0.9971	-6.05	-5.90	0.9925
Adenosine	-7.08	-5.64	0.9982	-5.87	-2.29	0.9991	-2.30	2.17	0.9996	-7.09	-10.04	0.9903
Cytosine	-5.44	2.91	0.9976	-4.65	5.91	0.9987	-3.05	6.21	0.9957	-5.07	-0.42	0.9937
Guanine	-5.10	6.02	0.9454	-6.44	0.71	0.8439	0.97	22.95	0.5749	-5.21	-0.48	0.9964
Cytidine	-6.26	2.85	0.9747	-6.68	0.64	0.9993	-2.25	13.60	0.9445	-7.97	-8.69	0.9934
Guanosine	-5.48	7.42	0.9984	-5.10	6.05	0.9997	2.71	33.51	0.9956	-6.64	-4.10	0.9949

$\Delta S'$ was calculated from the plot intercept (Eq. 2). $\Phi = V_M/V_S$, V_M was obtained from the flow rate and dead time t_0, assuming negligible extra-column volume. V_S was obtained by the geometric internal volume of the column minus V_M. Here, V_S is the total stationary volume, including the volume of bonded stationary phase and the volume of the supporting material. Since the V_S here is the total volume of stationary phase rather than the volume of the absorbing surface layer, we use the prime symbol ($\Delta S'$).
Mobile phase: acetonitrile/20 mM ammonium acetate, pH = 4.1, 90/10 (v/v); flow rate: 1.0 mL/min; UV detection: 254nm.

2.4 Conclusions

The retention behavior afforded by HILIC offers the potential for dramatic changes in selectivity compared to RPLC. The native CF6 based stationary phases have been successfully synthesized and evaluated. It appears that these new stationary phases have advantages over popular commercial columns in separating nucleic acid bases, nucleosides, xanthines, β-blockers and salicylic acid and its derivatives, and carbohydrates in the HILIC mode. Their performance in the HILIC mode can provide increased retention, improved selectivity and resolution for compounds, which are difficult to retain and separate in RP-HPLC. Additionally, CF6 columns are stable, have good efficiency, good reproducibility, and do not react with reducing sugars/carbohydrates. Consequently, they seem to be good for quantitative analysis. More detailed evaluations are currently underway and derivatization of the CF6 may further broaden its application.

Chapter 3

Develoment and evaluation of new zwitterionic HILIC stationary phases

based on 3-P,P-diphenylphosphonium-propylsulfonate

Abstract

New zwitterionic stationary phases were synthesized by covalently bonding 3-P,P-diphenylphosphonium-propylsulfonate to silica gel. The resulting materials possess both a negatively charged sulfonate group and a positively charged quaternary phosphonium group, which means that there is no net charge over a wide pH range. The retention mechanism and chromatographic behavior of polar solutes under HILIC conditions were studied on these zwitterionic phases. Compared to the commercial ZIC-HILIC column and a bare silica gel stationary phase, the newly synthesized zwitterionic stationary phases provided greater retention, higher peak efficiency and better peak symmetry in the HILIC mode. The analytes examined included: β-blockers, nucleic acid bases and nucleosides, salicylic acid and its analogues, and water soluble vitamins. Factors, such as the type of organic modifiers, solvent composition, pH and the buffer concentration of the mobile phase, have been considered as potential variables for controlling the chromatographic retention of polar analytes.

3.1 Introduction

Hydrophilic interaction liquid chromatography (HILIC) has been applied to the separation of polar compounds for more than 60 years by using polar stationary phases with organic-aqueous binary mobile phases. Typically, some water and a higher percentage of a water miscible organic solvent were used as HILIC mobile phases. This special LC mode was used in separating a mixture of fructose, glucose, and mannose on

ion exchange stationary phases as early as the 1950s [5]. Since 1975, this type of mobile phase has been developed for the analysis of carbohydrates, carboxylates, and amino acids using polar stationary phases (e.g., β-cyclodextrin, diol, amino, amide, etc.) [4]. Especially, the analysis of oligosaccharides achieved success on the native cyclodextrin based columns using HILIC-ESI-MS [58, 79]. In 1990 the acronym HILIC was coined for the analysis of hydrophilic substances, such as proteins, peptides and nucleic acids [9]. Recently, HILIC has emerged as an increasingly popular and a viable option to RPLC, because of the ability to retain and separate polar and hydrophilic analytes, which have often insufficient retention and resolution in RPLC.

There are a few commercially available columns designed for HILIC separations [3, 86, 87]. Among the different types of HILIC stationary phases, zwitterionic stationary phases play a unique role. The combination of positively and negatively charged sites on the sorbent surface provides unique opportunities to vary the separation selectivity. HPLC separation materials with zwitterionic functionalities have been known for many years [88] and have been widely applied in ion-exchange liquid chromatography to separate cations and anions simultaneously [86, 87, 89, 90]. Such stationary phases possess unique water-retaining properties due to the zwitterionic functionality. Recently, they have been developed and used for HILIC separations [62, 86, 91, 92]. In these cases, the zwitterionic nature does not promote strong ion exchange interactions but rather smaller electrostatic contributions from the charged groups. These qualities make zwitterionic stationary phases exceptionally well suited for HILIC separations.

The exact mechanism of HILIC separations remains open to question, but it probably involves several different types of interactions [3, 4, 10, 11]. For example, it has been postulated that there may be a partitioning of polar analytes between the highly organic mobile phase and the hydration layer that surrounds the polar surface [5, 12-14].

43

The existence of the water layer has been shown by McCalley and Neue [17]. They postulated that about 4-13% of the pore volume of a silica phase is occupied by a water layer when 75-90% acetonitrile in the eluent. In the case of zwitterionic stationary phases, both the zwitterionic functionality and any residual silanol groups are hydrated by water and promote a water enriched layer on the surface of the stationary phase. Additionally, silanol groups and zwitterionic functionalites provide the possibility of electrostatic interactions to HILIC separations [18]. As described by Alpert [9], the zwitterionic stationary phase exhibits an overall negative charge when using typical HILIC mobile phases due to the dissociation of residual silanol groups. Therefore some electrostatic repulsion interactions might occur between dissociated acidic analytes and the negatively charged stationary phase and some attractive electrostatic interactions might occur for protonated basic compounds in the HILIC mode. Beside the above possibilities, other interactions derived from functionalities need to be considered as well, such as π-π and/or n-π interactions, hydrogen bonding interactions, and/or dipole-dipole interactions. In some cases, hydrogen bonding interactions [7, 19, 20] and dipole-dipole interactions [22-24] between polar analytes and the stationary phase appear to be dominant.

In this study the preparation of new zwitterionic stationary phases is presented along with an investigation into their retention characteristics in the HILIC mode. A group of acidic, basic and neutral polar compounds were selected as model analytes for this study and the impact of mobile phase variables such as organic modifier, buffer concentration and buffer pH, on retention and selectivity were studied. The influence of the extent of coverage of the zwitterionic moieties on the supporting material and the effect of end-capping of silanol groups also were evaluated. Finally, the separations obtained using these zwitterionic HILIC stationary phases were compared to those

obtained using the commercially available silica based zwitterionic column ZIC-HILIC and a bare silica column.

3.2 Experimental

3.2.1 Reagents

The utilized supporting material was Daiso silica (Supelco, Bellefonte, PA) of 5 μm spherical diameter with 100 Å pore size and 440 m^2/g surface area. Anhydrous N,N-dimethylformamide (DMF), anhydrous toluene, anhydrous pyridine, anhydrous dioxane, 1,3-propanesultone, 2-diphenylphosphinoethyltriethoxysilane, diethyl ether, acetic acid, trimethylchlorosilane, ammonium acetate, chloroform and all polar analytes tested in this study were purchased from Sigma-Aldrich (Milwaukee, WI). HPLC grade organic solvents were obtained from EMD (Gibbstown, NJ). Water was purified by a Milli-Q Water Purification System (Millipore, Billerica, MA).

3.2.2 Synthesis of the zwitterionic stationary phase

3.2.2.1 Preparation of the zwitterionic selector

The zwitterionic selector based on 3-P,P-diphenylphosphonium-propylsulfonate was prepared. A mixture of 1,3-propanesultone (1.4 g, 11.4 mmol) and 2,2'-diphenylphosphinoethyl triethoxysilane (5.0 g, 13.2 mmol) was refluxed in anhydrous dioxane (20.0 mL) under argon atmosphere for 24 hrs. The solvent was evaporated and the resulting viscous liquid was thoroughly washed with 5 portions of diethyl ether (10.0 mL). The final product was isolated and dried *in vacuo* overnight with 80% yield. The zwitterionic selector is used immediately for the next step. ^{1}H NMR (500MHz, DMSO-d6): δ(ppm) 7.67(m, 10H), 4.45(t, 2H), 3.66(q, 6H), 3.20(t, 2H), 2.62(t, 2H), 2.09(m, 2H), 1.18(t, 9H), 0.68(t, 2H).

3.2.2.2 Preparation of zwitterionic stationary phase

Stationary phases with high (H-ZI, which has the maximum coverage after optimization) and low (L-ZI) loading of the zwitterionic functionality were prepared. A suspension of dry 5 μm silica gel (4.0 g) and the zwitterionic selector (2.0 g for H-ZI, and 1.0 g for L-ZI) in anhydrous dimethylformamide (80.0 ml) was heated at 100 ^{o}C for 12 hrs with slow stirring. Then the contents were filtered through a fine sintered glass funnel. The chromatographic medium was then washed with 50.0 ml portions of hot dimethylformamide, methanol, chloroform and acetone respectively. The zwitterionic stationary phase was dried in vacuo overnight at 40 ^{o}C. Elemental analysis of H-ZI: C% 12.0%; H% 1.6%; N% 0.1%. Elemental analysis of L-ZI: C% 8.0%; H% 1.4%; N% 0.1%.

3.2.2.3 Preparation of the end-capping stationary phase (EC-ZI)

End-capping of the H-ZI stationary phase (EC-ZI) was achieved by the reaction with trimethylchlorosilane. H-ZI silica gel (4.0 g) was suspended in anhydrous toluene (50.0 mL) and trimethylchlorosilane (4.0 mL) dissolved in pyridine (5.0 mL) was added dropwise over a period of 10 mins at room temperature. Then the reaction mixture was refluxed overnight and the silica material was filtered through a fine sintered glass funnel followed by subsequent washings using 50.0 mL portions of toluene, methanol, chloroform and acetone respectively. The end-capping stationary phase material was dried *in vacuo* overnight at 40 ^{o}C. Elemental analysis of EC-ZI: C% 14.0%; H% 1.7%; N% 0.1%.

3.2.3 Column preparation

The prepared materials (H-ZI, L-ZI and EC-ZI, as shown in Figure 3-1) were packed into stainless steel columns (250 mm × 4.6 mm i.d.) using an empirical slurry packing procedure. Around 3 g of the synthesized stationary phase was suspended in a 50 mL solution of acetonitrile/1.0 M ammonium nitrate (96/4, *v/v*) and slurry packed into

the stainless-steel column using acetonitrile as the push solvent. The packing pressure was 60 MPa and 2 μm SST frits were used for column packing. The HPLC column packing system is composed of an air driven fluid pump (HASKEL, DSTV-122), an air compressor, a pressure regulator, a low pressure gauge, two high pressure gauges (70 and 40 MPa, respectively), a slurry chamber, check valves, and several tubings.

3.2.4 Chromatographic evaluation

All experiments were conducted on Agilent HPLC series 1200 systems (Agilent Technologies, Palo Alto, CA), equipped with a quaternary pump, an autosampler, and a multiwavelength UV-vis detector. For data acquisition and analysis, the Chemstation software version Rev. B.01.03 was used on the system in Microsoft Windows XP environment. The injection volume was 5 μL and the flow rate of the mobile phase was 1.0 mL/min. Separations were carried out at room temperature unless otherwise specified. Each sample analysis was duplicated. The separation of standard mixtures was optimized by varying the mobile phase acetonitrile content between 60% and 95% and by varying the aqueous buffer concentration and buffer pH between 0-100 mM and pH = 3.0-6.5, respectively. The buffers were prepared by dissolving the appropriate amounts of ammonium acetate in deionized water. Adjustment of pH was done by the addition of 99.7% acetic acid to the aqueous buffer. By volume, appropriate amounts of acetonitrile and the buffer solution were mixed thoroughly and degassed by ultrasonication under vacuum for 5 min before use.

ZIC-HILIC (250×4.6 mm i.d., 5 μm and 200 Å, structure shown in Figure 3-1) and bare SiO_2 columns (250×4.6 mm i.d., 5 μm and 100 Å) were chosen for comparison of selectivities and efficiencies. The peak width of half height was used to calculate the peak efficiency. ZIC-HILIC was purchased from Merck SeQuant (Darmstadt, Germany). The SiO_2 column used was packed in house with Daiso silica. In order to evaluate the

potential of the ZI series columns for use in HILIC, and to compare the capabilities of the prepared materials to those commercial stationary phases, a selection of polar test compounds were used. These compounds include β-blockers (Figure 3-2), nucleic acid bases and nucleosides (Figure 3-3), water soluble vitamins (Figure 3-4) and salicylic acid and its analogues (Figure 3-5), all of which are common analytes of biological and pharmaceutical interest.

For the calculation of chromatographic data, t_0 was determined by the refractive index change caused by the sample solvent or by injecting toluene in the HILIC mode. Column efficiency was evaluated using uracil and cytosine as the test compounds. Three ZI series columns, the ZIC-HILIC column and the SiO_2 column were included in this efficiency test.
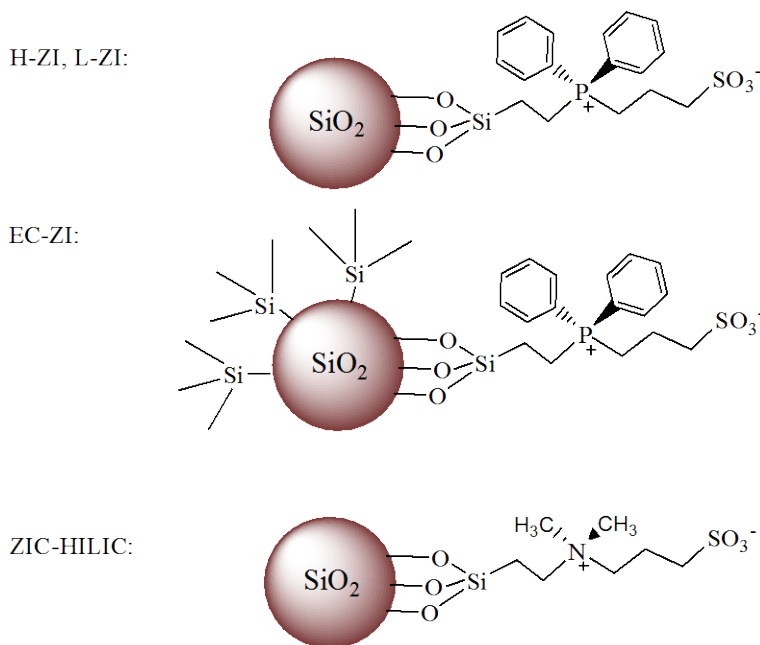
Figure 3-1 Structures of zwitterionic stationary phases and the ZIC-HILIC stationary phase.
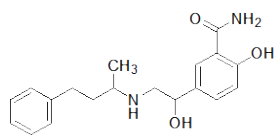
β-blockers:

Labetalol
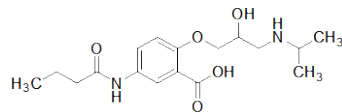
Acebutolol
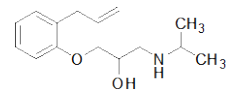
Alprenolol
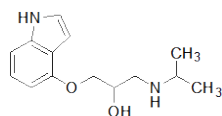
Pindolol
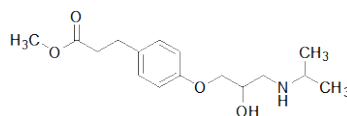
Esmolol
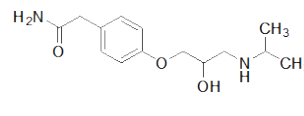
Atenolol
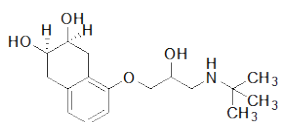
Nadolol
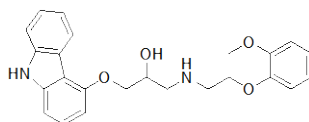
Carvedilol
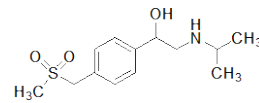
Sotalol
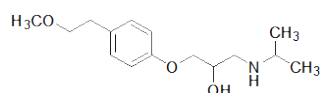
Metoprolol

Figure 3-2 Compound structures of β-blockers.

49
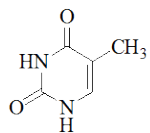
Nucleic acid base:
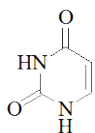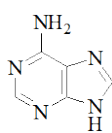
| Thymine | Uracil | Adenine | Cytosine | Guanine |
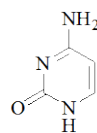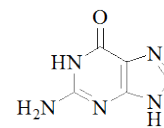
Nucleosides:
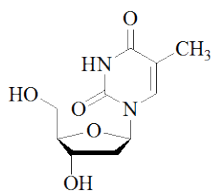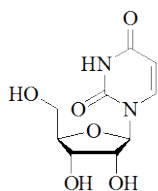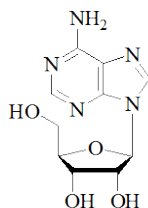
| Thymidine | Uridine | Adenosine | Cytidine | Guanosine |
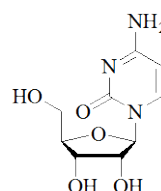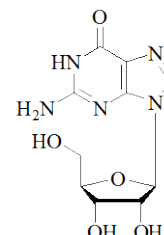
Figure 3-3 Compound structures of nucleic acid bases and nucleosides.

Salicylic acid and its analogous
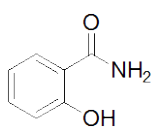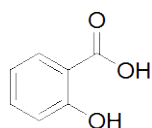
| Salicylamide | Salicylic acid | 4-Aminosalicylic acid | Acetylsalicylic acid | 3,4-Dihydroxyphenyl acetic acid |
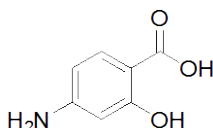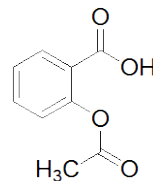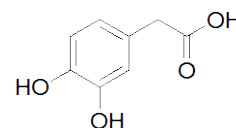
Figure 3-4 Compound structures of salicylic acid and its analogues.

Water soluble vitamins
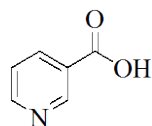
Nicotinic Acid (Vitamin B13)
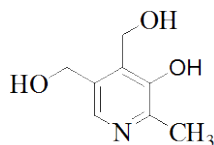
Pyridoxine (Vitamin B6)
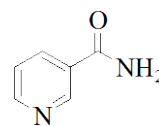
Nicotinamide (Vitamin B3)
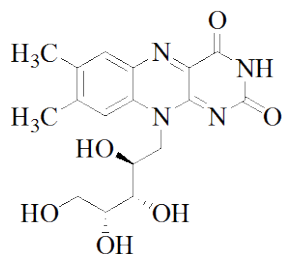
(-) Riboflavin (Vitamin B2)
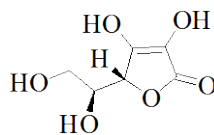
L-Ascorbic acid (Vitamin C)

Figure 3-5 Compound structures of water soluble vitamins.

3.3 Results and Discussion

3.3.1 Coverage of zwitterionic motifs

The structure of the newly synthesized zwitterionic stationary phases is shown in Figure 3-1. The H-ZI and L-ZI stationary phases share the same chemical structure but have different amounts of zwitterionic functionality bound to the supporting silica gel, which can be quantified from the carbon loading. The H-ZI has a higher amount of such functionality (C% is 12.0%) than does the L-ZI (C% is 8.0%). The EC-ZI stationary phase has the same amount of zwitterionic selector but has a higher carbon loading (C% is 14.0%) due to end-capping of the residual silanol groups of the H-ZI phase by reaction with trimethylchlorosilane. The ZI columns appear to show high column efficiency. The H-

ZI column had 14600 theoretical plates per 25 cm column for cytosine, and the L-ZI

column had 14800 plates, while the EC-ZI column had 10600 plates (Table 1).

Table 3-1 Evaluation of column efficiencies of the five tested columns.

	H-ZI	L-ZI	EC-ZI	ZIC-HILIC	SiO$_2$
Uracil (k)	0.75	0.72	0.53	0.69	0.66
Number of plates[a]	15500	15700	11400	9200	10800
Symmetry	1.01	1.21	1.28	1.49	2.82
Cytosine (k)	3.78	3.65	2.40	2.95	3.82
Number of plates[a]	14600	14800	10600	8800	10400
Symmetry	0.95	1.28	1.42	1.43	2.73

a. The number of theoretical plates given is per 25 cm column. Mobile phase condition: acetonitrile/20 mM ammonium acetate, pH=4.1, 90/10 (v/v); flow rate: 1.0 mL/min; UV detection: 254 nm.

Different coverage of zwitterionic functionality may alter the microstructure of the

stationary phase and the thickness of the water enriched layer due to the different water

binding capabilities of the residual silanol groups and zwitterionic functionalities [93]. The

H-ZI column and the L-ZI column perform well in separating polar analytes (structures as

shown in Figures 3-2~3-5) in the HILIC mode and produce similar separation profiles for

the same polar mixtures, as shown in Figures 3-6~3-9. In comparison with the L-ZI

column, the H-ZI column shows slightly stronger retention for most tested polar analytes

under the same mobile phase conditions. Furthermore, the H-ZI column produced slightly

better resolution values than the L-ZI. For example, labetalol/esmolol and

pindolol/metoprolol were partially separated on the H-ZI column (α = 1.05, R$_s$ = 0.9; α =

1.03, R$_s$ = 0.6, respectively) but these two pairs of analytes co-eluted on the L-ZI column.

The analogous end-capped (EC-ZI) column provided poor retention and worse

selectivities than the H-ZI and L-ZI columns (Figures 3-6~3-9). Poor separations of β-

blockers,nucleic acid bases and nucleosides and water soluble vitamins with partially

separated peaks and co-elution of peaks were observed on the EC-ZI column. This

reduction in selectivity and efficiency is mainly due to the introduction of the methyl end-capping groups, which are detrimental to the adsorbed water layer. Because the end-capping groups reduce the number of available silanols, they also reduce the chance of analytes interacting with silianol groups. Both of these factors affect retention and selectivity in HILIC.
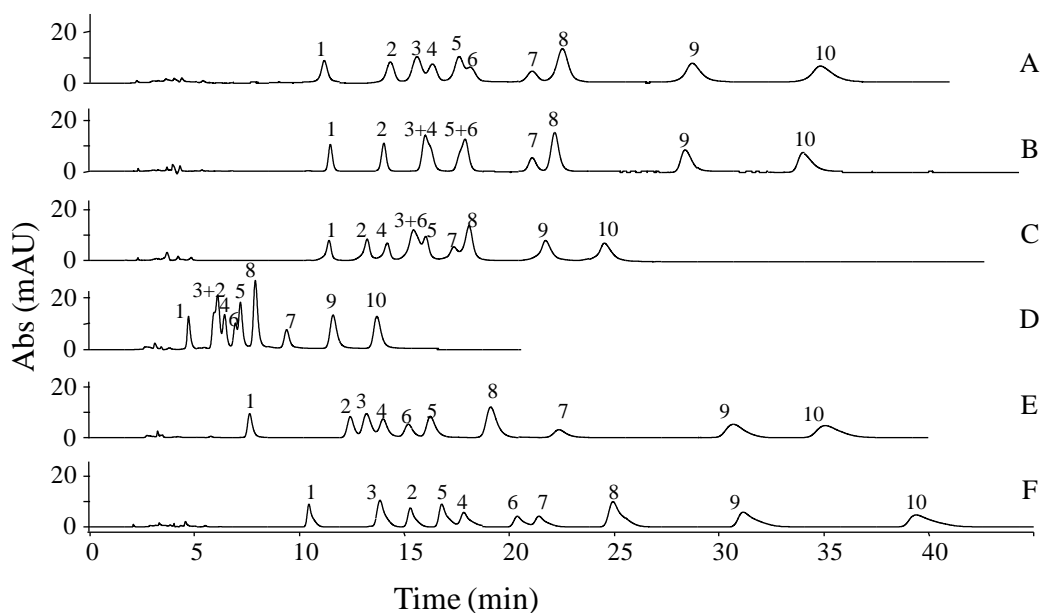
Figure 3-6 Separation of β-blockers on five HILIC columns. A, B, C, F are optimized chromatograms, on the H-ZI, the L-ZI, the EC-ZI, and the SiO_2 with a mobile phase of acetonitrile/20 mM ammonium acetate, pH = 4.1, 87/13 (*v/v*); D is the chromatogram on the ZIC-HILIC with a mobile phase of acetonitrile/20 mM ammonium acetate, pH = 4.1, 87/13 (*v/v*); E is the optimized chromatogram on the ZIC-HILIC with a mobile phase of acetonitrile/20 mM ammonium acetate, pH = 4.1, 92/8 (*v/v*). Flow rate: 1.0 mL/min; UV detection at 254 nm. Compounds: 1. Carvedilol; 2. Alprenolol; 3. Labetalol; 4. Esmolol; 5. Pindolol; 6. Metoprolol 7. Sotalol; 8. Acebutolol; 9. Nadolol; 10. Atenolol.
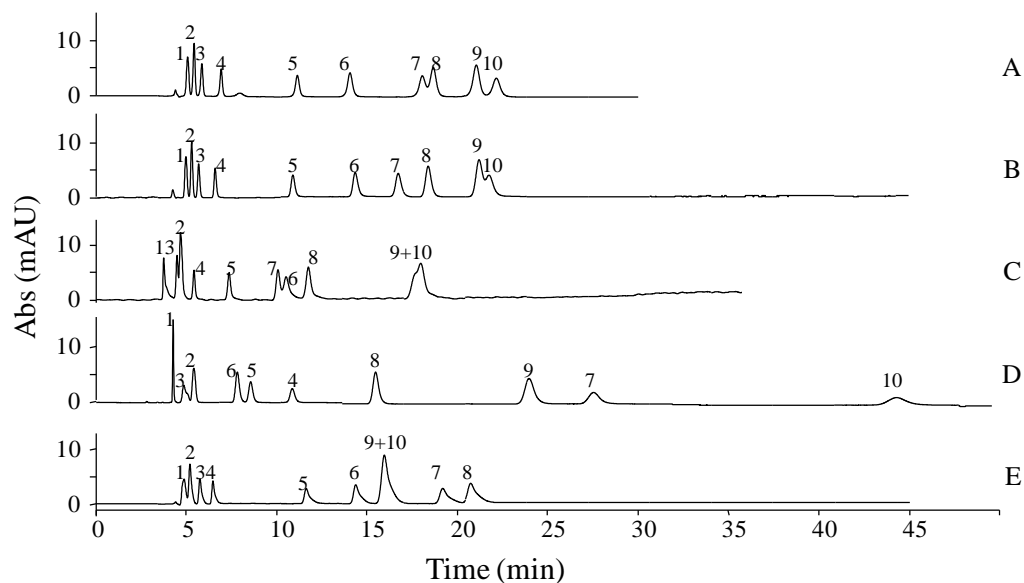
Figure 3-7 Separation of nucleic acid bases and nucleosides on five columns. A, B, C, D,

E are optimized chromatograms on the H-ZI, the L-ZI, the EC-ZI, the ZIC-HILIC and the

SiO$_2$ with a mobile phase of acetonitrile/20 mM ammonium acetate, pH = 4.1, 92/8 (*v/v*).

Flow rate: 1.0 mL/min; UV detection: 254 nm. Compounds: 1. Thymine; 2. Uracil; 3.

Thymidine; 4. Uridine; 5. Adenosine; 6. Adenine; 7. Cytidine; 8.Cytosine; 9. Guanine; 10.

Guanosine.
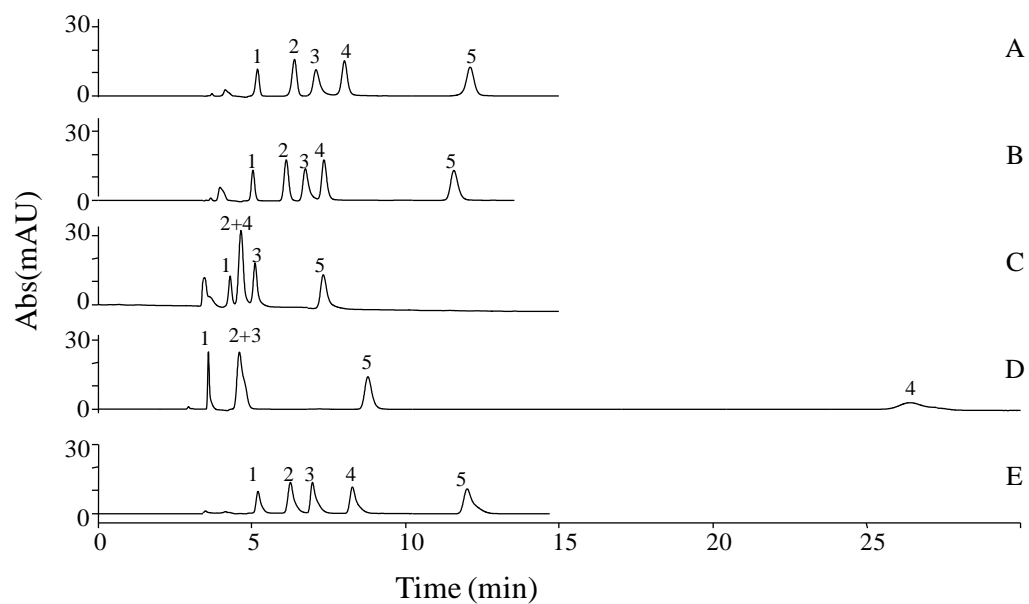
Figure 3-8 Separation of water soluble vitamins on five HILIC columns. A, B, C, D, E are optimized chromatograms on the H-ZI, the L-ZI, the EC-ZI, the ZIC-HILIC and the SiO$_2$ with a mobile phase of acetonitrile/40 mM ammonium acetate, pH = 4.1, 85/15 (*v/v*). Flow rate: 1.0 mL/min; UV detection at 254 nm. Compounds: 1. Nicotiamide; 2. Riboflavin; 3. Pyridoxin; 4. Ascorbic acid; 5. Nicotinic acid.
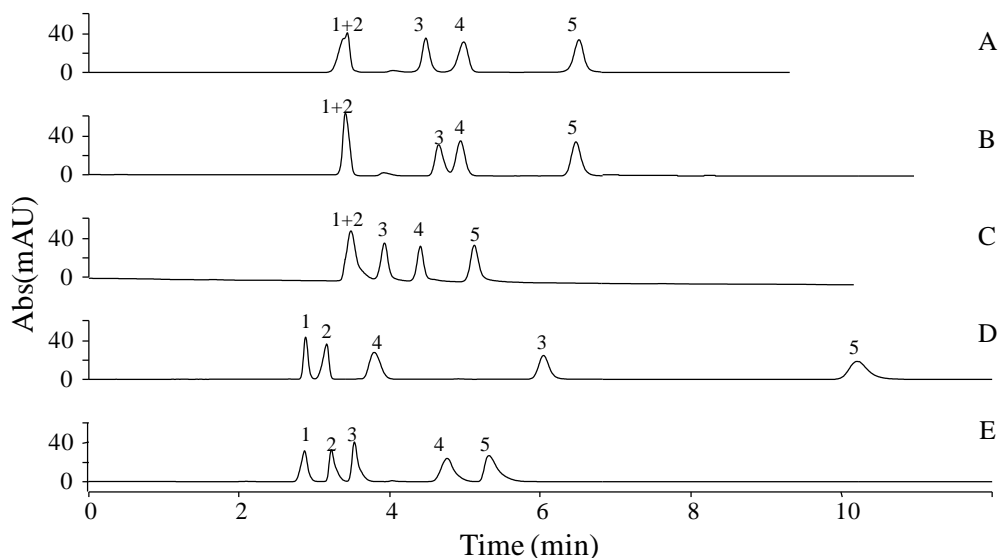
Figure 3-9 Separation of salicylic acid and its analogues on five HILIC columns. A, B, C, D, E are optimized chromatograms on the H-ZI, the L-ZI, the EC-ZI, the ZIC-HILIC and the SiO$_2$ with a mobile phase of acetonitrile/20 mM ammonium acetate, pH = 4.1, 85/15 (*v/v*). Flow rate: 1.0 mL/min; UV detection at 254 nm. Compounds: 1. Salicylamide 2. Salicylic acid; 3. Acetylsalicylic acid; 4. 4-Aminosalicylic acid; 5. 3,4-Dihydroxyphenylacetic acid.

3.3.2 A comparison of the HILIC mode separations on the H-ZI and the ZIC-HILIC columns

The ZIC-HILIC column is functionalized with a sulfopropylbetaine ligand (Figure 3-1) that overall confers a high capability of binding to water and various electrostatic interactions, but a low contribution of hydrogen bonding interactions [86]. The HILIC mode separations on the ZIC-HILIC and the H-ZI columns were initially compared using the optimized mobile phase on the H-ZI column. For a fair comparison, the mobile phase was then optimized on the ZIC-HILIC column as well. The H-ZI column shows its

56

potential in the HILIC mode separations, especially in the separations of β-blockers, nucleic acid bases, nucleosides and water soluble vitamins (analyte structures are shown in Figures 3-2~3-4, chromatograms shown in Figures 3-6~3-8). In the case of the separation of β-blockers, the H-ZI column not only provided greater retention but also offered better selectivities and resolutions (Figure 3-6) under its optimized mobile phase condition. With the exception of 2 pairs of partially separated analytes (labetalol/esmolol and pindolol/metoprolol), all adjacent peaks were baseline separated on the H-ZI with an analysis time of 40 min. Using the same mobile phase, the ZIC-HILIC column produced partial separation for alprennolol/labetalol/esmolol and metoprolol/pindolol with the analysis time of 20 min. While the ZIC-HILIC column gave greater selectivity values for partial separation of alprenolol/labetalol/esmolol and baseline separation for other β-blockers with its optimized mobile phase, also shown in Figure 3-6. The nucleic acid bases and nucleosides (Figure 3-7) were effectively separated on both columns. The overall analysis time was about 20 min on the H-ZI column whereas it was doubled to approximately 40 min on the ZIC-HILIC. Water soluble vitamins were baseline separated with a short analysis time (12 min) on the H-ZI column (Figure 3-8), while riboflavin and pyridoxine were partially separated with an analysis time of 25 min on the ZIC-HILIC column. However, the H-ZI column did not perform as well as did the ZIC-HILIC in the separation of salicylic acid and its analogues (Figure 3-5). A baseline separation was observed on the ZIC-HILIC, while salicylamide and salicylic acid co-eluted on the H-ZI column (Figure 3-9). Interestingly, the opposite elution order of 4-aminosalicylic acid and acetylsalicylic acid was only observed on the ZIC-HILIC column compared to the H-ZI column and other tested columns. The substantially different retention profiles on the H-ZI column and the ZIC-HILIC column with the same mobile phase condition or the optimized mobile phase condition are likely due to the different cationic functionalities

(aromatic quaternary phosphonium, P^+, on the ZI columns and aliphatic quaternary ammonium, N^+, on the ZIC-HILIC column). This indicates that π-π and/or n-π interactions are more prominent on the former zwitterionic type columns.

3.3.3 A comparison of the HILIC mode separations on the H-ZI and the SiO_2 columns

The SiO_2 column has a strong capability of binding water and therefore it has potential to achieve separations in the HILIC mode. Although the SiO_2 column provided better separation for labetalol/esmolol and pindolol/metoprolol than did the H-ZI column, it did not provide as good peak efficiencies and symmetries (Figure 3-6 and Table 3-1). The H-ZI column gave better selectivity and resolutions for nucleic acid bases and nucleoside mixtures (Figure 3-7). Cytosine and cytidine were partially separated on the H-ZI column (α = 1.03, R_s = 0.9), while they co-eluted on the SiO_2 column. Additionally, the opposite elution order between cytosine/cytidine and guanine/guanosine was observed on these two columns. Similar retention and selectivity of water soluble vitamins and salicylic acid and its analogues were observed on the H-ZI and SiO_2 columns (Figures 3-8 and 3-9) but tailing peaks were always observed on the SiO_2 column. These asymmetrical peaks were obtained mainly due to strong interactions between amino or phenol groups of the analytes and silanol groups on the surface of the stationary phase. The H-ZI column overcomes the drawback of peak tailing while maintaining high selectivity for the separation of polar compounds.

3.3.4 Nature and amount of organic modifier

The effect of the organic modifier in the mobile phase was examined by monitoring the separation of β-blockers on the H-ZI column. Three protic solvents (methanol, ethanol and isopropanol) and two aprotic solvents (acetonitrile and tetrahydrofuran) were used in this investigation. Different separation profiles were obtained on the H-ZI column with different organic modifiers and a 13% by volume

aqueous component (20 mM ammonium acetate, pH=4.1) as the mobile phase (Figure 3-10). It was found that higher retention and better selectivity were obtained on the H-ZI column using the aprotic solvents. The analysis times were similar (~35 min) when using either acetonitrile or tetrahydrofuran. However, different selectivities were obtained with these two organic modifiers. When using acetonitrile, labetalol/esmolol and pindolol/metoprolol were partially separated. When using tetrahydrofuran, labetalol had a shorter retention time and was separated from esmolol, whereas esmolol/metoprolol/pindolol were partially separated and sotalol/acebutolol co-eluted on the same column. The protic modifiers, such as methanol, ethanol and isopropanol, were not appropriate organic solvents for use in the HILIC mode separations as they produced short retention and poor selectivity for β-blockers. Similar results were reported by Chung et al [94] and S. Vikingsson et al [95]. They proposed that protic solvents (e.g., methanol, ethanol, or isopropanol) form hydrogen bonds to the analytes and thereby compete with hydrophilic sites on the stationary phase leading to reduced retention. However, they also strongly associate with hydrogen bonding groups on the stationary phase including silanol groups. It should be noted that the same effect of protic solvents was reported over 20 years ago for sugar separations [7].
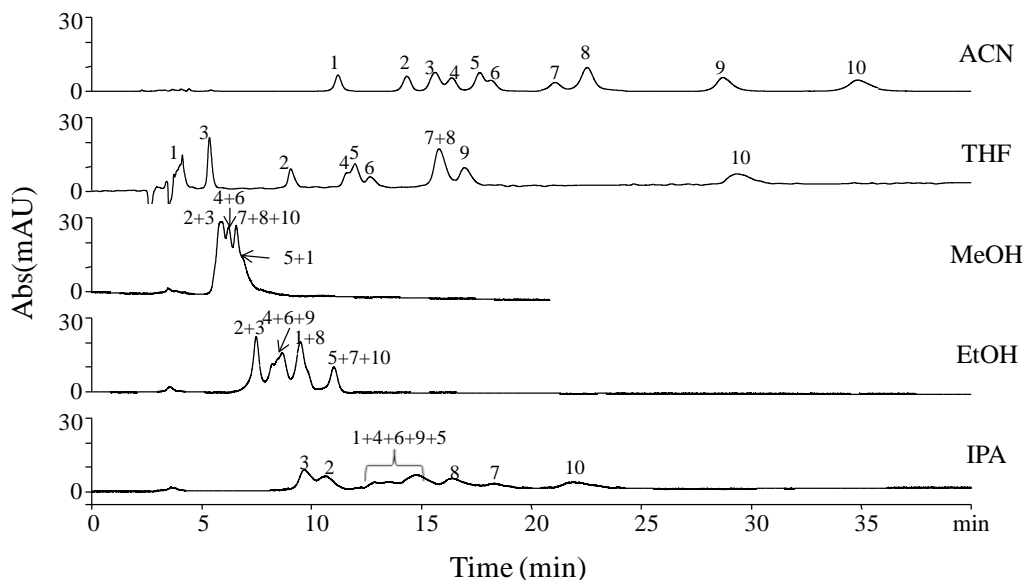
Figure 3-10 Effect of organic modifier on separation of β-blockers on the H-ZI column.

Mobile phase: various organic solvents with 20mM ammonium acetate, pH=4.1, 87/13

(*v/v*); flow rate: 1.0 mL/min; UV detection: 254 nm. Compounds: 1. Carvedilol; 2.

Labetalol; 3. Alprenolol; 4. Pindolol; 5. Esmolol; 6. Metoprolol 7. Sotalol; 8. Acebutolol; 9.

Nadolol; 10. Atenolol.

Acetonitrile is an exceptional solvent for HILIC separations, and it is miscible with

water in all proportions. Figure 3-11 shows plots of retention factors (*k*) versus the

volume fractions of acetonitrile in the mobile phase over a range of 5 – 95%.

Representative compounds include: basic (metoprolol, acebutolol, atenolol and cytosine),

acidic (nicotinic acid and 3,4-dihydroxyphenylacetic acid) and neutral (nicotiamide) types

of compounds. Their retention profiles do not show exact U-shaped curves when varying

organic composition of the mobile phase under a fixed buffer concentration and buffer pH.

These curves were much more accentuated in the organic component enriched region (>

60% acetonitrile) than in the water-rich region (< 40% acetonitrile) for the H-ZI column.

This is an indication of the HILIC mode retention behavior predominating rather than the HILIC/RPLC mixed-mode retention behavior, as described in previous reports [19, 75, 82, 95-97]. The weakest retention was observed when the acetonitrile content was about 40%. The β-blockers and nicotinic acid also show solubility limitations when using a mobile phase of acetonitrile content higher than 95% or lower than 5%. Similar patterns have been observed on a wide variety of stationary phases (including the silica column and the ZIC-HILIC column). Such curves are also in agreement with data from earlier studies involving various HILIC stationary phases with different mobile phase conditions [76, 82, 85, 98, 99].
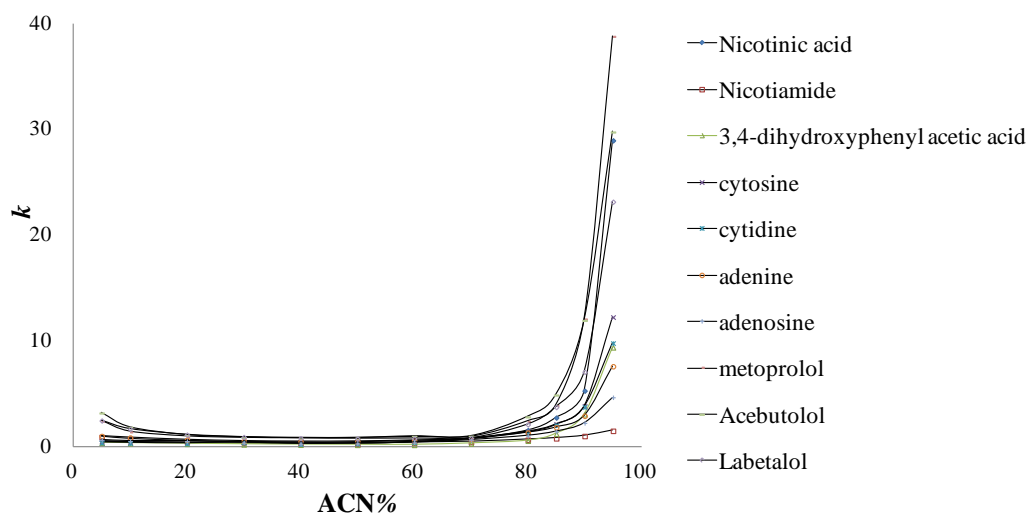
Figure 3-11 Effect of acetonitrile content on the retention (k) of tested analytes on the H-ZI column. Mobile phase: acetonitrile/20 mM ammonium acetate, pH = 4.1; flow rate: 1.0 mL/min; UV detection at 254 nm.

3.3.5 Buffer pH and buffer concentration

The pH of the mobile phase not only influences the degree of ionization of the samples but also affects many stationary phases. However the mobile phase pH does

not affect the ionization of zwitterionic groups on the stationary phase, since these functionalities are permanent charges. It is well known that both buffer pH and analyte ionization change when organic solvents are introduced to aqueous buffer solutions [100-103]. Uncharged analytes, such as nucleic acid bases and nucleosides, were virtually unaffected by pH variations on all tested columns. However there were significant impacts on the retention of charged compounds as shown in Figure 3-12. The retention of nadolol (pK_a = 9.7) and atenolol (pK_a = 9.6) increased with increasing buffer pH. This is possibly due to the stronger electrostatic attractive interactions between the basic compounds and the more negatively charged stationary phases at a higher buffer pH. The retention of acidic compounds was also affected by the buffer pH. For example, nicotinic acid shows an increase in retention as the pH of the buffer in the mobile phase increases from 3.2 to 4.1 and a slight decrease in retention in the pH region of 4.1 to 5.0. This unique retention behavior with pH results from the fact that this compound has two ionizable groups: one tertiary amine (protonated, pK_a = 3.01) and one carboxylic acid group (pK_a = 3.77). Therefore as the pH changes this molecule goes from positively charged to neutral to negatively charged.
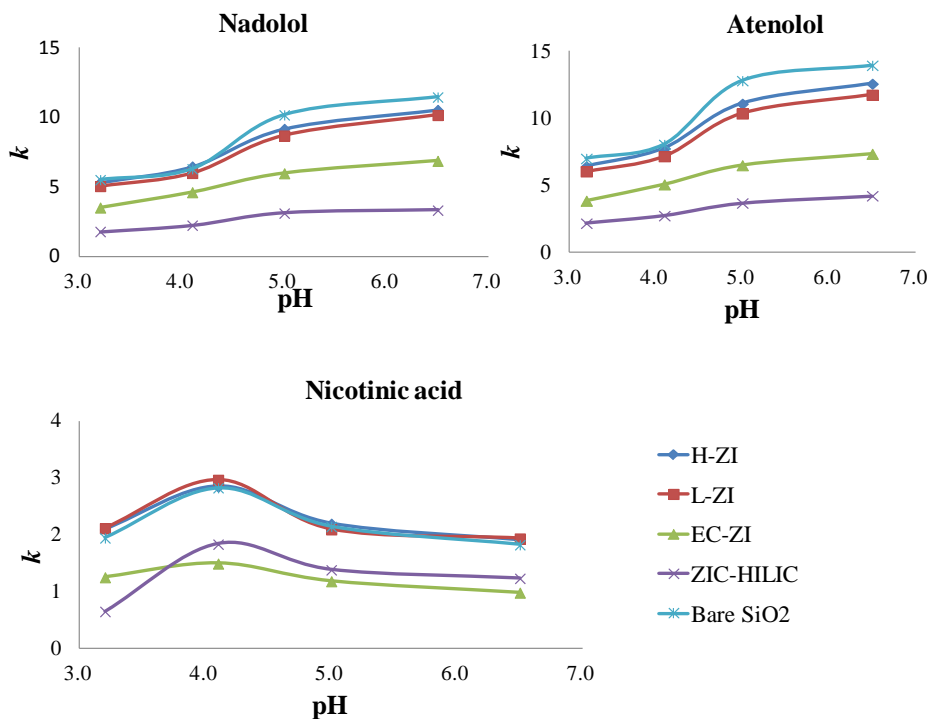
Figure 3-12 Effect of buffer pH on the retention (k) of tested analytes. Mobile phase: acetonitrile/20 mM ammonium acetate, 85/15 (*v/v*); flow rate: 1.0 mL/min; UV detection at 254 nm.

An increase in buffer concentration increases the ionic strength of the mobile phase, thereby producing differences in the retention behavior of many analytes. Figure 3-13(a) shows that the compounds (cytosine, cytidine, guanine and guanosine) were retained longer on the H-ZI column with higher buffer concentrations. Guanosine and guanine co-eluted with 5 mM ammonium acetate but were baseline separated with 100 mM ammonium acetate. For acidic compounds, the retention of nicotinic acid increased from around 8 min using 5 mM buffer to around 12 min using 40 mM buffer (Figure 3-13(b)). A similar increase in retention was observed for ascorbic acid on the H-ZI column.

Similar effects of buffer concentration for uncharged and acidic compounds have been reported on a variety of HILIC columns as well [55, 59, 75, 93, 97, 102]. Additionally, in the case of acidic compounds, the higher ionic strength could further weaken any electrostatic repulsion interactions with the overall negatively charged stationary phase [18]. However, a significant decrease in retention on the H-ZI column with an improvement in peak efficiencies was observed for nadolol and atenolol (the β-blockers representatives) when using higher buffer concentrations (Figure 3-13(c)). This trend is well known and also has been reported for basic compounds on other HILIC columns [55, 93, 104, 105]. This is likely due to the weakening of π-π and/or n-π interactions, electrostatic attractive interactions and hydrogen bonding interactions between these basic analytes and the stationary phases.
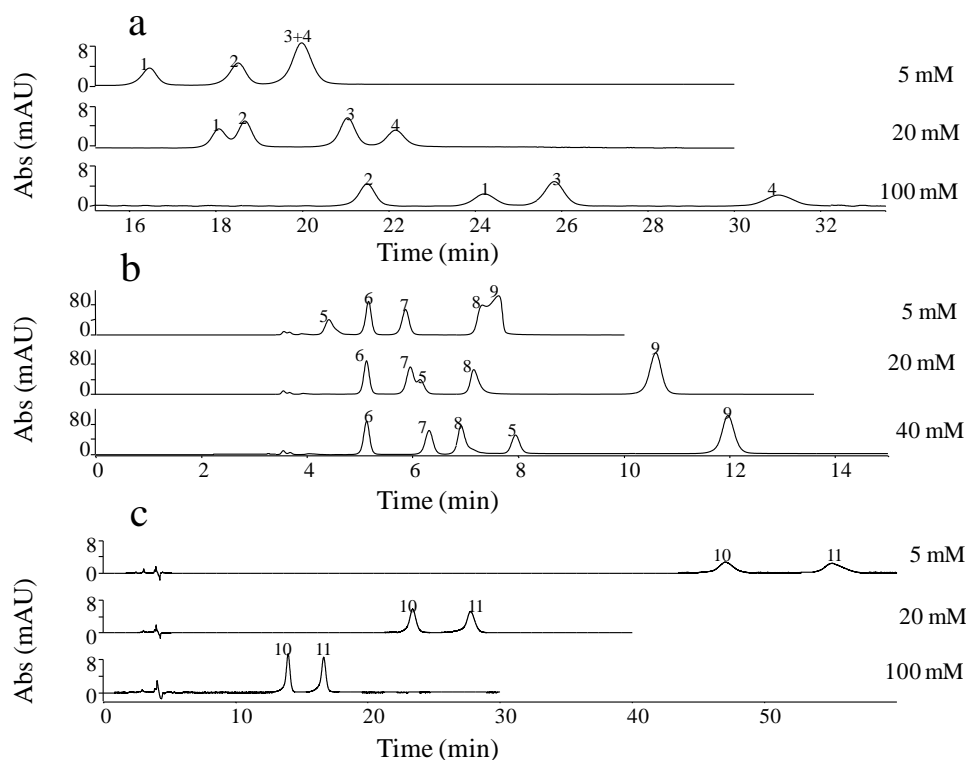
Figure 3-13 Effect of buffer concentration on the retention of the tested analytes on the H-ZI column. Flow rate: 1.0 mL/min; UV detection at 254 nm. A:1. Cytidine ; 2. Cytosine; 3. Guanine; 4. Guanosine with acetonitrile/ammonium acetate, pH = 4.1, 92/8 (*v/v*); B: 5. Ascorbic acid; 6. Nicotiamide; 7. Riboflavin; 8. Pyridoxine; 9. Nicotinic acid with acetonitrile/ammonium acetate, pH = 4.1, 85/15 (*v/v*); C: 10. Nadolol. 11. Atenolol with acetonitrile/ammonium acetate, pH = 4.1, 85/15 (*v/v*).

3.4 Conclusions

New zwitterionic stationary phases have been successfully synthesized and show excellent capabilities in separating a variety of polar analytes. After a comparison of surface coverage and the effect of end-capping, it appears that the H-ZI column (higher coverage and without end-capping) had the best separation capabilities among ZI series

column. The H-ZI column also shows advantages over popular commercial stationary phases (the ZIC-HILIC and SiO2 columns) for many HILIC separations (β-blockers, nucleic acid bases and nucleosides and water soluble vitamins). The retention behavior in the HILIC mode was investigated by varying factors such as the organic modifier, the mobile phase composition, the buffer concentration and the buffer pH. It was confirmed that aprotic solvents are the preferred organic modifiers in HILIC separations, such as acetonitrile. In the organic-rich region (>60% acetonitrile), the HILIC mode retention behavior predominated on the ZI columns. There is an obvious influence of buffer pH on charged analytes but slight influence on neutral analytes. It was also found that an increasing buffer concentration increases retention of neutral and acidic compounds but decreases retention of basic compounds.

Acknowledgements

Chapter 4

Thermodynamic studies of a zwitterionic stationary phase

in hydrophilic interaction liquid chromatography

Abstract

A zwitterionic 3-P,P-diphenylphosphonium-propylsulfate stationary phase called HZI was synthesized for hydrophilic interaction liquid chromatography (HILIC). A set of fifteen solutes including apolar aromatic compounds, positively charged β-blockers, polar nucleic acid bases, nucleosides and negatively charged compounds was used to prepare van't Hoff plots between 10 and 70 ^{o}C with HILIC mobile phases containing between 10 and 20% 20 mM or 50 mM ammonium acetate buffer (pH = 4.1) in acetonitrile. The unique π-π interaction capability of the HZI phase is evidenced by the low but significant retention of the apolar aromatic compounds in the HILIC mode as well as by the strong retention of the aromatic containing β-blockers. The linear van't Hoff plots gave the ΔH^o and ΔS^o thermodynamic changes of the solute transfer from the mobile to the stationary phase. Plotting the ΔH^o values versus the corresponding ΔS^o ones produced a line excluding the three apolar aromatic solutes and a negatively charged compound. The excluded compounds corresponded to curved van't Hoff plots. If the non-linearity of van't Hoff plots is classically explained by changes in solute transfer interactions, we showed that it could also be explained by a temperature induced change in the hydrated stationary phase volume seen by the solutes.

4.1 Introduction

The use of polar stationary phases in combination with hydro-organic mobile phases containing high percentages of an organic modifier that is a relatively poor

hydrogen bonding solvent (e.g. acetonitrile, tetrahydrofuran or acetone) has been used for over 30 years to separate polar analytes [6-8, 21, 49-52, 106-109]. Today, these chromatographic approaches are most commonly referred to as hydrophilic interaction liquid chromatography (HILIC), a term introduced by Alpert in 1990 [9]. HILIC is one of the faster growing chromatographic modes due to its convenient practical features: HILIC does not need to change the chromatographic system; it simply needs the proper column-solvent combination [3, 4, 110, 111]. Although HILIC is considered as an alternative to reversed phase LC for polar solutes, it is mechanistically closer to normal phase LC. The mobile phase composition is most often made by acetonitrile, a polar aprotic solvent, with small percentages (less than 40%) of water. The HILIC stationary phase must be polar or even charged (ionic or zwitterionic bonded moieties). Originally, it was proposed that the high acetonitrile content accentuated H-bonding between the polar stationary phase and analytes (*i.e.* carbohydrates or amino-acids [7, 8, 21]).

Subsequently it was proposed that, after equilibrium, a very polar water rich layer is formed at the polar stationary phase surface. A partitioning mechanism of polar solutes may occur between the bulk mobile phase and the water-enriched layer of the HILIC stationary phase. The mobile phase water content allows for the fine tuning of the HILIC separations on an opposite way compared to RPLC: the mobile phase with less water produces higher solute retentions [9, 55]. This simplistic mechanism was recently challenged as it appears that different possible interactions are possible depending on the stationary phase functional groups [3, 4, 111, 112].

The increasing use of HILIC spurred the development of a large number of different stationary phases with polar, ionic or zwitterionic bonded groups [3, 20, 75, 113, 114]. Recently we proposed a diphenyl phosphonium-propylsulfonate zwitterionic stationary phase for HILIC separation that we called HZI [115]. This original HZI HILIC

68

phase bears permanent charges closely associated to aromatic rings. Comparing the separation capabilities of this new zwitterionic HILIC stationary phases to a bare silica column and a commercial ZIC-HILIC column, differences were observed in solute retention and peak efficiency working with a set of aromatic polar as well as apolar solutes [115]. These results provided the impetus for us to make a full thermodynamic study to examine solute interactions with the HZI zwitterionic stationary phase in order to obtain insights on retention mechanisms. Van't Hoff plots were established using the same set of solutes with different acetonitrile-buffer mobile phases containing between 10 and 20% v/v buffer. Two levels of buffer salt (ammonium acetate) were also used to investigate ionic strength effects.

4.2 Experimental

4.2.1. The zwitterionic 3-P,P-diphenylphosphonium-propylsulfate stationary phase

The stationary phase was synthesized bonding ethyl-3-P,P'-diphenylphosphonium-propylsulfate triethoxy silane on Daiso silica (Supelco-Sigma-Aldrich, Bellefonte, PA), a 5 μm spherical silica with 10 nm (100 Å) pore size and 440 m^2/g surface area following the procedure extensively described [115]. Table 4-1 lists the full characteristics of the HZI HILIC zwitterionic stationary phase whose 1.95 g were packed into a 25x0.46 cm column. The hold-up volume, V_m, was taken as the first detector deviation observed (refractive index changes) on sample solvent injections. The stationary phase volume was estimated using a known method [116] with a bonded surface area of 650 m^2 inside the 25 cm column and a thickness of the bonded layer of 0.9 nm giving an estimated 0.6 cm^3 or mL for the V_s volume of the bonded moieties (Table 4-1).
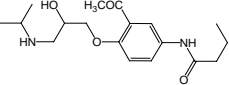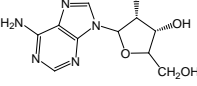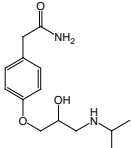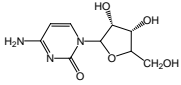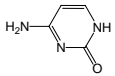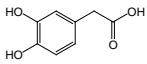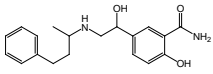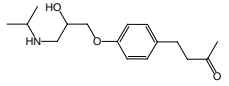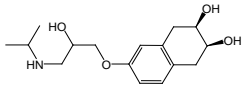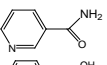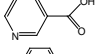
Table 4-1 Physico chemical characteristics of the zwitterionic HILIC stationary phase and

packed HZI column.

Structure	Parameter	value	unit
	Base material	DaisoGel Silica	SP-100-5-P
	Particle shape	Spherical	-
	Particle diameter	5	μm
	Pore size	10	nm
	Pore volume	1.1	mL/g
	Surface area (bare)	440	m^2/g
	Surface area (bonded)	330	m^2/g
	Particle size distribution	<1.25	D40/D90
	Bonded m.w.	411	Dalton
	Bonded C percentage	12	%
	Bonded density	1.75	$\mu mol/m^2$
	Column length	25	cm
	Column diameter	4.6	mm
	Packed silica mass	1.95	g
	Packed moles	1.13	millimoles
	Estimated V_S	0.6	mL
	Hold-up volume V_m	2.9	mL
	Phase ratio Φ	0.2	-

4.2.2. Chemicals

Acetonitrile (ACN), ammonium acetate and all test solutes were obtained from Sigma Aldrich (Saint Louis, MO). Water was purified by a Milli-Q-water purification system (Millipore, Billerica, MA). Table 4-2 gives the structure and properties of the 15 test solutes that include β-blockers, nucleic acid bases and nucleosides, polar vitamins and apolar aromatic compounds. The three aromatic compounds are not ionizable. Two acid compounds were negatively charged at the mobile phase pH 4.1. The ten remaining compounds were bases positively charged at pH 4.1 (Table 4-2). The listed octanol/water calculated coefficients corresponds to the molecular form of each compound. They give an idea of relative hydrophobicity.

Table 4-2 Test solutes used in the thermodynamic studies with the HZI column

Code	Compound	Structure	m.w.	pK_a	pH 4.1 charge	Log $P_{o/w}$
1	Acebutolol		336	9.4	+	1.7
2	Adenine		135	3.2; 5.4; 10	+	-0.1
3	Adenosine		267	2.7; 5.2	+	-1.1
4	Atenolol		266	9.6	+	0.16
5	Benzene		78	n.i.	0	2.13
6	Cytidine		243	4.2; 12.5	+	-2.2
7	Cytosine		111	4.8; 10	+	-1.0
8	Dopac		168	4.2	-	1.0
9	Labetalol		328	7.3; 9.4	+	2.7
10	Metoprolol		267	9.4	+	1.6
11	Nadolol		309	9.6	+	1.2
12	Nicotinamide		122	3.3	+	-0.35
13	Nicotinic acid		123	4.8	-	0.36
14	Toluene		92	n.i.	0	2.73
15	Xylene		106	n.i.	0	3.16

Dopac is 3,4-dihydroxyphenyl acetic acid.
n.i.: non ionizable.
pK_a: acid dissociation constant in pure water at 20°C.
Log $P_{o/w}$ calculated by the KOWWIN™ software for the molecular form of the compound.

4.2.3. Chromatographic conditions

An Agilent HPLC series 1200 system (Agilent Technologies, Palo Alto, CA) equipped with a quaternary pump, autosampler, column oven and multiwavelength UV detector was used for all HILIC studies. The injection volume was set at 5 μL and the mobile phase flow rate was always 1 mL/min. The van t'Hoff plot were obtained within the 10-70 ^{o}C temperature range with the HZI column described in Table 4-1 and Ref. [115].

Mobile phases were prepared mixing the desired amount of pH 4.1 ammonium acetate buffer at 20 mM or 50 mM to pure acetonitrile. The buffer pH was adjusted to exactly 4.1 by pure acetic acid additions. An ultrasonic bath was used to degas the mobile phases for 5 min just after mixing ACN and buffer.

4.3 Results and Discussion

4.3.1. Solute retention: HILIC versus RPLC

Alpert postulated that hydrophilic interaction chromatography involves partitioning of polar analytes between the hydrated stationary phase and the bulk mobile phase [9]. Acetonitrile is a polar non hydrogen bond donor solvent appropriate to promote the HILIC mode when methanol, a polar and H-bond capable solvent is much less effective. On the whole 0-100% water content in ACN, the HILIC domain corresponds to the low 0-20% side and the RPLC domain is the water-rich side (40-100% *v/v*).
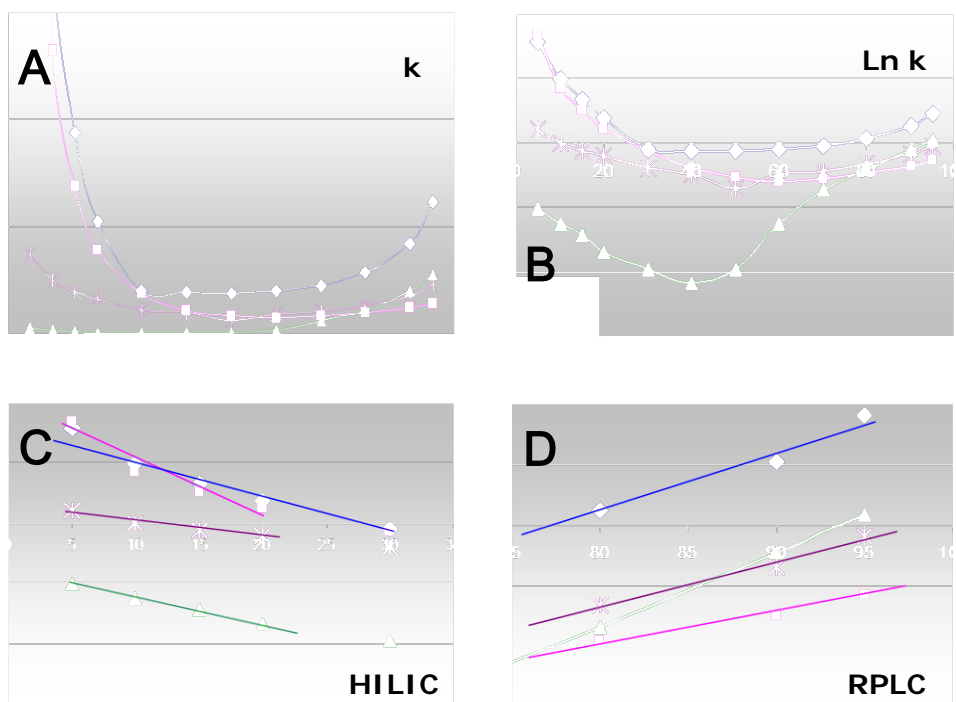
Figure 4-1 Retention factors of three polar analytes and xylene on the HZI 25 x 0.46 cm column. A). k versus the mobile phase buffer content; B). ln k versus buffer percentage; C). enlargement of the HILIC side (5-30% buffer *v/v*); D). enlargement of the RPLC side. Mobile phase: ACN-20 mM ammonium acetate buffer at pH 4.1, 20 ^{o}C, flow rate 1 mL/min, detection UV 254 nm.

U-shaped curves are obtained when plotting solute retention factors versus the water content over the 0-100% range. Figure 4-1 illustrates this point showing the retention factors of four solutes versus the mobile phase 5-95% water content. The same set of data is shown in a k versus water content scale (Figure 4-1A) and a ln k versus water volume fraction (Figure 4-1B). Figure 4-1C is an enlargement showing the HILIC

side (water content between 5 and 30% *v/v*) with the ln k versus water content lines showing negative slopes: the solute retention factors decrease when the mobile phase water content increases. Figure 1D shows the RPLC side with water volume fraction between 75 and 95%. There, the analytes with ln k versus water content lines have positive slopes: the solute retention factors increase when the mobile phase water content increases.

Figure 4-1 also shows that the most hydrophobic solute of the set (xylene, log P = 3.16, Table 4-1) is retained in HILIC mode even if it is the first eluting solute with the smallest retention factor (k = 0.12 in ACN/buffer 95/5 *v/v*; Figure 4-1C). Xylene was selected as a completely unretained void volume marker in HILIC mode [108]. If some retention is observed with the HZI stationary phase, it means that some π-π interaction can take place between the aromatic rings of the bonded zwitterionic group and that of xylene (Table 4-1). This interaction increases somewhat when there is less water hydrating the adjacent phosphonium positively charged group. The xylene k factor increases rapidly in the RPLC mode when more than 60% water is present in the mobile phase (k = 1.1 in ACN/buffer 5/95 *v/v*; Figure 4-1D). The π-π interactions become far less significant with the appearance and dominance of the classical hydrophobic effect.

When the mobile phase contained between 10 and 30% buffer volume fractions (HILIC mode), the positively charged β-blockers were systematically the most retained compounds of the set in all mobile phase conditions and temperatures (Figure 4-2). The three aromatic apolar compounds were logically, in the HILIC mode, the first eluting compounds always in the order xylene first, toluene and benzene last within seconds. They had to be injected individually in triplicate to obtain accurate retention data. The observed selectivity for the nucleosides, nucleic acid bases and polar vitamins were composition as well as temperature dependent. For example, Figure 4-2, left, shows that

3,4-dihydroxy phenylacetic acid also called dopac (Compound #8) eluted just after adenine (Compound #2) at 10 ^{o}C with the ACN-20 mM buffer 90/10 *v/v* mobile phase. At 70 ^{o}C, dopac (#8) elutes well before adenine (#2; Figure 4-2 left). The two compounds elute together between 40 and 50 ^{o}C.
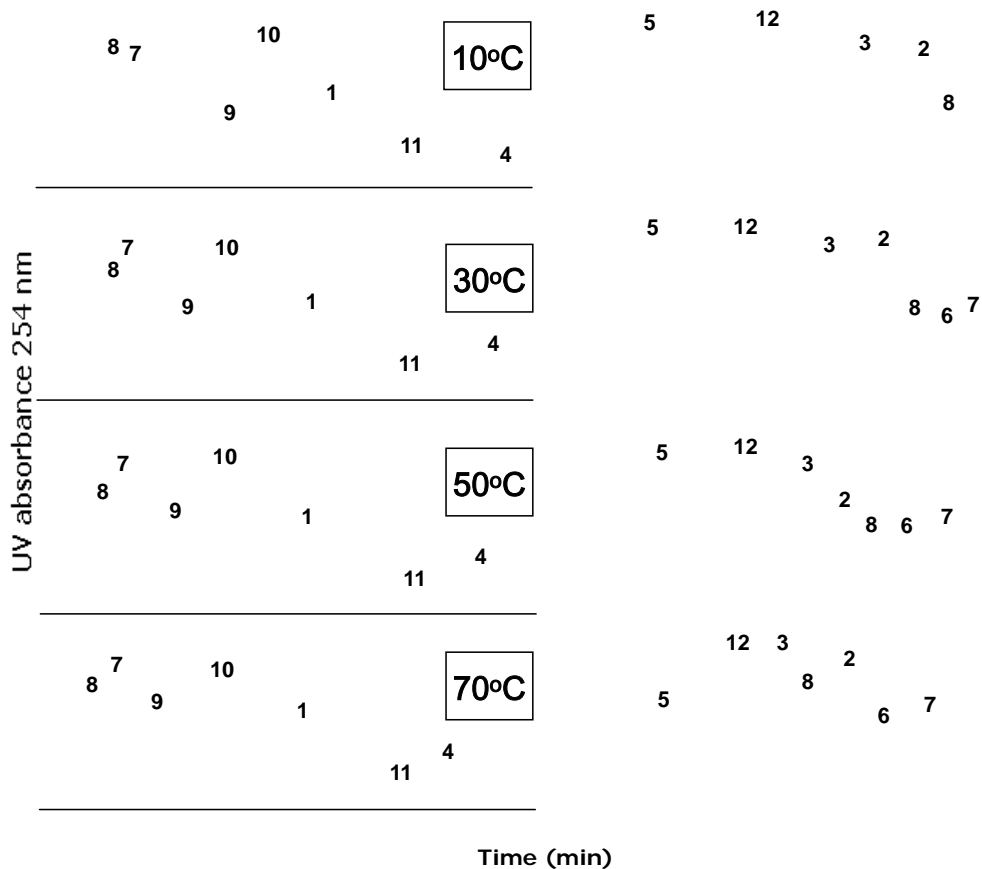
Figure 4-2 Effect of temperature on test solute retention obtained with the 90/10 ACN-20 mM ammonium acetate buffer mobile phase at 1 mL/min on the HZI column (25 x 0.46 cm). Compound code is listed in Table 4-2. Left chromatograms: Long retained β-blockers (Peaks #1, 4, 9, 10 and 11). Right chromatograms: Nucleosides and nucleic acids (Peaks #2, 3, 6 and 7), dopac (Peak #8), nicotinamide (Peak #12) and benzene (Peak #5).

4.3.2. Effect of temperature on retention: van't Hoff plots

Temperature changes have a significant impact on solute selectivity because they modify mobile phase viscosity, solute diffusion coefficients and the solute-stationary phase interactions. The main reason for studying the relationship between solute retention factors and temperature was to gain insights into retention mechanisms involved between solutes of different properties and zwitterionic stationary phases used in the HILIC mode [3, 4, 85, 110, 111, 115].

Mobile phase temperature, T, and solute retention factors, k, are related by the van't Hoff equation:

$$\ln k = -\frac{\Delta H^o}{RT} + \frac{\Delta S^o}{R} + \ln \emptyset \tag{1}$$

where ΔH^o and ΔS^o are respectively the enthalpy and entropy change corresponding to the chemical exchange of the solute going from the mobile phase to the stationary phase; R is the gas constant (=8.314 J K^{-1} mol^{-1}) and Φ is the phase ratio V_S/V_m.

Figure 4-3 shows the van't Hoff plots of the Table 4-2 solutes for the 85/15 % *v/v* ACN-buffer 20 mM mobile phase. The same trend was observed for different HILIC mobile phases: most of the solutes gave linear plots with positive slopes. The most retained β-blockers were not sensitive to temperature changes (Figure 4-2, left) producing relatively "flat" van't Hoff plots or with very slightly negative slopes (Figure 4-3, left). Some solutes, namely labetalol (#9), dopac (#8), and the three apolar aromatic compounds benzene (#5), toluene (#14) and xylene (#15), gave curved plots (Figure 4-3, right).

| 70 | 60 | 50 | 40 | 30 | | 70 | 60 | 50 | 40 | 30 |

dopac

(K^{-1})

(K^{-1})
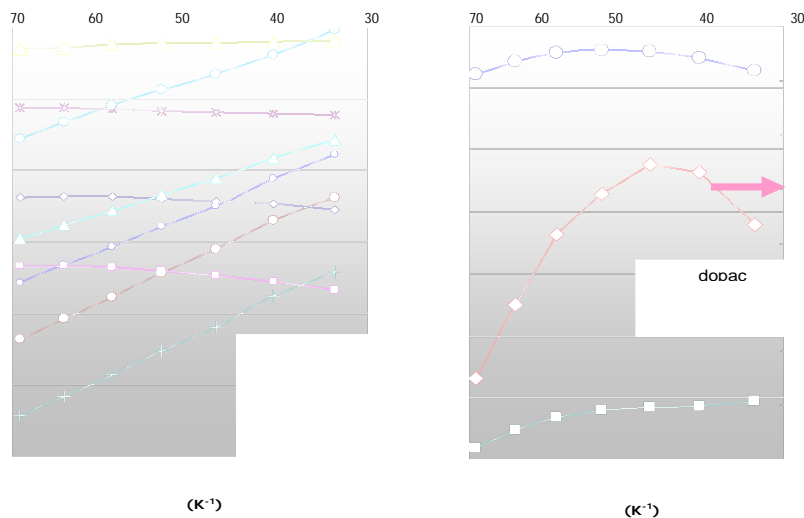
Figure 4-3 Van't Hoff plots of the Table 2 test solutes on the HZI column and a mobile phase ACN/20 mM ammonium acetate buffer 85/15 *v/v* between 10 and 70 ^{o}C. Left diagrams: linear plots with a positive slope for cytosine (#7), adenine (#2), adenosine (#3), cytidine (#6), and nicotinic acid (#13) (left 0-1.2 scale) and a horizontal or slightly negative slope for nadolol (#11), acebutolol (#1), metoprolol (#10) and atenolol (#4) (right 1.2-2.2 scale). Right diagrams: curved plots for dopac (#8) and labetalol (#9) (left 0-1.4 scale) and benzene (#5) (right -2.7- -2.3 scale).

4.3.3. Thermodynamic data

Eq. 1 indicates that the slope of a linear van't Hoff plot gives the corresponding solute enthalpy change, ΔH^{o}, of the solute transfer from the mobile phase to the stationary phase. If the column phase ratio, Φ, is known, the intercept of the plot gives the solute transfer entropic variation, ΔS^{o}. Table 4-3 lists a selection of these data obtained for different HILIC mobile phases containing between 10 and 20% of 20 mM or 50 mM ammonium acetate buffer in acetonitrile (temperature range: 10-70 ^{o}C) (full data available upon request). Figure 4-4 (top) shows the enthalpy results versus the buffer

volume fraction in the 20 mM HILIC mobile phase. Figure 4-4 (bottom) is the ΔH^o versus ΔS^o plot for three HILIC mobile phase compositions.
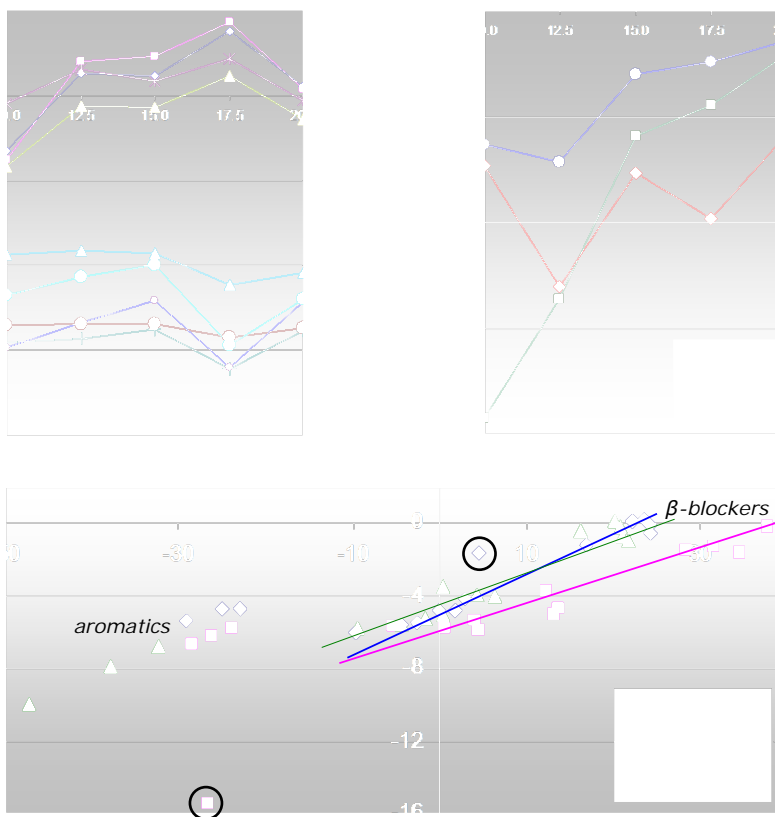
Figure 4-4 Top: Enthalpy variation plotted versus the 20 mM HILIC mobile phase water content for the Figure 4-3 solutes. Bottom: ΔH^o plotted versus ΔS^o for the Table 4-2 solutes for three mobile phase compositions. The aromatic and β-blocker compounds are located on both sides of the plots. The circled outsider is dopac compound #8 (not an outsider with 50 mM mobile phase). Mobile phase: ACN with indicated ammonium acetate and concentration volume fraction, flow rate 1 mL/min. Column zwitterionic HZI 25 x 0.46 cm.

Table 4-3 Enthalpy and entropy changes for the HILIC mobile phase containing 20 mM ammonium acetate – HZI stationary phase solute transfer.

	Enthalpy variation ΔH (kJ/mol)												
water %	Acebutolol	Adenine	Adenosine	Atenolol	Cytidine	Cytosine	Dopac	Metoprolol	Nadolol	Nicotineamide	Nicotinic acid	Labetalol	benzene*
20	0.2036	-5.481	-5.521	-0.554	-4.840	-4.169	-1.658	0.142	-0.132	-5.977	-4.803	-1.129	-4.663
17.5	1.4993	-5.686	-6.427	0.459	-6.400	-4.439	-3.534	1.728	0.866	-5.999	-5.858	-1.936	-7.854
15	0.4696	-5.391	-5.505	-0.272	-4.836	-3.720	-4.709	0.927	0.324	-5.884	-3.981	-2.406	-6.146
12.5	0.504	-5.389	-5.719	-0.251	-5.333	-3.659	-10.91	0.809	0.621	-6.087	-4.270	-5.699	-10.42
10	-1.301	-5.407	-5.802	-1.661	-5.939	-3.729	-15.45	-1.519	-0.179	-5.679	-4.686	-5.065	-5.844
17.5 50 mM	-0.1641	-5.211	-5.601	-0.994	-5.022	-3.957	-3.474	0.134	-0.697	-5.846	-4.016	-0.441	-6.811

	Entropy variation ΔS (J/mol K)												
water %	Acebutolol	Adenine	Adenosine	Atenolol	Cytidine	Cytosine	Dopac	Metoprolol	Nadolol	Nicotineamide	Nicotinic acid	Labetalol	benzene*
20	23.47	-2.571	-4.408	24.31	-0.148	2.929	4.47	22.05	24.22	-9.673	1.695	16.92	-22.96
17.5	29.26	-2.672	-6.367	29.47	-3.502	3.293	0.330	28.73	29.22	-9.541	0.256	15.68	-33.5
15	29.16	0.408	-1.748	30.41	3.302	7.585	-0.025	28.92	30.78	-7.913	9.183	16.77	-26.35
12.5	32.37	1.208	-1.629	33.78	3.194	9.321	-17.38	31.39	34.93	-8.229	10.67	8.33	-40.49
10	31.44	4.143	0.647	34.49	4.406	12.34	-26.68	28.24	37.77	-5.258	13.66	13.20	-23.98
17.5 50 mM	20.71	-1.749	-4.348	21.64	0.409	4.211	0.382	20.17	20.92	-9.384	6.368	16.23	-32.28

The toluene and xylene data are not listed being very close to the benzene data. Their representative points are plotted in Figure 4-4.

The first observation is the clear difference in thermodynamic behavior of the three aromatic compounds: benzene, toluene and xylene. They all three clearly stand apart from the rest of the Table 4-2 compound set (Figure 4-4, bottom) with a large negative ΔS^o term listed in Table 4-3 for benzene between -23 J/mol K for the 20% water rich HILIC mobile phase down to -40.5 J/mol K with only 12.5% water. The corresponding ΔH^o enthalpy change is between -4.7 and -10.4 kJ/mol for benzene. This indicates an entropy driven mechanism: the enthalpic retention contribution (first tern of eq. 1) is completely cancelled by the entropic term (second term of eq. 1). Similar thermodynamic values were obtained for toluene and xylene (Figure 4-4 bottom). It is pointed out that the aromatic retention factors are very small with all 10-20% HILIC mobile phases (between k = 0.11 for xylene with 10% buffer and 0.03 with 20% buffer) showing a relative error as large as 30% and that these three compounds always produced curved van't Hoff plots (Figure 4-3, right). However, the entropy driven weak retention of the aromatic compounds can be explained by π-π interaction between these aromatic compounds and the HZI aromatic rings. Such interaction would induce a solute arrangement onto the stationary phase that would produce decreased entropy.

The second class of compounds standing out is the β-blockers: they are both the most retained compounds by the HZI stationary phase and the least sensitive to temperature changes (Figure 4-3, left). Some of them even show sometimes a slight increase in retention with the increase in temperature (*e.g.* metoprolol and acebutolol). This behavior is due to a very little enthalpy terms reaching small positive values in some cases as seen in Table 4-3. The β-blockers ΔH^o values are between 0.142 kJ/mol for metoprolol and -0.554 kJ/mol for atenolol in the HILIC mobile phase containing acetonitrile and 20% of 20 mM ammonium acetate. Labetalol returned curved plots and is set apart to be studied especially. As evidenced by eq. 1, a small or nil ΔH^o value in its

forst term cancels the temperature dependence of ln k. The β-blockers are positively

charged at the mobile phase pH 4.1. They showed the highest retention at all

temperatures and buffer contents with the HZI column [115]. They have opposite

thermodynamic parameters compared to those of aromatic compounds: a large positive

entropy variation is associated to a weak enthalpy change. The small ΔH^o were

responsible for the observed almost flat van't Hoff plots (Figure 4-3, left). The β-blocker

retention factors are essentially due to the positive entropic term (eq. 1, Figure 4-2, left

and Table 4-3). The strong entropy increase when β-blockers interact with the HZI

stationary phase suggests a multi-mode interaction. The cationic character of this class of

compounds will produce strong charge-charge interaction with the positive (repulsion)

and negative (attraction) centers of the HZI bonded ligand. The presence of an aromatic

ring and several hydroxyl groups on all β-blockers adds π-π and H-bond interactions

increasing the solute affinity for the HZI stationary phase. Labetalol stands somewhat

apart with a small but significant enthalpy term (-1.129 kJ/mol with 20% 20 mM buffer,

Table 4-3) associated to a positive entropy term smaller than that of the other β-blockers

tested. It is interesting to note that labetalol is the only β-blocker with two aromatic rings

which may enhance the π-π interactions explaining the small but significant difference

with the other β-blockers. A recent study did not find any pronounced effects from π-π

interactions comparing 22 polar HILIC stationary phases including several zwitterionic

ones but none with two aromatic rings on a charged atom. It did find a strong effect of

charge-charge interactions [112].

For all other compounds, on the temperature range tested, the thermodynamic

study (Table 4-3) returned a positive contribution on solute retention of the enthalpy term,

ΔH^o, that is stronger that the negative contribution of the $T\Delta S^o$ entropic term. This

indicates a classical enthalpy driven retention mechanism not calling for any more

comments. The changes in retention induced by increasing the buffer concentration were already described: decrease of positively charged β-blockers solute retention and minor effects on pyrimidine solutes [115].

The ΔH^o values were plotted versus the corresponding ΔS^o values (Table 4-3 and Figure 4-4, bottom). Setting apart the three apolar aromatic compounds, a relatively acceptable alignment is observed for the Table 4-2 compounds (Figure 4-4, bottom). The regression coefficients of the ΔH^o versus ΔS^o lines are respectively 0.978 and 0.918 for the 20 mM ACN-buffer 80/20 and 90/10 *v/v* HILIC mobile phases excluding the outsider dopac #8 (circled point in Figure 4-4, bottom). This alignment indicates similar mechanism [117, 118]. This result is interesting since it seems to say that charged compounds interact similarly with the HZI zwitterionic stationary phase regardless of their charge. This conclusion should be moderated by the fact that our set of compounds includes mostly positively charged solutes. Nevertheless, two solutes: #8 and #11, are negatively charged at the working pH = 4.1. If dopac (#8) is somewhat an outsider at 20 mM ionic strength, the nicotinic acid (#13) thermodynamic parameters fit with the Figure 4-4 (bottom) regression lines (data in Table 4-3).

Π-π interaction seems to play a significant role in the HZI retention and selectivity of π-containing solutes [115]. Indeed the ΔH^o and ΔS^o values obtained for all β-blocker solutes produced points in Figure 4-4 that do not stand apart from the other solute representative points: all points belong to the Figure 4-4 ΔH^o versus ΔS^o lines. The additional π-π, H-bonding and partition interactions are stronger in magnitude for β-blockers with a strong positive entropic contribution and limited enthalpy contribution. The other charged solutes show balanced contributions with similar effects in magnitude but opposite effects in retention of the enthalpic and entropic contributions (Table 4-3).

Increasing the ionic strength of the mobile phase decreases charge-charge interactions. Anionic dopac is no more an outsider with 50 mM ammonium acetate mobile phases but the global ΔH^o versus ΔS^o picture remains the same: the apolar aromatic compounds stand apart with their negative entropy driven mechanism and the β-blockers have a similar positive entropy driven mechanism with diminished interaction producing lower retention factors (Figure 4-4, bottom).

4.3.3 Curved van't Hoff plots

Five compounds listed in Table 4-2 had curved van't Hoff plots with some (dopac and labetalol) or all (aromatic compounds) studied HILIC mobile phases as illustrated by Figure 4-3 (right). Curved van't Hoff plots were commonly observed in HILIC thermodynamic studies [85, 110, 119]. The problem is usually ignored or expedited stating that a change in retention mechanism occurs in the temperature range studied which makes sense when it is obvious that multiple forces are at play as in our case [110]. Temperature changes may have different effects on different interactions. However, Chester and Coym raised another possible explanation for curved van't Hoff plots: phase ratio variation [120]. Following them, the slope of the van't Hoff equation (eq. 1) is a derivative with four terms:

$$\frac{\partial \ln k}{\partial (1/T)} = \frac{-\Delta H^o}{R} - \frac{1}{RT}\left(\frac{\partial(\Delta H^o)}{\partial(1/T)}\right) + \frac{1}{R}\left(\frac{\partial(\Delta S^o)}{\partial(1/T)}\right) + \frac{\partial \ln \emptyset}{\partial(1/T)} \tag{2}$$

A constant mechanism on the temperature range studied associated to stable phase ratio produce a nil value for the three partial derivatives of eq. 2 and the van't Hoff slopes is directly related to ΔH^o. If a change in mechanism occurs, the second and third terms of eq. 2 are not nil and the observed curvature is indeed explained. But the curvature is explained as well assuming a constant mechanism with constant ΔH^o and ΔS^o terms and phase ratio variations. These constant thermodynamic terms can be

estimated on a narrow temperature range, and then ln Φ can be calculated using eq. 1 for the whole temperature range [120].

Our results shows that the curved van't Hoff plots have at least three aligned points at high temperatures. The curvature is mostly seen at low temperatures (*e.g.* benzene Figure 4-3). Then, the ΔH^o and ΔS^o values were estimated on the 50-70 ^{o}C linear range of the ln k versus $1/T$ plots (left side of Figure 4-3) and used to calculate the ln Φ values for all other temperatures. Figure 4-5 shows the Φ values obtained for different solutes with curved van't Hoff plots in the same ACN/buffer (20 mM, top, or 50 mM, bottom) ammonium acetate 85/15 volume fraction (Figure 4-5 left) and for dopac in different HILIC mobile phases (Figure 4-5, right). The first observation is that the trend is always the same: the phase ratio seen by the solutes increases with temperature. Such Φ increase with temperature was the trend seen by Chester and Coym observing the densely grafted C18 stationary phase changes with temperature [120]. These results could well be an artifact. Since the ΔH^o and ΔS^o solute parameters were obtained at high temperatures using the $\Phi = 0.2$ value, it is obvious that calculated Φ values will tend toward 0.2 at high temperatures as seen in Figure 4-5.
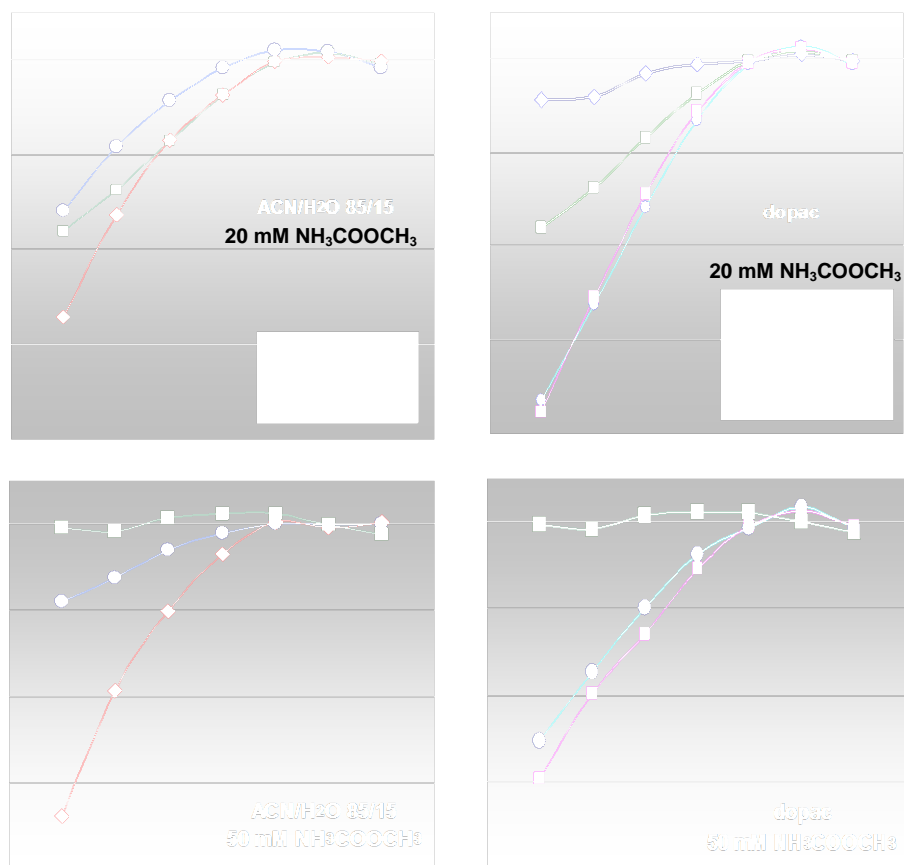
Figure 4-5 HZI calculated column phase ratio Φ ($=V_S/V_m$) for solutes producing curved van't Hoff plots. Left: Phase ratio for three solutes in the ACN/buffer 85/15 v/v. Right: Phase ratio for Dopac (Compound #8) in different HILIC mobile phases. Top: mobile phases with 20 mM ammonium acetate; bottom: mobile phases with 50 mM mobile phases. The zwitterionic HZI column: 25 x 0.46 cm, flow rate: 1 mL/min.

If the observed trend is significant, it means that the solutes showing curvilinear van't Hoff plots see an accessible stationary phase volume increasing with temperature. One HILIC mechanism describes a hydrated layer formed on the polar stationary phase [3, 17]. The hydrated layer volume increases with the acetonitrile water content up to about 30% [17]. A small-angle neutron scattering study of ACN/water mixtures on the water molar fraction 0.2-0.6 corresponding to a volume fraction range 8-34% in a temperature interval between 6 and 34 ^{o}C evidenced significant structural changes [121]. Colder ACN/water mixtures were much more structured with stronger water-water molecular interaction (water pools) than warmer mixtures of the same composition. It can be speculated that the water concentration variation induced at the HILIC stationary phase surface is affected by colder temperature so that the more organized cold layer has a reduced volume accessible to solutes.

Once again, if the variable Φ ratio is relevant, Figure 4-5 (left) shows that all concerned solutes (toluene and xylene not shown overlapping with benzene) see similar Φ ratio in the same 20 mM mobile phase. The Φ ratio variability decreases when the mobile phase water volume fraction increases (Figure 4-5, right). In the mobile phase ACN/20 mM buffer 80/20 *v/v*, the van't Hoff linear regression coefficients of labetalol and dopac were respectively 0.989 and 0.971 (slight curvature). Only the poorly retained aromatic compounds #5, 14 and 15 showed clearly curved van't Hoff plots. The Φ ratio variation is greatly reduced in 50 mM buffer containing mobile phase. Figure 4-5 (bottom left) shows that only the non ionic apolar benzene solute shows a curved plot with 50 mM 85/15 *v/v* buffer concentration. All plots, but the aromatic ones, were linear with more than 15% 50 mM buffer concentrations (Figure 4-5 bottom right). As already shown, increased ionic strength screen interacting columbic or polar forces [115]. Also,

86

increasing the mobile phase water content decreases the water concentration differences between bulk mobile phase and stationary phase surface [3, 17].

4.4 Conclusions

Thermodynamic studies of a set of polar and apolar solutes interacting with a recently proposed zwitterionic HILIC stationary phase gave insights into the retention mechanism. The main result is that the two aromatic rings attached to the positively charged phosphonium group can expressed themselves introducing π-π interactions that were not seen with other commercially available HILIC stationary phases. Solutes containing phenyl rings will show different HILIC selectivity when separated on the HZI column.

Curved van't Hoff plots were obtained for several solutes. If changes in entropy and enthalpy over the temperature interval cannot be excluded given the different forces at play in the retention mechanism, it is suggested that the hydrated layer on the stationary phase surface could have a temperature dependent composition and physico chemical state so that the solutes could see a changing stationary phase volume.

Chapter 5

Evaluation of aromatic-derivatized cyclofructans 6 and 7 as HPLC chiral selectors

Abstract

The two best aromatic-functionalized cyclofructan chiral stationary phases, R-naphthylethyl-carbamate cyclofructan 6 (RN-CF6) and dimethylphenyl-carbamate cyclofructan 7 (DMP-CF7), were synthesized and evaluated by injecting various classes of chiral analytes. They provided enantioselectivity toward a broad range of compounds, including chiral acids, amines, metal complexes, and neutral compounds. It is interesting that they exhibited complementary selectivities and the combination of two columns provided enantiomeric separations for 43% of the test analytes. These extensive chromatographic results provided useful information about method development of specific analytes, and also gave some insight as to the enantioseparation mechanism.

5.1 Introduction

In the past two and a half decades, enantiomeric separations have developed from a highly challenging method into a routine laboratory technique.[122] This is mainly because of the rapid development of a plethora of HPLC chiral stationary phases (CSPs). Given the large number and types of CSPs, method development for a specific enantiomeric compound can involve time-consuming screening of a large number of CSPs. Therefore, researchers continue to investigate new chiral stationary phases, in hopes of finding either a more universal column, which is widely effective for different classes of compounds, or columns with a well defined (and therefore predictable) selectivity.

Developing a new chiral selector with a broad range of enantioselectivies has been a challenge, and derivatization of a naturally-occurring molecule has proven to be a successful strategy, which can broaden the application range of the original chiral selector. [123-140] For example, aromatic derivatization (dimethylphenyl, R- and S-naphthylethyl, dinitrophenyl) of β-cyclodextrin greatly extended its utility in the normal phase mode.[124-129] Native cellulose and amylose are known to be poor chiral selectors, while dimethylphenyl-substituted ones (Chiralpak AD and OD) are among the most widely useful CSPs. [39, 130, 132, 133, 141] Aided by additional π-π interactions and dipolar interactions, the aromatic-derivatized chiral selector may provide totally different mechanisms of chiral recognition, compared to the original one.

A new class of macrocyclic oligosaccharides, cyclofructans, has recently received considerable attention in the area of enantiomeric separations. Cyclofructans are composed of six or more β-(2→1) D-fructofuranose units, name as CF6, CF7, CF8, and etc. [142] They were first reported in 1989 and they have been used in a variety of industrial applications, such as moderators of food and drink bitterness and astringency, inhibitors for odor and taste of iron. [143, 144] However, its application as a chiral selector for HPLC, CE and GC has been investigated only recently by our group. [65-67, 145] Both LC and CE studies have demonstrated that native cyclofructan 6 (CF6) has limited capabilities for chiral recognition. [65, 66, 66, 145] However, additional studies indicated that optimally derivatized-CF6 had considerable promise as a chiral selector. [65] By varying the nature and degree of substitution of the substituent(s), the functionalized cyclofructans could be "tuned" to separate different classes of molecules. While aliphatic-substituted CF6 has been thoroughly examined, [145] aromatic derivatives have not.

Therefore, the purpose of the present work is to examine the potential and overall chiral selectivities of aromatic-derivatized CF6 and CF7. In order to evaluate their applicability, a large number of racemic compounds, including chiral acids, amines, metal complexes, and neutral compounds, were injected on the two best chiral stationary phases, R-naphthylethyl-carbamate CF6 (RN-CF6) and dimethylphenyl carbamate CF7 (DMP-CF7). Also, effects of the chiral selector structure on enantioseparations are discussed.

5.2 Experimental

5.2.1 Materials

Anhydrous toluene, anhydrous pyridine, trifluoroacetic acid (TFA), ammonium nitrate, 3-(triethoxysilyl)propyl isocyanate, 1,6-diisocyanatohexane, (3-aminopropyl)dimethylethoxysilane, R-1-(1-naphthyl)ethyl isocyanate, 3,5-dimethylphenyl isocyanate, and most of racemic analytes tested in this study were purchased from Sigma-Aldrich (Milwaukee, WI, USA). Ru(II) complexes were donated by Dr. MacDonnell (Department of Chemistry and Biochemistry, the University of Texas at Arlington). CF6 was obtained by fermentation and crystallization as described previously. [70, 146, 147] CF7 was purified as reported previously. [148] Acetonitrile (ACN), isopropanol (IPA), heptane, ethanol (ETOH), and methanol (MEOH) of HPLC grade were obtained from EMD (Gibbstown, NJ). Water was obtained fromm Millipore (Billerica, MA). Kromasil and Daiso silica (5μm spherical diameter, 100 Å, 120 Å, 200 Å pore size) were obtained from Supelco (Bellefonte, PA). The aromatic-substituted CF6 and CF7 chiral stationary phases were synthesized, according to the previous paper. [65] Then they were slurry-packed into 25cm×0.46cm (i.d.) stainless steel columns.

5.2.2 HPLC method

The chromatographic system used was an Agilent 1100 HPLC (Agilent Technologies, Palo Alto, CA, USA), consisting of a diode array detector, an autosampler, a binary pump and a temperature-controlled column chamber. For all HPLC experiments, the injection volume and the flow rate were 5 μL, 1mL/min, respectively. The column temperature was 20 ^{o}C, if not specified otherwise. The mobile phase was degassed by ultrasonication under vacuum for 5 min. The analytes were dissolved in ethanol, or the appropriate mobile phases (the concentration was ~3 mg/mL). The stock analyte solution was further diluted with the mobile phase if necessary. In the normal phase mode, heptane/ethanol (or isopropanol) with/without trifluoroactic acid was used as the mobile phase. The mobile phase of the polar organic mode was composed of acetonitrile/methanol with 0.2% ammonium nitrate (weight percentage).

For the calculation of retention factors (k_1, k_2), t_0 was determined by the peak of the refractive index change due to the sample solvent or by injecting 1,3,5-tri-tert-butylbenzene in the normal phase mode.

5.3 Results and Discussions

Screening chromatographic results of the RN-CF6 CSP and the DMP-CF7 CSP

Preliminary studies showed that aromatic functionalization of cyclofructans significantly broadened the application range of these CSPs. [65] Therefore, different aromatic-substitution groups on cyclofructan6 (CF6) and cyclofructan7 (CF7), including dimethylphenyl, methylphenyl, naphthylethyl, dichlorophenyl, and chlorophenyl, were tested. It was found that two of these CSPs provided the best performance and they showed the broadest selectivity for the tested racemic analytes. They are the R-naphthylethyl-carbamate CF6 (RN-CF6) and dimethylphenyl-carbamate CF7 (DMP-CF7).

It was also found that better selectivity and resolution were often obtained in the normal phase mode on the aromatic functionalized cyclofructan stationary phases. [65] Therefore, the current study focuses on a systematic chromatographic evaluation of the RN-CF6 and DMP-CF7 stationary phases, mainly in the normal phase mode.

A set of 220 racemic compounds with various functionalities were used to evaluate these two columns. Racemic analytes were divided into five groups: acids, amines (including primary, secondary and tertiary amines), alcohols, ruthenium complexes, and other neutral compounds. It was reported that enantiomers of ruthenium complexes were quickly separated with high selectivities by the R-naphthylethyl β-cyclodextrin column (Cyclobond RN), [149] which is closely related to the structure of the RN-CF6 stationary phase. Therefore, these Ru(II) complexes were tested in order to compare the performance of cyclofructan- and cyclodextrin-based stationary phases. Earlier studies indicated that the RN-CF6 CSP provided enantioselectivities for a few unique primary amines, which the isopropyl-CF6 column could not easily separate.[145] Therefore, in this study, several primary-amine containing compounds (grouped into "amines") were selected to investigate the capability of CF6- and CF7-based CSPs for separating primary amines.

Table 5-1 Summary of optimized chromatographic data achieved on RN-CF6 and DMP-CF7 chiral stationary phases.

#	Compound name	Structure	CSP	k_1	α	R_s	Mobile phase[a]
A. Chiral acids							
1	Phenethylsulfamic acid		RN-CF6	1.52	1.20	1.6	60H40E0.1TFA
2	Carbobenzyloxy alanine		DMP-CF7	9.10	1.10	1.7	95H5E0.1TFA0C

Table 5-1—*Continued*
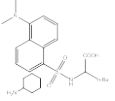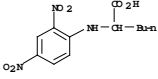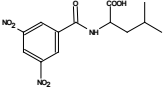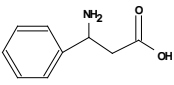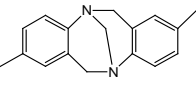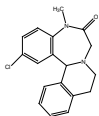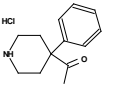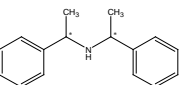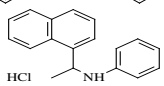
3	Dansyl-norleucine cyclohexylammonium salt		DMP-CF7	2.42	2.03	8.6	80H20E0.1TFA
4	N-2,4-DNP-DL-norleucine		DMP-CF7	9.93	1.10	1.5	95H5E0.1TFA
5	N-(3,5-dinitrobenzoyl)-DL-leucine		RN-CF6	0.84	1.49	4.5	50H50E0.1TFA
			DMP-CF7	16.90	1.13	3.0	95H5E0.1TFA
6	N-(3,5-Dinitrobenzoyl)-DL-phenylglycine		RN-CF6	2.50	1.16	2.2	50H50E0.1TFA
			DMP-CF7	21.66	1.07	0.8	95H5E0.1TFA
7	3-(Benzyloxycarbonyl)-4-oxazolidinecarboxylic acid		DMP-CF7	4.11	1.05	0.9	90H10E0.1TFA
8	DL-3-Amino-3-phenylpropionic acid		DMP-CF7	8.25	1.04	0.7	80H20E0.1TFA

B. Amines

1	Tröger's base		RN-CF6	0.79	1.50	5.2	70H30E
			DMP-CF7	3.19	1.29	3.7	80H20E0.1TFA
2	2-Chloro-5,9,10,14B-tetrahydro- 5-Me-isoquino(2,1-d)(1,4)benzodiazepin-6(7H)-		RN-CF6	2.58	1.02	0.4	60H40E0.1TFA
3	4-Acetyl-4-phenylpiperidine hydrochloride		DMP-CF7	5.14	1.05	0.7	80H20E0.1TFA
4	Bis-[(R/S)-1-phenylethyl] amine hydrochloride		RN-CF6	3.59	1.15	2.4	90H10E0.1TFA
5	N-Benzyl-1-(1-naphthyl) ethylamine hydrochloride		RN-CF6	8.92	1.02	0.6	95H5E0.1TFA

Table 5-1—*Continued*
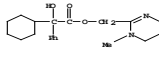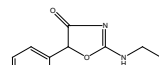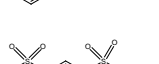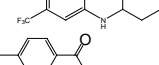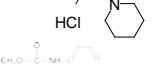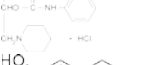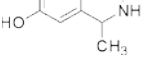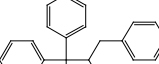
6	α,α-Diphenylprolinol		RN-CF6	15.03	1.12	1.7	90H10E0.1TFA
7	Oxyphencyclimine hydrochloride		RN-CF6	13.68	1.12	1.5	60H40E0.1TFA
8	5-Phenyl-2-(2-propynyl-amino)-2-oxazolin-4-one		DMP-CF7	5.21	1.08	1.5	80H20E0.1TFA
9	Bendroflumethiazide		RN-CF6	1.81	1.16	2.0	60H40E0.1TFA
10	Tolperisone hydrochloride		RN-CF6	5.52	1.12	1.8	70H30E0.1TFA
11	Diperodon hydrochloride		RN-CF6	7.42	1.11	1.2	70H30E0.1TFA
12	1-Methyl-6,7-dihydroxy-1,2,3,4-tetrahydroisoquinoline hydrobromide		RN-CF6	4.33	1.17	2.0	60H40E0.1TFA
			DMP-CF7	12.12	1.05	0.6	80H20E0.1TFA
13	2-Amino-1,1,3-triphenyl-1-propanol		RN-CF6	3.40	1.10	1.5	80H20E0.1TFA
			DMP-CF7	3.12	1.02	0.5	80H20E0.1TFA
14	N-p-Tosyl-1,2-diphenylethylenediamine		RN-CF6	8.28	1.24	2.9	80H20E0.1TFA
			DMP-CF7	5.43	1.13	1.4	80H20E0.1TFA
15	DL-alanine-β-naphthylamide hydrochloride		RN-CF6	10.03	1.10	1.5	80H20E0.1TFA

C. Alcohols

1	α-Methyl-9-anthracenemethanol		RN-CF6	11.30	1.06	1.3	99H1I0.1TFA0C

Table 5-1—*Continued*

#	Name	Structure					
2	1-Anthracen-2-yl-ethanol		DMP-CF7	14.59	1.05	1.0	99H1E
3	Benzoin		RN-CF6	9.30	1.06	1.5	99H1I0.1TFA0C
			DMP-CF7	7.79	1.09	1.5	99H1E
4	α-Methyl-2-naphthalenemethanol		DMP-CF7	9.90	1.02	0.5	99H1E
5	6-(4-chlorophenyl)-4,5-dihydro-2-(2-hydroxybutyl)-3(2H)-pyridazinone		DMP-CF7	13.63	1.03	0.6	95H5E0.1TFA
6	N,N'-Dibenzyl-tartramide		RN-CF6	8.21	1.04	0.9	90H10E0.1TFA
			DMP-CF7	22.76	1.03	0.8	95H5E0.1TFA
7	Furoin		RN-CF6	5.24	1.02	0.5	90H10E0.1TFA
			DMP-CF7	17.46	1.04	0.7	98H2E0.1TFA
8	3-(4-Chlorophenyl)-2-ethyl-2,3,5,6-tetrahydroimidazol [2,1-b]-thiazol-3-ol		DMP-CF7	5.05	1.10	0.7	80H20E0.1TFA
9	Cromakalim		DMP-CF7	17.24	1.08	1.5	95H5E0.1TFA
10	1,1'-Binaphthyl-2,2'-dimethanol		RN-CF6	6.37	1.02	0.6	95H5E0.1TFA
			DMP-CF7	7.44	1.05	0.7	80H20E0.1TFA

D. Ru(II) complexes

#	Name	Structure					
1	[Ru(phen)₃](Cl₂)		RN-CF6	0.62	1.49	3.8	60M/40A/0.2 NH_4NO_3[b]
			DMP-CF7	3.81	1.14	1.3	80M/20A/0.2 NH_4NO_3

Table 5-1—*Continued*
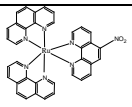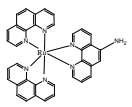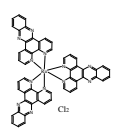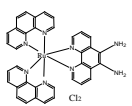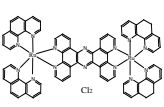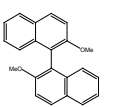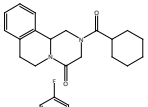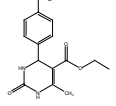
#	Compound	Structure	Method				Conditions
2	[Ru(phen)₂nitrophen](Cl₂)		RN-CF6	0.46	1.65	4.1	60M/40A/0.2 NH₄NO₃
			DMP-CF7	3.52	1.25	1.8	80M/20A/0.2 NH₄NO₃
3	[Ru(phen)₂aminophen](Cl₂)		RN-CF6	0.54	1.53	3.9	60M/40A/0.2 NH₄NO₃
			DMP-CF7	2.81	1.15	1.3	80M/20A/0.2 NH₄NO₃
4	[Ru(dppz)₃](Cl₂)		RN-CF6	0.78	2.90	11.4	60M/40A/0.2 NH₄NO₃
			DMP-CF7	2.63	1.44	2.7	80M/20A/0.2 NH₄NO₃
5	[Ru(phen)₂phendiamine] (Cl₂)		RN-CF6	0.59	1.51	3.3	60M/40A/0.2 NH₄NO₃
			DMP-CF7	4.02	1.16	1.2	80M/20A/0.2 NH₄NO₃
6	[Ru(phen)₂dppz](Cl₂)		RN-CF6	0.67	1.80	5.8	60M/40A/0.2 NH₄NO₃
			DMP-CF7	6.25	1.32	2.2	80M/20A/0.2 NH₄NO₃
7	[Ru₂(phen)₄(tpphz)](Cl₄)		RN-CF6	2.24	2.67	6.9	60M/40A/0.2 NH₄NO₃
			DMP-CF7	16.24	1.30	0.9	80M/20A/0.2 NH₄NO₃

E. Others

#	Compound	Structure	Method				Conditions
1	2,2'-Dimethoxyl-1,1'-binaphthyl		RN-CF6	6.20	1.02	0.5	95H5E0.1TFA
2	Praziquantel		RN-CF6	9.69	1.05	1.0	95H5E0.1TFA
3	4-(4-Fluoro-phenyl)-6-methyl-2-oxo-1,2,3,4-tetrahydro pyrimidine-5-carboxylic acid ethyl ester		DMP-CF7	14.85	1.12	2.6	95H5E0.1TFA

Table 5-1—*Continued*
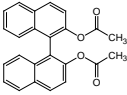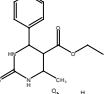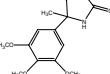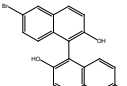
#	Name		Method				Condition
4	1,1'-Bi(2-naphthyl diacetate)		RN-CF6	0.83	1.12	1.5	70H30E0.1TFA
			DMP-CF7	4.18	1.13	2.2	99H1E
5	N-2'-Acetylamino-[1,1']binaphthalenyl-2-yl)-acetamide		DMP-CF7	23.45	1.04	0.9	95H5E0.1TFA
6	6-Methyl-4-phenyl-2-thioxo-1,2,3,4-tetrahydro-pyrimidine-5-carboxylic acid ethyl ester		DMP-CF7	12.92	1.11	1.5	98H2E0.1TFA
7	5-Methyl-5-(3,4,5-trimethoxyphenyl)hydantoin		RN-CF6	13.08	1.04	1.1	90H10E0.1TFA
			DMP-CF7	13.36	1.05	1.5	90H10E0.1TFA
8	5,5',6,6',7,7',8,8'-Octahydro(1,1'-binaphthalene)-2,2'-diol		RN-CF6	6.80	1.20	4.9	99H1I0.1TFA
			DMP-CF7	5.13	1.05	0.7	80H20E0.1TFA
9	3,3'-Dibromo-5,5',6,6',7,7',8,8'-octahydro(1,1'-binaphthalene)-2,2'-diol		RN-CF6	4.89	1.28	5.2	99H1I0.1TFA
			DMP-CF7	5.13	1.04	0.7	80H20E0.1TFA
10	2,2'-Diamino-1,1'-binaphthalene		RN-CF6	2.03	1.18	2.7	70H30E
			DMP-CF7	4.36	1.48	5.0	80H20E0.1TFA
11	6,6'-Dibromo-1,1'-bi-2-naphthol		RN-CF6	3.67	1.11	2.3	90H10E0.1TFA
			DMP-CF7	3.70	1.17	2.6	90H10E0.1TFA

Table 5-1—*Continued*

#	Name	Structure	Method				
12	1,1'-Bi-2-naphthol		RN-CF6	3.33	1.07	1.7	90H10E0.1TFA
			DMP-CF7	3.91	1.23	5.0	90H10E0.1TFA
13	DL-N-Acetylhomocysteine thiolactone		RN-CF6	12.08	1.03	0.8	90H10E0.1TFA
14	Althiazide		RN-CF6	3.04	1.20	2.7	60H40E0.1TFA
			DMP-CF7	12.42	1.09	1.5	80H20E0.1TFA
15	Benzyl-6-oxo-2,3-diphenyl-4-morpholine carboxylate		RN-CF6	7.08	1.05	1.6	95H5E0.1TFA
			DMP-CF7	6.26	1.06	1.5	95H5E0.1TFA
16	1.1'-Bi-2-naphthol bis(trifluoromethanesulfonate)		RN-CF6	7.80	1.07	1.2	100HEP0C
17	Camphor p-tosyl hydrazon		DMP-CF7	7.53	1.18	3.4	95H5E0.1TFA
18	4-Chlorophenyl 2,3-epoxypropyl ether		DMP-CF7	2.52	1.12	1.9	95H5E0.1TFA0C
19	3,4-dihydroxyphenyl-alfa-propylacetamide		DMP-CF7	6.15	1.06	1.0	80H20E0.1TFA
20	1,5-Dimethyl-4-phenyl-2-imidazolidinone		RN-CF6	11.17	1.06	1.5	95H5I0.1TFA
			DMP-CF7	11.10	1.07	1.5	95H5E0.1TFA
21	2,3-Dihydro-7a-methyl-3-phenylpyrrolo[2,1-b]oxazol-5(7aH)-one		RN-CF6	2.19	1.15	2.1	90H10E0.1TFA
			DMP-CF7	8.26	1.07	1.6	99H1E

Table 5-1—*Continued*
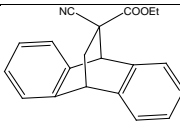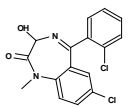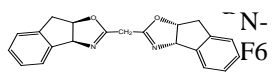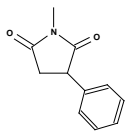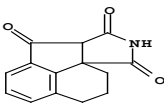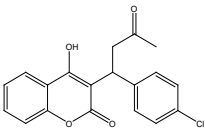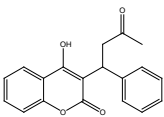
22	Ethyl 11-cyano-9,10-dihydro-endo-9,10 -ethanoanthracene-11-carboxylate		RN-CF6	3.07	1.08	1.7	99H1E0.1TFA
			DMP-CF7	1.94	1.57	5.2	95H5E0.1TFA
23	2,3-O-Isopropylidene 2,3-dihydroxy-1,4-bis(disphenylphosphino)butane		RN-CF6	10.89	1.05	0.8	90H10E0.1TFA
			DMP-CF7	5.80	1.02	0.5	80H20E0.1TFA
24	Lormetazepam		RN-CF6	9.57	1.04	0.8	90H10E0.1TFA
25	[3aS/R-[2(3'aR*,8'aS*),3'aα/β, 8'aα/β]] -(-)-2,2'-Methylenebis [3a,8a-dihydro-		N-F6	9.84	1.21	1.2	70H30E0.1TFA
26	Phensuximide		RN-CF6	6.12	1.05	1.5	95H5E0.1TFA
			DMP-CF7	15.98	1.09	1.2	98H2E0.1TFA
27	3a,4,5,6-Tetrahydro-succininido[3,4-b]acenaphthen-10-one		RN-CF6	4.31	1.08	1.5	80H20E0.1TFA
			DMP-CF7	12.60	1.10	2.1	90H10E0.1TFA
28	3-(α-Acetonyl-4-chlorobenzyl)-4-hydroxycoumarin		RN-CF6	11.54	1.10	1.8	95H5E0.1TFA
			DMP-CF7	12.16	1.30	4.5	95H5E0.1TFA
29	Warfarin		RN-CF6	12.20	1.10	1.9	95H5I0.1TFA
			DMP-CF7	11.54	1.17	2.6	95H5E0.1TFA

Table 5-1—*Continued*
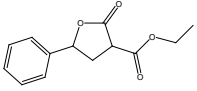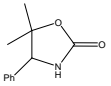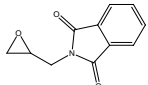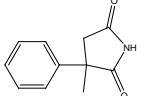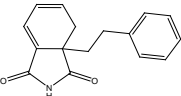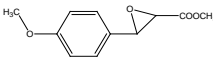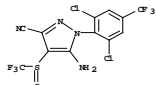
#	Name	Structure					
30	2-Carbethoxy-gamma-phenyl-gamma-butyrolactone		RN-CF6	12.79	1.09	1.0	99H1I0.1TFA0C
			DMP-CF7	11.79	1.12	2.4	98H2E0.1TFA0C
31	5,5-dimethyl-4-phenyl-2-oxazolidinone		DMP-CF7	8.26	1.08	1.8	95H5E0.1TFA
32	N-(2,3-Epoxypropyl)-phthalimide		DMP-CF7	14.59	1.08	1.7	98H2E0.1TFA
33	α-Methyl-alpha-phenyl-succinimide		RN-CF6	10.28	1.05	1.5	95H5E0.1TFA0C
			DMP-CF7	9.77	1.09	2.0	95H5E0.1TFA
34	Phenethylphthalimide		RN-CF6	4.07	1.08	1.3	99H1I0.1TFA0C
			DMP-CF7	3.82	1.25	3.2	99H1E
35	Methyl trans-3-(4-methoxyphenyl)glycidate		RN-CF6	7.22	1.02	0.6	90H10E0.1TFA
			DMP-CF7	14.07	1.09	1.9	95H5E0.1TFA
36	cis-3,4-benzo-6-azabicyclo[3.2.0]heptan-7-one		RN-CF6	5.31	1.07	1.5	90H10E0.1TFA0C
			DMP-CF7	22.03	1.04	0.8	98H2E0.1TFA
37	cis-4,5-benzo-7-azabicyclo[4.2.0]octan-8-one		RN-CF6	8.27	1.05	1.3	95H5E0.1TFA0C
			DMP-CF7	17.70	1.03	0.6	98H2E0.1TFA
38	Fipronil		RN-CF6	17.42	1.07	1.7	98H2E0.1TFA0C

100

Table 5-1—*Continued*
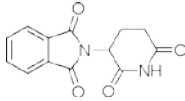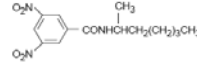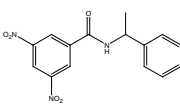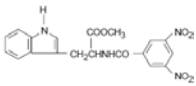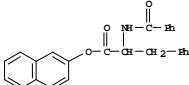
39	5-Methyl-5-phenyl hydantoin		DMP -CF7	14.73	1.16	5.0	95H5E0.1TFA
40	trans-Stilbene oxide		RN- CF6	1.70	1.05	1.1	100HEP0C
41	Thalidomide		RN- CF6	12.65	1.05	1.1	80H20E0.1TFA
42	3,5-DNB-2-aminoheptane		RN- CF6	0.86	1.13	1.5	70H30E0.1TFA
43	3,5-Dinitro-N-(1-phenylethyl)benzamide		RN- CF6	0.96	2.05	9.8	50H50E0.1TFA
44	4-Phenyl-2-oxazolidinone		DMP -CF7	7.12	1.05	1.0	90H10E0.1TFA
45	4-Phenylthiazolidine-2-thione		RN- CF6	13.27	1.04	1.3	95H5E0.1TFA0C
46	4-Benzyloxazolidine-2-thione		RN- CF6	6.98	1.02	0.5	90H10E0.1TFA
			DMP -CF7	6.90	1.15	2.9	90H10E0.1TFA
47	4-Benzylthiazolidine-2-thione		DMP -CF7	4.25	1.09	1.9	90H10E0.1TFA
48	4-Benzyl-5,5-dimethyl-2-oxazolidinone		RN- CF6	7.06	1.02	0.6	90H10E0.1TFA
49	4-Benzyl-3-chloroacetyl-2-oxazolidinone		RN- CF6	3.73	1.02	0.5	90H10E0.1TFA
50	4-Isopropylthiazolidine-2-thione		DMP -CF7	5.65	1.08	1.8	95H5E0.1TFA
51	cis-4,5-Diphenyl-2-oxazolidinone		RN- CF6	14.80	1.05	1.5	95H5E0.1TFA0C
			DMP -CF7	13.63	1.09	1.9	95H5E0.1TFA

Table 5-1—*Continued*

				k_1	α	R_s	
52	N-Benzoyl-DL-phenylalanine beta-naphthyl ester		RN-CF6	5.92	1.06	0.5	90H10E0.1TFA0C
			DMP-CF7	14.80	1.08	1.5	95H5E0.1TFA0C
53	3,5-DNB-Tryptophan methyl ester		RN-CF6	5.52	1.12	1.8	70H30E0.1TFA
			DMP-CF7	5.75	1.14	5.0	80H20E0.1TFA
54	N-Benzoyl-DL-phenylalanine beta-naphthyl ester		DMP-CF7	8.52	1.06	1.1	95H5E0.1TFA

(a) Abbreviation:

Mobile phases: H: heptane; I: isopropanol; E: ethanol; A: acetonitrile; M: methanol; TFA: trifluoroacetic acid.

OC: the column temperature is 0 ˚C.

(b) 0.2% NH_4NO_3 is the weight percentage.

Table 5-1 lists the chromatographic data for all compounds separated by the RN-CF6 and DMP-CF7 CSPs. The chromatographic data include retention factor (k_1), selectivity (α), and resolution (R_s). In the case of Ru complexes (group D in Table 5-1), it was necessary to use the polar organic mode plus salt addition (such as ammonium nitrate) to obtain elution in a reasonable time. Optimized separations of all other compounds were achieved in the normal phase mode. The chromatograms in Figure 5-1 (20 ^{o}C vs 0 ^{o}C) demonstrate effects of temperature on these enantioseparations. The selectivity of separating 4-chlorophenyl 2,3-epoxypropyl ether was improved from 1.07 to 1.12 when decreasing the column temperature. Usually, decreasing the column temperature increases enantioselectivity, retention, and resolution. Therefore, decreasing the column temperate to 0 ˚C can be an effective strategy during the optimization process.
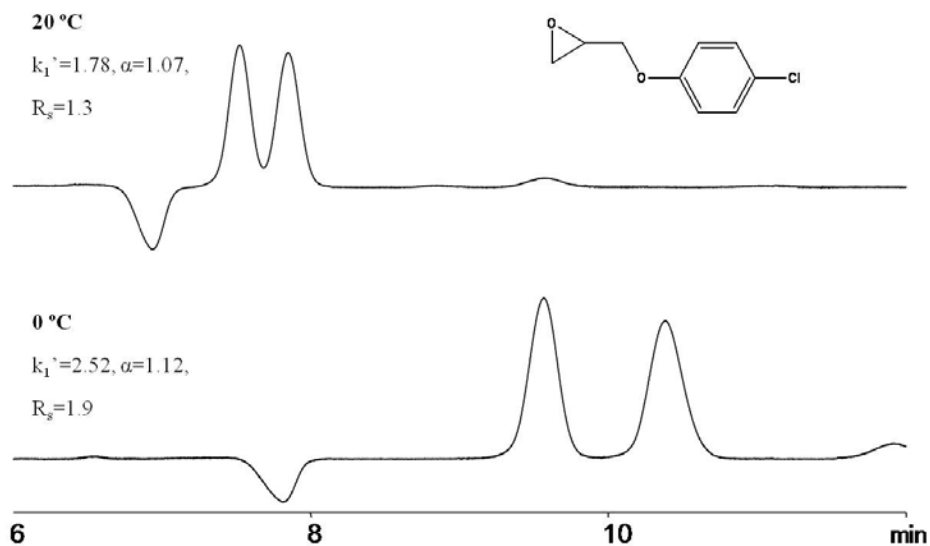
Figure 5-1 The column temperature effect on enantioseparations by the DMP-CF7 chiral

stationary phase. The analyte and mobile phase are 4-chlorophenyl 2,3-epoxypropyl

ether and 95Hep5EtOH0.1TFA, respectively.

The data in Table 5-1 indicates that the number of successful separations for

each class of analyte obtained on two columns is 8, 15, 10, 7, 54, respectively. The total

number of separations achieved on the combination of RN-CF6 and DMP-CF7 are 94.

Enantiomers of 63 compounds out of 94 were baseline separated. 43% of the tested

compounds, which were randomly chosen, were separated on these two CSPs. The

representative chromatograms of a chiral acid, secondary amine, tertiary amine, alcohol,

Ru(II) complex, and a neutral compound, are shown in Figure 5-2.
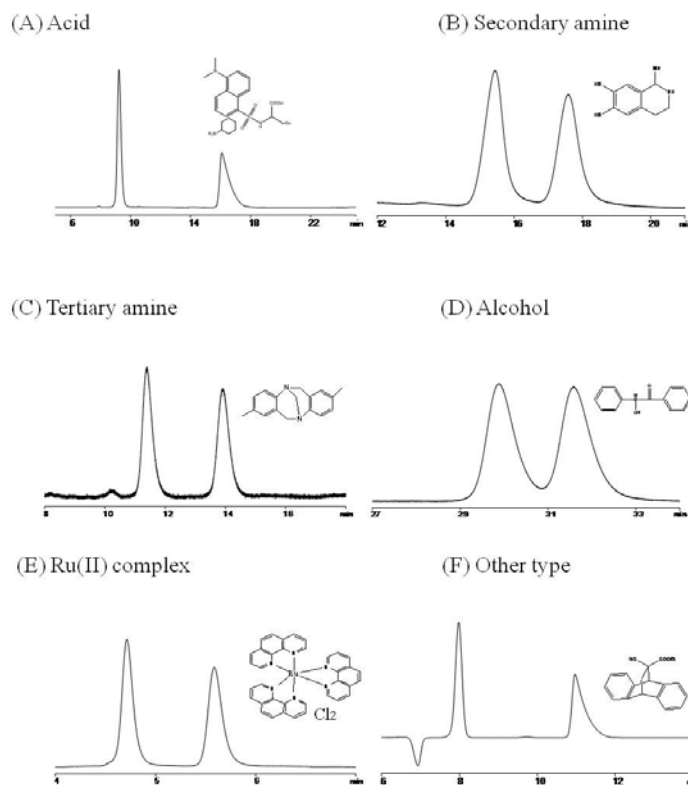
Figure 5-2 Representative chromatograms showing enantioseparations of various types of compounds. The analytes, stationary phases, and d mobile phases are: (A) Dansyl-norleucine cyclohexylammonium salt, DMP-CF7, 80H20E0.1TFA; (B) 1-Methyl-6,7-dihydroxy-1,2,3,4-tetrahydroisoquinoline hydrobromide, RN-CF6, 60H40E0.1TFA; (C) Tröger's base, DMP-CF7, 80H20E0.1TFA; (D) Benzoin, RN-CF6, 99H1I0.1TFA (0 ^{o}C); (E) [Ru(phen)$_3$]Cl$_2$, RN-CF6, 60M/40A/0.2 NH$_4$NO$_3$; (F) Ethyl 11-cyano-9,10-dihydro-endo-9,10-ethanoanthracene-11-carboxylate, DMP-CF7, 95H5E0.1TFA.

The data in Table 5-1 and Figure 5-2 indicates that the RN-CF6 and DMP-CF7 CSPs provide excellent enantioselectivity toward a wide range of analytes. Compared to native CF6 and CF7, their capabilities for chiral recognition were significantly improved. This can be explained by the fact that derivatization of native cyclofructans effectively

disrupts internal hydrogen bonding, relaxing (denaturing) the molecule and exposing its entire surface. [65, 145] In addition, the presence of the aromatic and carbonyl groups provide ample opportunities for π-π interactions and dipolar interactions, as well as additional steric interaction sites. These are the type of interactions that play a pronounced role in chiral recognition in nonpolar solvents (the normal phase mode) rather than in polar solvents. It should be also noted that the CF-based chiral stationary phases were very robust and not irreversibly altered when changing from one mobile phase mode to another. The cyclofructan-bonded CSPs did not show a detectable deterioration in the separation performance after extensive use (~1,000 injections in six months).

These results also indicate that the performance of cyclofructan stationary phases was significantly different from other known crown-ether based CSPs, although cyclofructans also contain crown-ether cores. CF-based CSPs provided chiral recognition toward a variety of compounds in the normal phase mode, while other known crown-ether CSPs show limited selectivity except for primary amines and they are preferably used with acidic aqueous mobile phases. [150-154]

5.3.1 Complementary selectivity provided by RN-CF6 and DMP-CF7

Figure 5-3 summarizes the separations obtained on the RN-CF6 CSP, the DMP-CF7 CSP and a combination of the two columns. The total number of separations achieved on the RN-CF6 CSP and the DMP-CF7 CSP are 69, and 69, respectively. Of these, there were 43 baseline separations on the RN-CF6 column and 41 on the DMP-CF7 column. Enantiomers of 25 compounds were separated only by the RN-CF6 CSP, while another 25 were separated only with the DMP-CF7 CSP. It was often observed that some analytes were baseline separated on the RN-CF6 column, while only a partial separation or no separation was observed on the DMP-CF7 CSP, and vice versa.

Therefore, the RN-CF6 and DMP-CF7 CSPs demonstrated complementary enantioselectivities.
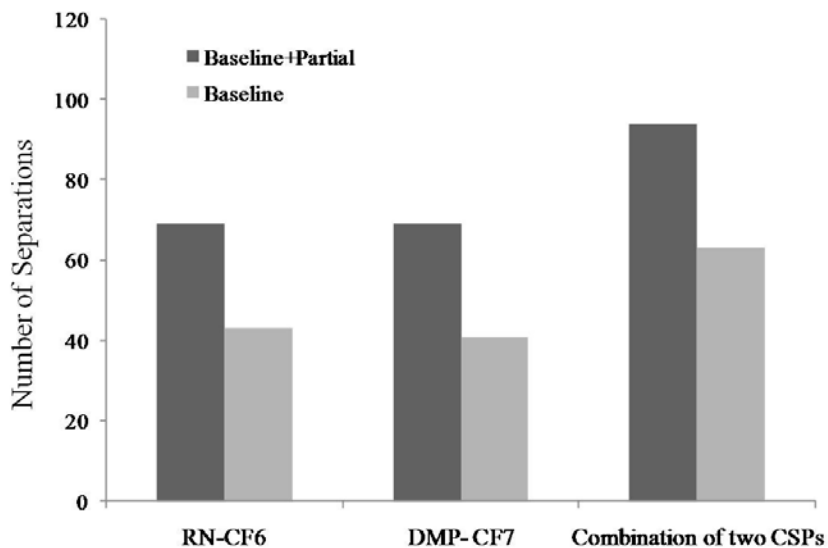
Figure 5-3 Summary of enantioseparations obtained on the RN-CF6 and DMP-CF7 based chiral stationary phases.

Figure 5-4 gives two examples of the complementary selectivity provided by these columns. Enantiomers of bendroflumethiazide were baseline separated with the RN-CF6 CSP with a high selectivity (α=1.16) while no separation was observed on the DMP-CF7 CSP (Figure 5-4A). The RN-CF6 column gave a partial separation of 4-benzyloxazolidine-2-thione with a tiny shoulder (α=1.02) while the DMP-CF7 column provided high selectivity (α=1.15) and a baseline separation (Figure 5-4B).
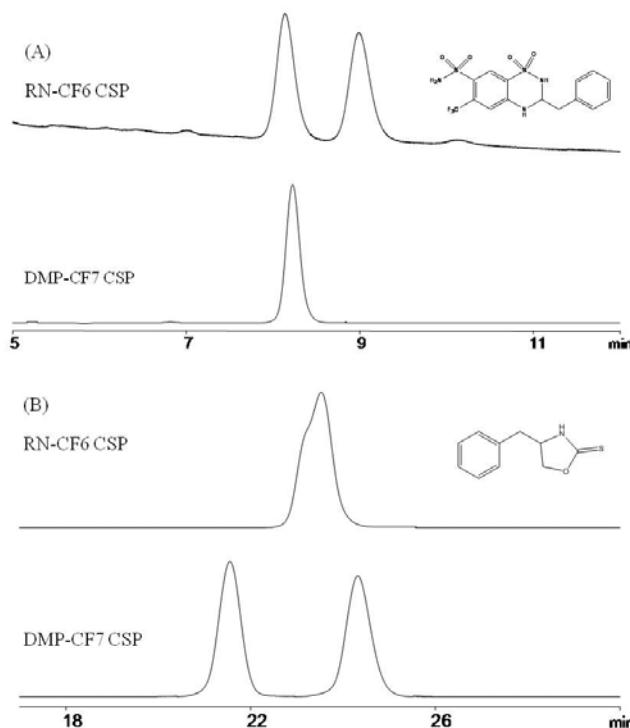
Figure 5-4 Comparison between RN-CF6 and DMP-CF7 stationary phases. The analyte and mobile phase are (A) bendroflumethiazide, 60heptane/40ethanol/0.1TFA; (B) 4-benzyloxazolidine-2-thione, 90heptane/10ethanol/0.1TFA.

Although the overall success rates of the RN-CF6 and DMP-CF7 CSPs are the same (31%), their capabilities for chiral recognition for various classes of compounds are different. For example, only 2 out of 8 in group A (chiral acids), 4 out of 15 in group B (amines), and 4 out of 10 in group C (alcohols) were separated by both columns. The others compounds (over 60%) in these three groups were only separated by one column (either the RN-CF6 or the DMP-CF7 CSP). However, for group E (others), these two stationary phases shared a bigger overlap and about 50% analytes in group E (Table 5-1) were separated by both columns. For Ru complexes (group D), both columns provided

enantiomeric separation, although the RN-CF6 CSP gave a much higher selectivity than the DMP-CF7 CSP.

Considering the success rate of two columns for different groups of compounds, the DMP-CF7 CSP obtained greater success than the RN-CF6 CSP when separating chiral acids, based on the fact that 8 analytes were separated by the DMP-CF7 CSP compared to 3 by the RN-CF6 CSP. It was also found that the RN-CF6 CSP provided a higher enantioselectivity toward chiral amines (group B) than the DMP-CF7 CSP in most of cases. The characteristic that the RN-CF6 and DMP-CF7 columns offered complementary selectivities for different groups of compounds is advantageous when selecting columns for separating a large number of different compounds.

5.3.2 Effects of the size of the cyclofructan ring, i. e., CF6 vs CF7 on
enantioseparations

The effects of the size of the central crown ether core (*i. e.*, 18-crown-6 vs 21-crown-7) in CF6 and CF7 can be examined by comparing DMP-CF6 (data shown in ref. 27) and DMP-CF7 as LC chiral selectors. The capabilities of chiral recognition provided by DMP-CF6 and DMP-CF7 CSPs are quite different. The DMP-CF7 column provided significantly different resolution for over 60 % of analytes separated by the DMP-CF6 CSP. Generally, the DMP-CF7 CSP gave better performance than the DMP-CF6 CSP for separating acidic and neutral analytes. For example, enantiomers of dansyl-norleucine cyclohexylammonium salt were well separated with an extremely high selectivity (α = 2.03) by the DMP-CF7 CSP while only a partial separation was obtained on the DMP-CF6 CSP (shown in Figure 5-5). For amine containing compounds, the DMP-CF6 column gave higher selectivity than the larger DMP-CF7 based CSP. Also, this was true for all derivatized-CF6 stationary phases and respective CF7 columns. Therefore, the size of

the cyclofructan ring plays a significant role in interactions between amine containing analytes and the chiral selector.
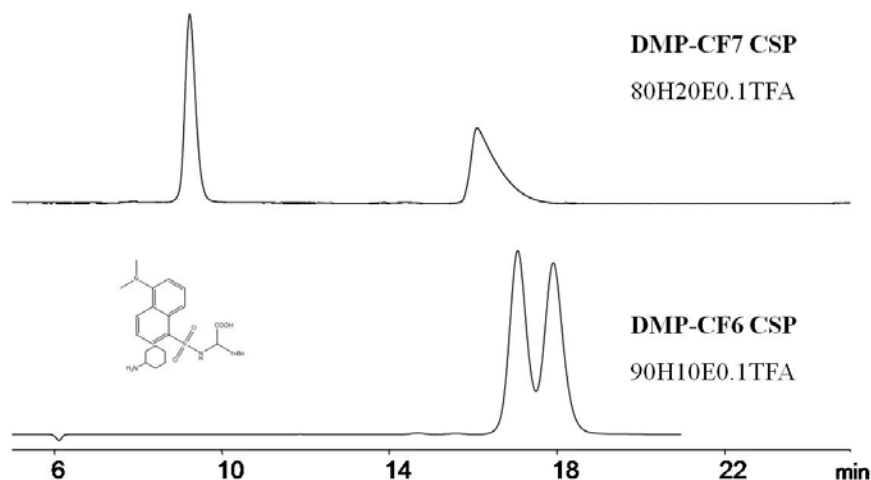
Figure 5-5 Comparison between DMP-CF6 and DMP-CF7 CSPs. The analyte is dansyl-norleucine cyclohexylammonium salt.

The selectivity of the RN-CF6 and RN-CF7 stationary phases also were compared. The relative performance of the RN-CF6 and RN-CF7 CSPs was opposite to that found for the DMP functionalized cyclofructans. Indeed, it was the smaller RN-CF6 CSP that usually provided better resolution than the larger RN-CF7 CSP. Also, it is noted that the chromatographic differences between the RN-CF6 and RN-CF7 CSPs are much smaller compared to the more substantial difference between the DMP-CF6 and DMP-CF7 columns.

The difference between CF6 and CF7 is the central crown ether size and the number of available hydroxyl groups. Although CF6 and CF7 differ only by one fructose unit, their spatial structures are quite different according to computational modeling studies. [70] Also, the separation of CF6 and CF7 on a HILIC stationary phase showed that their number of available hydroxyl groups was quite different. [148] There is a much

bigger difference in the separation of CF6 and CF7, than is found for the comparable separation of α-, β-, and γ-cyclodextrin. This may be due to the extensive internal hydrogen bonding of cyclofructans. [148]

Currently, there is no reported crystal structure of CF7 and it is difficult to give more detailed explanations about the chromatographic differences between CF6 and CF7-based stationary phases without further study. However, the chromatographic results clearly indicated that the size and geometry of cyclofructan is an important factor in interactions between cyclofructans and chiral analytes.

5.3.3 Effects of the nature of the derivatization group on enantioseparations

The nature of the derivatization group also contributes to chiral recognition. Our earlier studies of various aliphatic- and aromatic-derivatized CF6 stationary phases support this contention. [65] The nature of the aromatic group plays an important role since the derivatizing groups change the interactions between analyte and stationary phase (*i.e.*, steric repulsion, π-π interaction, dipolar interactions, etc). Also, the R-naphthylethyl moiety itself is chiral, and its defined stereogenic configuration may contribute additional interaction sites.

Special attention was paid to the separations of racemic ruthenium(II) complexes. The RN-CF6 stationary phase provided significantly better selectivity toward Ru complexes than other derivatized-CF6 stationary phases, such as DMP-CF6, R/S-methylphenyl-CF6. [65] This fact indicated that the nature of the derivative plays a major role in the chiral recognition process between the Ru complex and the chiral selector. Comparisons between RN-CF6 and SN-CF6 provide further insights about the chiral recognition mechanism. The configuration of the naphthylethyl carbamate moieties is opposite for the "RN" (R-naphthylethyl) and "SN"-CF6 (S-naphthylethyl) stationary phases. RN-CF6 easily separates enantiomers of Ru(II) complexes, with

enantioselectivities ranging from 1.49-2.90. The SN-CF6 column can also baseline separate all of the tested complexes, with enantioselectivities ranging from 1.17-1.97 (data not shown). The most important fact is that enantiomers of these metal complexes were separated on RN- and SN-CF6 columns with opposite elution orders. This indicates that the substituent significantly contributed to the chiral recognition. The stereogenic configuration of the naphthylethyl carbamate group is a major factor for chiral recognition, and the cyclofructan 6 plays a secondary role. If CF6 played no role in the enantiomeric selectivity for these complexes, then the SN-CF6 CSP would produce exactly opposite enantiomeric separations. However, this is not the case.

Although the exact orientation of the aromatic groups of derivatized-CFs is not known, it is likely that chiral recognition is the sum of many different interactions arising from different parts of the bonded chiral selector. Both the derivative group and the core cyclofructan play an important role in enantiomeric separations.

5.3.4 Effects of the analyte structure

To try to understand the separation mechanism, it helps to look at closely related compounds, where slight structural changes greatly alter enantioselectivity. In Group E, compounds 44-51 are a series of structurally related compounds, which all contain a five-member ring, having -O-CO-NH-, or -S-CO-NH-, or -S-CS-NH- units.

For example, 4-phenyl-2-oxazolidinone (E44) and 4-phenylthiazolidine-2-thione (E45) have similar chemical structures, in which the only difference is that the -O-CO-NH- moiety in compound E44 is replaced by -S-CS-NH- in E45. Chromatographic results indicate that the RN-CF6 stationary phase provided enantioselectivity toward E45, but not E44, while the DMP-CF7 column separated racemic E44, but not E45. Another analogous example is the comparison of 4-benzyloxazolidine-2-thione (E46) and 4-benzylthiazolidine-2-thione (E47). E46 contains a -O-CS-NH- unit, while E47 has a -S-

CS-NH unit. The other functionalities are the same. The RN-CF6 CSP provided enantioseparation only for E46. The DMP-CF6 column showed significantly different selectivity toward E46 and E47 (1.15 vs 1.09). The structural difference between E44/E45, and E46/47 mainly affected dipolar interactions or hydrogen bonding interactions. The facts that the CSPs provided hugely different selectivities indicated that dipolar interactions or hydrogen bonding interactions play an import role in chiral recognition of cyclofructan chiral selctors.

Π-π interactions and steric interactions may significantly contribute to enantiomeric separations on cyclofructan-based stationary phases as well. For example, compared with E44, compound E51 has an additional phenyl group, which can provide additional π-π interactions and increase the steric bulkiness of the analyte. The fact that the DMP-CF7 stationary phase only separated racemic E44 while the RN-CF6 CSP exhibited chiral recognition only for E51, demonstrated that π-π and/or steric interactions can significantly affect chiral recognition interactions between the chiral selector and analyte.

5.4 Conclusions

The RN-CF6 and DMP-CF7 stationary phases provided chiral recognition toward a variety of compounds, including acidic, basic, neutral organic compounds, and metal complexes. It is interesting that they exhibited complementary selectivity and the combination of two columns provided enantioseparations for 43% of test analytes. Generally, better separation of amine containing compounds was obtained on the RN-CF6 stationary phases, while the DMP-CF7 column worked more effectively for acidic compounds in most cases. It was found that both the crown ether ring and the nature of the derivative group on the cyclofructans affected selectivity and enantiomeric separations.

These extensive chromatographic results offered useful information for method development of specific chiral analytes and a better knowledge of enantioseparation mechanism. Also, they provide insight concerning design of new chiral stationary phases. Currently, the studies in which both ionic groups (anionic or cationic) and aromatic groups are inserted in one CF molecule, are underway, in hopes of finding more widely-applicable chiral selectors.

Chapter 6

Enantiomeric impurities in chiral catalysts, auxiliaries and synthons used in

enantioselective syntheses: Part 4

Abstract

The enantiomeric purity of chiral reagents used in asymmetric syntheses directly affects the reaction selectivity and the product's enantiomeric excess. In this work, 46 recently available chiral compounds were evaluated to determine their actual enantiomeric compositions. They have not been assayed previously and/or have been introduced after 2006, when the last comprehensive evaluation of commercially available chiral compounds was reported. These compounds are widely used in asymmetric syntheses as chiral synthons, catalysts, and auxiliaries. The effective enantioselective analysis methods include HPLC approaches using Chirobiotic, Cyclobond and LARIHC series chiral stationary phases and a GC approach using Chiraldex chiral stationary phases. Accurate, efficient assays for selected compounds are given. All enantiomeric test results were categorized within five impurity levels (i.e., <0.01%, 0.01-0.1%, 0.1-1%, 1-10% and >10%). Different date of the same reagent from the same company could have different levels on enantiomeric impurities. The majority of the tested reagents were found to have less than 0.1% enantiomeric impurities. Only one of the chiral compounds was found to have enantiomeric impurities exceeding 10%.

6.1 Introduction

Enantioselective reactions are of great importance to chemists involved in asymmetric syntheses. When enantiomeric reagents with unknown purities are used, the underestimated contaminants, including various amounts of enantiomeric impurities, in

the "single-enantiomer" reaction will produce various amounts of enantiomeric impurities in the product, making the "apparent e.e." value less than might be expected. Furthermore, when using a chiral reagent or catalyst to add an additional stereogenic center to a chiral substrate, kinetic effects could further increase the amount of unwanted stereoisomeric impurities. In biological processes, these undesired enantiomeric byproducts usually have different impacts on pharmacokinetics or pharmacodynamics and thus give different therapeutic results [155].

The enantiomeric purity of a product is mainly due to three factors: (a) the enantioselectivity of the reaction; (b) the enantiomeric excess of the starting material and/or the catalyst/auxiliary used; and (c) the susceptibility for the desired product to racemize, especially during work-up or storage [156, 157]. Although the stereoselectivity of asymmetric synthetic processes continues to improve, an awareness of the enantiomeric composition of chiral reagents remains essential. Zukowski once reported the importance of enantiomeric purity of Jacobsen's catalyst in the quality control of the product [158]. Unfortunately, the presence and effects of enantiomeric impurities in commercially available chiral reagents often are neglected by the supplier and the consumer. The only impurities noted as being present are usually nonisomeric substances. Therefore, it is useful to know the enantiomeric purity of the most common, commercial, chiral reagents for enantioselective syntheses. Also it has been shown that the batch to batch enantiomeric purity of the same compound from the same supplier can differ considerably [156]. Thus having a facile method available to evaluate chiral reagents also is useful.

Previously, we have reported detectable amounts of enantiomeric impurities in nearly 300 commercial chiral compounds, which are widely applied in asymmetric synthesis as chiral catalysts/catalyst ligands, synthons (synthetic building blocks), chiral

auxiliaries, and chiral resolving agents [156, 157, 159]. The majority of chiral reagents were determined to have moderate to low levels (<1%) of enantiomeric impurities, while some had unexpectedly high levels (>10%). The general level of enantiomeric impurities reported in 2006 was lower than that reported in 1998-1999.

New chiral compounds, catalysts, auxiliaries, and synthons are continuously being developed. The most useful ones often become commercially available. Herein, we evaluate new chiral compounds that have not been assayed previously and/or have been introduced after 2006, when the last comprehensive evaluation of commercial chiral compounds was reported [159].

6.2 Experimental

6.2.1 Materials

The HPLC columns (25 cm×4.6 mm, i.d.) used were LARIHC CF6-P (isopropyl carbamated-cyclofructan 6 [65, 145]), Cyclobond I 2000 (native β cyclodextrin [160]), Cyclobond I 2000 RSP (2-hydroxylpropyl-β-cyclodextrin [161]), Cyclobond I 2000 SN ((S)-naphthylethyl carbamated-β-cyclodextrin [125, 126]), Cyclobond I 2000 DNP (dinitrophenyl ether linked-β-cyclodextrin [129]), Chirobiotic T (teicoplanin [162]), Chirobiotic TAG (teicoplanin aglycone [163]), Chirobiotic V (vancomycin [47, 164]), Chirobiotic V2 (vancomycin [165]). The LARIHC CF6-P column was obtained from AZYP, LLC (Arlington, TX). The other used columns were obtained from Supelco, LLC (Bellefonte, PA). GC analysis was performed using a 30 m × 0.25 mm i.d., 0.12 µm film thickness Chiraldex G-TA (2,6-di-O-pentyl-3-trifluoroacetyl-β-cyclodextrin [166, 167]) column and a 20 m × 0.25 mm i.d., 0.12 µm film thickness G-BP (2,6-di-O-pentyl-3-butyryl-γ-cyclodextrin [168]), which were also obtained from Supelco, LLC (Bellefonte, PA). All HPLC grade solvents, including methanol, acetonitrile, ethanol, heptane, were

purchased from EMD (Gibbstown, NJ). Water was purified by a Milli-Q Water Purification System (Millipore, Billerica, MA). Acetic acid, trifluoro-acetic acid, trifluoroacetic anhydride, triethylamine, ammonium acetate and all chiral compounds used in this study were obtained from Sigma-Aldrich (Milwaukee, WI).

6.2.2 Apparatus and methods

All LC enantiomeric separations were performed on an Agilent 1100 HPLC series system equipped with a quaternary pump, an autosampler, a diode array dectection (DAD) system and thermostat (Agilent Technologies, Palo Alto, CA). Data acquisition and analysis were obtained from the Chemstation software version Rev. B.01.03 in Microsoft Windows XP environment. Separations were carried out at room temperature unless stated otherwise. The wavelengths of UV detection were set at 210 nm, 230 nm, 254 nm and 280 nm. The injection volume and flow rate were set as 5 μL and 1.0 mL/min, respectively. All GC enantiomeric analyses were performed on an Agilent 6850 GC series system equipped with a flame ionization detetector (FID) and an autosampler (Agilent Technologies, Palo Alto, CA). Data acquisition and analysis were obtained from Chemstation plus software (Rev. B.01.02). All analyses were performed with a helium carrier gas flow rate of 1 mL/min and a split ratio of 100/1. The oven temperature was held isothermally. The injection port and the detector were set at 250 $^{\circ}$C and 280 $^{\circ}$C, respectively. Each sample was analyzed in duplicate. All enantioselective methods for quantification of 46 commercially available chiral reagents in HPLC and GC are detailed in Table 6-1 and Table 6-2, respectively. A method number from Table 6-1 is listed for each compound and the result is in Table 6-3.

Table 6-1 Optimal HPLC enantiomeric separation methods for determining e.e. valuses.

Method[a]	Column[b]	Mobile phase[c] (%, *v/v*)
LC-1	LARIHC CF6-P	ACN:MeOH:TEA:AA=90:10:0.4:0.6
LC-2	LARIHC CF6-P	MeOH:Buffer=20:80
LC-3	LARIHC CF6-P	Hep:EtOH:TFA=97:3:0.1
LC-4	LARIHC CF6-P	Hep:IPA:TFA=70:30:0.1
LC-5	Chirobiotic V	Hep:EtOH:TFA=92:8:0.1
LC-6	Chirobiotic V $\times$ 2	ACN:MeOH:TEA:AA=95:5:0.2:0.3 at 5 ^{o}C
LC-7	Chirobiotic T	Hep:EtOH:TFA=98:2:0.1
LC-8	Chirobiotic TAG	ACN:MeOH:TEA:AA=70:30:0.2:0.3
LC-9	Chirobiotic TAG $\times$ 2	ACN:MeOH:TEA:AA=75:25:0.2:0.3 at 10 ^{o}C
LC-10	Chirobiotic V2 $\times$ 2	ACN:MeOH:TEA:AA=20:80:0.2:0.3
LC-11	Cyclobond I 2000 RSP	ACN:MeOH:TEA:AA=90:10:0.2:0.3
LC-12	Cyclobond I 2000 RSP	ACN:MeOH:TEA:AA=97:3:0.4:0.2
LC-13	Cyclobond I 2000 RSP	MeOH:Water:TEA:AA=35:65:0.6:0.9

a. This notation is used to identify the separation techniques in Table 6-3.
b. Trade names for the HPLC columns used. Further information on these columns can be found in the Experimental section.
c. Mobile phase: ACN=acetonitrile; MeOH= methanol; EtOH= ethanol; IPA=isopropyl alcohol; Buffer=20 mM ammonium acetate, pH=4.1; TEA=triethylamine; AA=acetic acid; TFA=trifluoroacetic acid.

Table 6-2 Optimal GC enantiomeric separation methods for determinig e.e. valuses.

Method[d]	Column[e]	Length (m)	Temperature (^{o}C)	Flow rate (ml/min)
GC-1[f]	Chiraldex G-TA	30	100	1
GC-2	Chiraldex G-TA	30	90	1
GC-3	Chiraldex G-TA	30	40	1
GC-4[f]	Chiraldex G-BP	20	100	1
GC-5[f]	Chiraldex G-BP	20	110	1

d. This notation is used to identify the separation techniques in Table 6-3.
e. Trade names for the GC columns used. Further information on these columns can be found in the Experimental section.
f. Analyte with amino group was derivatized with trifluoroacetic anhydride to help the selectivity of separation and the volatility of analytes.

Typical enantioselective HPLC analysis for chiral reagents are shown in Figure 6-1. All results were calculated from at least three parallel measurements of samples of different concentrations. The methods listed in Table 6-1 gave more than baseline separations of enantiomers, with resolutions greater than 3.0 (R_s >3.0). Such high resolutions are necessary in order to detect small amounts of enantiomeric impurities in the presence of a large amount of the dominant enantiomers. When the level of enantiomeric impurity is greater than 1%, enantiomeric impurities can be directly quantified by peak areas for an appropriate concentration, as shown in Figure 6-1(a). When the level of enantiomeric impurity is lower than 1%, peak areas quantification is not always reliable as based on instrumental integration devices. The larger peak of the dominant enantiomer is usually off scale since a relatively large amount often must be injected. The concentration of the major compound which the large peak represents can be outside the linear dynamic range of the detector and often overloads a column. In these cases, the area of the largest peak can be underestimated. To solve this problem, the enantiomeric impurity should be quantified first by increasing the injection amount, then the dominant peak is measured by serial dilution to an appropriate concentration, as shown in Figure 6-1(b). If the enantiomeric impurity peak cannot be detected even after increasing the amount of the major analyte to overloaded condition on the column, then the level of the enantiomeric impurity is less than the detection limit for the method (which is 0.01% for this study, as shown in Figure 6-1(c).
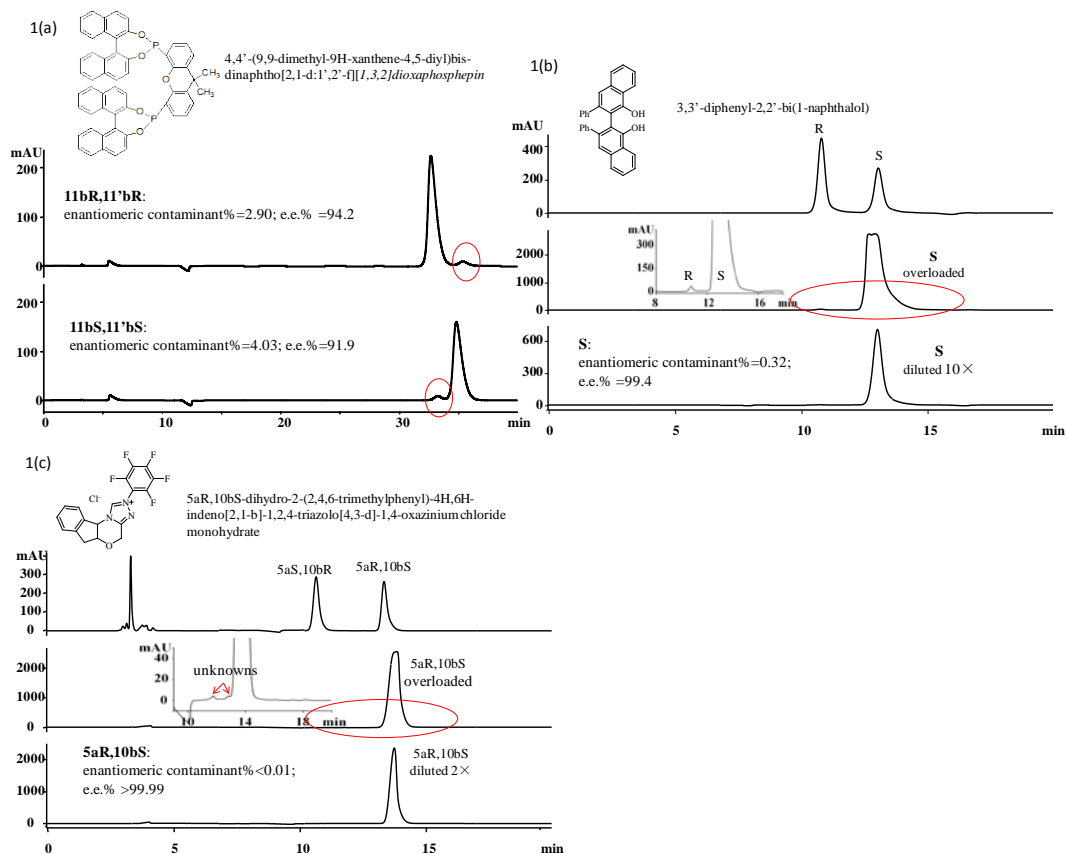
Figure 6-1 Typical enantiomeric impurities quantification.

6-1(a). Quantification of enantiomeric impurities in 4,4'-(9,9-Dimethyl-9H-xanthene-4,5-diyl)bis-dinaphtho[2,1-d:1',2'-f][1,3,2]dioxaphosphepin were determined on the Chirobiotic T column. Mobile phase: heptane/ethanol/trifluoroacetic acid 98/2/0.1, flow rate 1.0 mL/min, UV: 254 nm.

6-1(b). Quantification of enantiomeri impurity in (S)-3,3'-Diphenyl-2,2'-bi(1-naphthalol) on the LARIHC CF6-P column. Mobile phase: heptane/ethanol/trifluoroacetic acid 97/3/0.1, flow rate 1.0 mL/min, UV: 254 nm.

6-1(c). Quantification of enantiomeri impurity in (5aR,10bS)-Dihydro-2-(2,4,6-trimethylphenyl)-4H,6H-indeno[2,1-b]-1,2,4-triazolo[4,3-d]-1,4-oxazinium chloride monohydrate was determined on the LARIHC CF6-P column. Mobile phase: acetonitrile/methanol/triethylamine/acetic acid 90/10/0.4/0.6, flow rate 1.0 mL/min, UV: 254 nm.

120

6.3 Results and Discussion

This is the first time the LARIHC CF6-P column was used in the quantification of enantiomeric impurities of chiral reagents. This new stationary phase was developed in 2009, bonded isopropyl carbamated cyclofructan to silica gel. It shows superior selectivity for chiral primary amines, particularly, in the presence of organic solvents and even supercritical fluids [65, 145]. Surprisingly, the LARIHC CF6-P column also was successfully applied in quantification of some non-amine enantiomers, such as (5aR,10bS/5aS,10bR)-dihydro-2-(pentafluorophenyl)-4H,6H-indeno[2,1-b][1,2,4]triazolo[4,3-d][1,4]oxazinium chloride, (R/S)-3,3'-diphenyl-2,2'-bi(1-naphthalol) and (R/S)-1,1'-bi-2-naphthyl dimethanesulfonate. In addition, the LARIHC CF6-P column was used in the reversed phase mode to separate (3,5-dioxa-4-phosphacyclohepta [2,1-a:3,4-a']dinaphthalen-4-yl) dimethylamine. The Chirobiotic V2 column, a new version of vancomycin based chiral stationary phase, was another impressive column in this study. 23% of the total chiral compounds had enantiomeric impurities quantified on the Chirobiotic V2 column. It performed better than other Chirobiotic series columns both in baseline separation of enantiomers and quantification of enantiomeric impurities in Table 6-3.

Table 6-3 The enantiomeric composition of chiral catalysis, auxiliaries, synthons and resolving agents used in asymmetric syntheses.

Use in synthesis	Name and structure chiral reagent	Enantiomeric impurity %	Enantiomeric excess (e.e. %)	Method Number
Rovis Catalysts (the chiral NHC catalysts): (1). Used in intramolecular Stetter reactions. [169-171] (2). Used in an inverse electron demand Diels–Alder reaction of activated enals and α,β-unsaturated imines. [172, 173]	5a(R),10b(S)- Dihydro-2-(pentafluorophenyl)-4H,6H-indeno[2,1-b][1,2,4]triazolo[4,3-d][1,4]oxazinium chloride monohydrate 5a(S),10b(R)- Dihydro-2-(pentafluorophenyl)-4H,6H-indeno[2,1-b][1,2,4]triazolo[4,3-d][1,4]oxazinium chloride monohydrate	(5aS,10bR): <0.01	(5aR,10bS): > 99.99	LC-1
		(5aR,10bS): 0.03	(5aS,10bR): 99.9	

Table 6-3—*Continued*
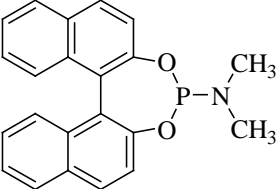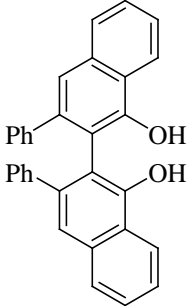
MonoPhos™ Ligands: Used in asymmetric allylic substitution reactions. [174]	(R)-(−)-(3,5-Dioxa-4-phosphacyclohepta[2,1-a:3,4-a']dinaphthalen-4-yl)dimethylamine (S)-(+)-(3,5-Dioxa-4-phosphacyclohepta[2,1-a:3,4-a']dinaphthalen-4-yl)dimethylamine	S: <0.01 R: <0.01	R: >99.99 S: >99.99	LC-2

VANOL ligand: (1). Used in asymmetric Diels-Alder, imine aldol, and aziridination reactions. [175-177] (2). Used in the addition of sulfonamides to Boc-activated aryl imines. [178-182] (3). A biaryl derived catalyst, used in the synthesis of chiral β-amino esters. [183, 184]	(R)-VANOL (R)-3,3'-Diphenyl-2,2'-bi(1-naphthalol) (S)-VANOL (S)-3,3'-Diphenyl-2,2'-bi(1-naphthalol)	S: 0.19 R: 0.32	R: 99.6 S: 99.4	LC-3

Table 6-3—*Continued*
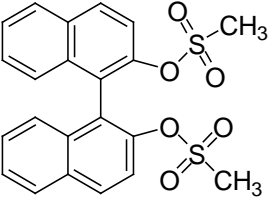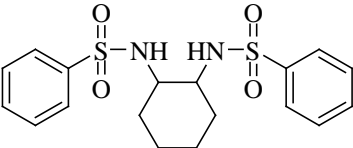
BINOL and Derivatives: (1). Used in asymmetric epoxidations. [185-188]	(R)-(−)-1,1'-Bi-2-naphthyl dimethanesulfonate (S)-(+)-1,1'-Bi-2-naphthyl dimethanesulfonate 	S: 0.07	R: 99.9	LC-4
		R: <0.01	S: >99.99	
(1). Used in asymmetric synthesis of acyclic epoxy alcohols and allylic epoxy alcohols. [189] (2). Used in the conjugate addition of aryl methyl ketone derived enamines to nitroalkenes. [190] (3). Used in practical the asymmetric synthesis of β-lactones. [191]	(1R,2R)-(+)-N,N'-Di-p-tosyl-1,2-cyclohexanediamine (1S,2S)-(−)-N,N'-Di-p-tosyl-1,2-cyclohexanediamine 	(1S,2S): <0.01 (1R,2R):<0.01	(1R,2R): >99.99 (1S,2S): >99.99	LC-5

Table 6-3—*Continued*

(1). Used in the carbon dioxide and epoxides coupling reactions to form cyclic carbonates. [192]	(R,R)-N,N'-Bis(3,5-di-tert-butylsalicylidene)-1,2-cyclohexanediaminoaluminum chloride	(S,S): <0.01	(R,R): >99.99	LC-5
(2). Used in the α-addition of isocyanides to aldehydes. [193]	(S,S)-N,N'-Bis(3,5-di-tert-butylsalicylidene)-1,2-cyclohexanediaminoaluminum chloride	(R,R): <0.01	(S,S): >99.99	
(3). Used in the enantioselective addition of indoles to arylnitroalkenes to enantiomerically enriched tryptamine precursors. [194] (4). Used in the asymmetric cyanohydrin synthesis. [195] (5). Applied in enantioselective conjugate cyanation of unsaturated imides [196-197] and enantioselective conjugate addition of indoles to simple α,β-unsaturated ketones. [198]				
Trost Ligands: (1). Used in asymmetric allylic alkylations. [199-202]	(R,R)-DACH-pyridyl Trost ligand (S,S)-DACH-pyridyl Trost ligand	(1S,2S): 0.25	(1R,2R): 99.5	LC-6
		(1R,2R): <0.01	(1S,2S): > 99.99	

Table 6-3—*Continued*
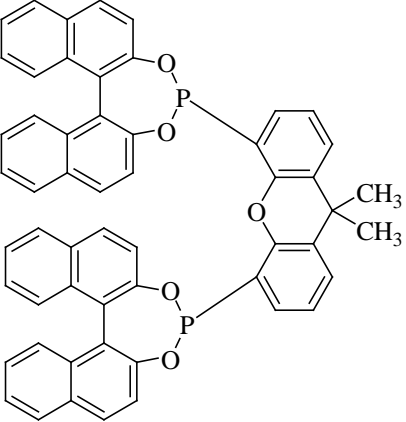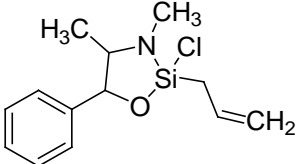
Reetz Ligands: (1). Applied in Noyori-type asymmetric transfer hydrogenation of prochiral ketones. [203]	(11bR,11'bR)-4,4'-(9,9-Dimethyl-9H-xanthene-4,5-diyl)bis-dinaphtho[2,1-d:1',2'-f][1,3,2]dioxaphosphepin (11bS,11'bS)-4,4'-(9,9-Dimethyl-9H-xanthene-4,5-diyl)bis-dinaphtho[2,1-d:1',2'-f][1,3,2]dioxaphosphepin	(11bS,11'bS): 2.90	(11bR,11'bR): 94.2	LC-7
		(11bR,11'bR): 4.03	(11bS,11'bS): 91.9	
Leighton's Strained Silacycles: (1). Used in enantioselective allylation and crotylation reactions [204, 205], such as the allylation of acylhydrazone. [206] (2). Used in the enantioselective synthesis of tertiary carbinamines. [207]	(4R,5R)-2-Allyl-2-chloro-3,4-dimethyl-5-phenyl-1-oxa-3-aza-2-silacyclopentane (4S,5S)-2-Allyl-2-chloro-3,4-dimethyl-5-phenyl-1-oxa-3-aza-2-silacyclopentane	(4S,5S): <0.01	(4R,5R): >99.99	LC-8
		(4R,5R): <0.01	(4S,5S): >99.99	

126

Table 6-3—*Continued*
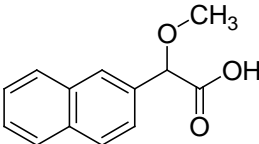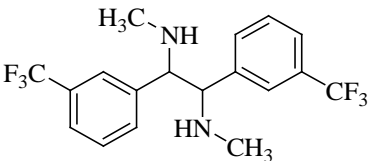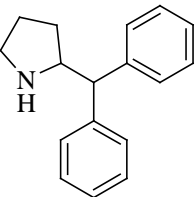
New chiral anisotropic reagents, NMR tools to elucidate the absolute configurations of long-chain organic compounds. [208]	(R)-α-Methoxy-2-naphthylacetic acid (S)-α-Methoxy-2-naphthylacetic acid	S: 0.14 R: 1.14	R: 99.7 S: 97.7	LC-9
Used in the stereoconvergent alkyl-alky Suzuki cross-coupling of unactivated electrophiles [209], activated secondary alkyl electrophiles [210], and unactivated homobenzylic halides [211].	(1R,2R)-(+)-N,N'-Dimethyl-1,2-bis[3-(trifluoromethyl)phenyl]ethanediamine (1S,2S)-(−)-N,N'-Dimethyl-1,2-bis[3-(trifluoromethyl)phenyl]ethylenediamine	(1S,2S)[g]: 2.24 (1S,2S)[h]: 1.17 (1R,2R)[a]: <0.01 (1R,2R)[b]: 0.14	(1R,2R)[g]: 95.5 (1R,2R)[h]: 97.7 (1S,2S)[a]:>99.99 (1R,2R)[b]: 99.7	LC-10
Used as chiral solvating agents to determine the enantiomeric composition of chiral carboxylic acids directly by NMR analysis, chiral pyrrolidines. [212]	(R)-(+)-2-(Diphenylmethyl)pyrrolidine (S)-(−)-2-(Diphenylmethyl)pyrrolidine	S: <0.01 R: <0.01	R: >99.99 S: >99.99	LC-10

Table 6-3—*Continued*

CBS Catalysts: Used in the asymmetric reduction of prochiral ketones, α-hydroxy acids, α-amino acids, C2 symmetrical ferrocenyl diols, propargyl alcohols. [213-219]	(R)-(+)-2-Methyl-CBS-oxazaborolidine (S)-(−)-2-Methyl-CBS-oxazaborolidine	S: <0.01	R: >99.99	LC-10
		R: <0.01	S: >99.99	
Used to generate chiral Lewis acids and then applied in the enantioselective Diels-Alder reaction. [219-221]	(R)-(+)-o-Tolyl-CBS-oxazaborolidine solution (0.5 M in toluene) (S)-(−)-o-Tolyl-CBS-oxazaborolidine solution	S: <0.01	R: >99.99	LC-10
		R: <0.01	S: >99.99	

Table 6-3—*Continued*
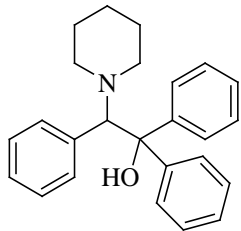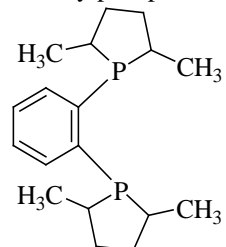
(1). Used in the enantioselective arylation of aldehydes. [222] (2). Used in a formal synthesis of (+)-Incrustoporin. [223] (3). Used in the enantioselective addition of diethylzinc to benzaldehyde. [224]	(R)-(−)-2-Piperidino-1,1,2-triphenylethanol (S)-(+)-2-Piperidino-1,1,2-triphenylethanol R: <0.01	S: <0.01 S: >99.99	R: >99.99	LC-10
DuPhos and BPE Phospholane Ligands and Complexes: (1). Used as chiral auxiliary in asymmetry [2+2+2] cycloaddition of α,ω-diynes. [225] (2). Used in asymmetric alkylation of N-diphenylphosphinoylimines. [174] (3). Used in the rhodium-complex catalyzed asymmetric hydrogenation. [226]	(−)-1,2-Bis[(2R,5R)-2,5-dimethylphospholano]benzene (+)-1,2-Bis[(2S,5S)-2,5-dimethylphospholano]benzene (2R,5R): <0.01	(2S,5S): <0.01 (2S,5S): >99.99	(2R,5R): >99.99	LC-11

129

Table 6-3—*Continued*
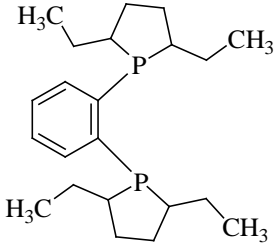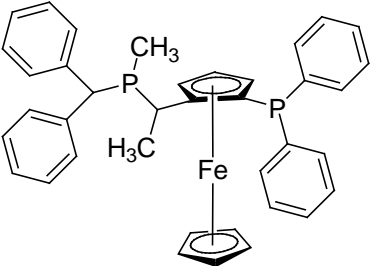
DuPhos and BPE Ligands: (1). Used in the synthesis of chiral β2-amino acids by asymmetric hydrogenation. [227] (2). Used in the rhodium-catalyzed intermolecular alkyne hydroacylation. [228] (3). Used in the asymmetric hydrogenantion of protected allylic amines. [229]	(−)-1,2-Bis[(2R,5R)-2,5-diethylphospholano]benzene (+)-1,2-Bis[(2S,5S)-2,5-diethylphospholano]benzene	(2S,5S): <0.01	(2R,5R): >99.99	LC-12
		(2R,5R): <0.01	(2S,5S): >99.99	
		R: <0.01	S: >99.99	
P-Phos, PhanePhos and BoPhoz™ Ligands: Used in rhodium-catalyzed hydrogenations. [230-232]	(R)-N-Methyl-N-diphenylphosphino-1-[(S)-2-diphenylphosphino)ferrocenyl]ethylamine (S)-N-Methyl-N-diphenylphosphino-1-[(R)-2-(diphenylphosphino)ferrocenyl]ethylamine	S,R: 1.08	R,S: 97.8	LC-13
		(R,S): 0.10	(S,R): 99.8	

130

Table 6-3—*Continued*
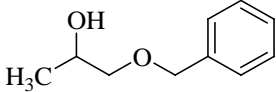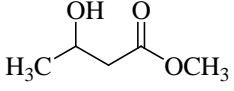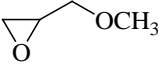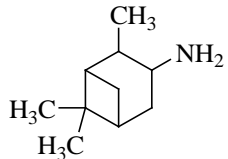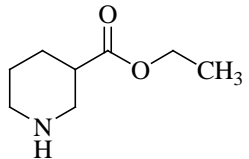
(1). Complex esters as antiwear agents. [233] (2). Used in the synthesis of enantiomeric N-(2-phosphonomethoxypropyl) derivatives of purine and pyrimidine bases. [234]	(R)-(−)-1-Benzyloxy-2-propanol (S)-(+)-1-Benzyloxy-2-propanol ![structure] 	S: 0.66 R: 0.33	R: 98.7 S: 99.3	GC-1
(1). Used to increase NADPH availability in *Escherichia coli*. [235] (2). Used in the total synthesis of fully hydroxy-protected mycolactones and their stereoisomerization upon deprotection. [236] (3). Used as a building blocker in the synthesis of (2S)-2-methyltetrahydropyran-4-one. [237] (4). Applied in situ modification of nickel catalysts to the enantio-differentiating hydrogenation of methyl acetoacetate. [238]	Methyl (R)-3-hydroxybutyrate Methyl (S)-3-hydroxybutyrate ![structure] 	S: <0.01 R: 0.51	R: >99.99 S: 99.0	GC-2
(1). Used as a building blocker in the azaphosphatranes organocatalyzing of carbonate synthesis from CO_2 and epoxides. [239] (2). Used in the asymmetric synthesis of β-hydroxy-cyclopentadienyl ligands and of their bidentate lanthanide complexes. [240] (3). Used as a building blocker in the asymmetric reaction of oxiranes with S-phenyl thioesters catalyzed by quaternary onium salts or crown ether-metal salt complexes. [241]	(R)-(−)-Glycidyl methyl ether (S)-(+)-Glycidyl methyl ether ![structure] 	S: 0.65 R: 0.14	R: 98.7 S: 99.7	GC-3

Table 6-3—*Continued*

(1). Used as a building blocker in the enantioselective Tsuji allytation. [242] (2). Used in the asymmetric epoxidation of alkenes mediated by chiral iminium slats. [243-246] (3). Used as a chiral derivatizing agent for GC analysis of optical carboxylic acids. [247]	(1R,2R,3R,5S)-(−)-Isopinocampheylamine (1S,2S,3S,5R)-(+)-Isopinocampheylamine	S: 0.11 R: 0.68	R: 99. 8 S: 98.6	GC-4
(1). Used as a building blocker in the synthesis of potent and highly selective inhibitors. [248] (2). Used as a building blocker in the synthesis of stereoisomers of antithrombotic nitpecotamides. [249] (3). Used as a building blocker in the oxidative C-arylation of free (NH)-heterocycles. [250]	(R)-Ethyl piperidine-3-carboxylate (E)-Ethyl piperidine-3-carboxylate	S: 10.9 R: 9.59	R: 78.2 S: 80.8	GC-5

g. (1R,2R)-(+)-N,N'-Dimethyl-1,2-bis[3-(trifluoromethyl)phenyl]ethanediamine and (1S,2S)-(−)-N,N'-Dimethyl-1,2-bis[3-(trifluoromethyl)phenyl]ethylenediamine were purchased in March 2012

h. (1R,2R)-(+)-N,N'-Dimethyl-1,2-bis[3-(trifluoromethyl)phenyl]ethanediamine and (1S,2S)-(−)-N,N'-Dimethyl-1,2-bis[3-(trifluoromethyl)phenyl]ethylenediamine were purchased in March 2013.

In this study, the majority of the tested chiral compounds (54%) were found to have less than 0.01% enantiomeric impurities. Approximately 7% of the compounds had from 0.01% to 0.1% enantiomeric impurities, while 24% of the tested compounds had 0.1-1% enantiomeric impurities. Finally, 13% of the tested chiral compounds had enantiomeric impurities at the 1-10% levels and only one of the chiral reagents was found to have enantiomeric impurities exceeding 10%. The level of enantiomeric contaminants found in chiral reagents in the present work was compared with those that were assayed in 1998-1999 and 2006 [156, 157, 159], and the results are shown in Figure 6-2. The number of chiral compounds with only trace levels of enantiomeric impurities approached 54% in this study, whereas fewer chiral compounds of this purity were available prior to 1998-1999, with 20% having less than 0.01% enantiomeric impurities at that time [156, 157]. The highest enantiomeric impurity in chiral compounds was found in the assay of (R)-ethyl piperidine-3-carboxylate. It was determined by GC method to have 10.9% of enantiomer. However, the highest enantimeric impurity in the 1998-1999 analysis work was (R)-tert-butyl-4-formyl-2,2-dimethyl-3-oxazolidine, which contained 15.1% of the (S)-enantiomer. In 2006, (R)-1-indanol was reported to have a 13.8% enantiomeric impurity. The overall decrease in levels of enantiomeric impurities in the more modern reagents is apparent. This is likely the result of continual improvements in enantioselective syntheses and the increasing attention to enantiomeric purity quality control in the manufacturing process.
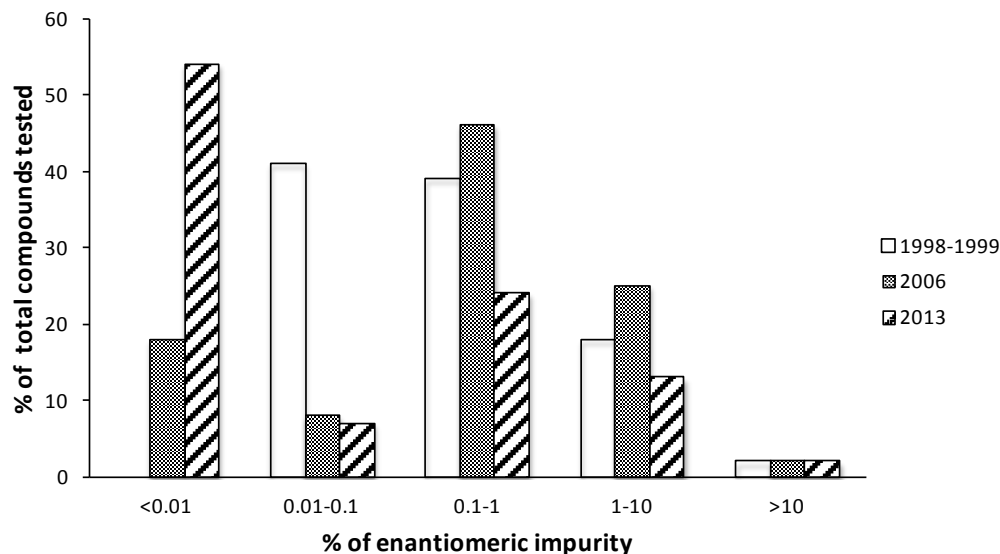
Figure 6-2 Comparison of results obtained in this study (2013) and previous results
obtained in 2006 and 1998-1999.

Finally, it should be noted that when enantiomers of a compound/reagent are
both available, it is not uncommon for them to have different e.e. values. This is clearly
observed in the assay of N,N'-dimethyl-1,2-bis[3-(trifluoromethyl)phenyl] ethanediamine.
The R,R-configuration compound had 2.24% of the S,S-enantiomer, but the S,S-reagent
had less than 0.01% of the R,R-enantiomer. These results are consistent with findings in
other studies. In addition, enantiomeric impurities were variable from batch to batch of
chiral regents, even which were purchased from the same source [156]. For example,
(1R,2R)-N,N'-dimethyl-1,2-bis[3-(trifluoromethyl) phenyl] ethanediamine contained
(1S,2S)-enantiomer impurity 2.24% (purchased in March 2012 from Sigma-Aldrich) and
1.17% (purchased in March 2013 from Sigma-Aldrich), respectively.

Obviously, it is beneficial to use highly pure chiral reagents in asymmetric
syntheses. This can be achieved by further improved isolation and purification of chiral

compounds in the manufacturing process. As new chiral compounds are constantly being developed and applied in asymmetric synthesis, it remains important to provide some information as to the enantiomeric composition and to have available facile approaches for separation and quantification.

Chapter 7

Navive/derivatized cyclofructan 6 bound to resin via "click" chemistry

as stationary phases for achiral/chiral separations

Abstract

Resin bound cyclofructan 6 (CF6) based stationary phases were prepared by immobilizing functionalized 4-azido-β-cyclofructan 6 (or its derivatives) to chloromethyl modified styrene divinylbenzene (MCI GEL™ CSP50/P10 CMS) via a 1,2,3-triazole linker. The resin bound native CF6 stationary phase (CF6-CMS) appears to have potential in HILIC separations of different types of polar compounds. The isopropyl carbamate derivatized stationary phases (IP-CF6-CMS) can be used as pH stable chiral stationary phases (CSPs) in HPLC. Under the optimum mobile phase conditions, 37 different types of chiral compounds have been separated on the IP-CF6-CMS column. The optimum mobile phase contained of acetonitrile/methanol/triethylamine/acetic acid 70/30/0.2/0.5 is utilized as the starting condition for enantiomeric separations on the IP-CF6-CMS column. Lowering the separation temperature also is beneficial for these separations. The selectivity for some analytes on the IP-CF6-CMS column is comparable with that on the silica gel based LARIHC-CF6 column. These results indicated that there is potential for using these less expensive, but stable resin based cyclofructan columns for HILIC or chiral separations in process chemistry. Finally, using 1-(1-naphthyl)-ethylamine as the model analyte, the column demonstrated excellent stability and reproducibility.

7.1 Introduction

Cyclofructans obtained by enzymatic conversion of inulin, are new types of macrocyclic oligosaccharides [63, 64]. They consist of six or more β-(2→1) linked D-

fructofuranose units and their names are commonly abbreviated as CF6, CF7, CF8, etc. Among cyclofructans, CF6 has attracted most attention due to its highly defined geometry and its availability in pure form [70]. Each β-(2→1) linked D-fructofuranose unit contains one primary hydroxyl group and two secondary hydroxyl groups, which provide these molecules with a hydrophilic character. The unique CF6 structure makes it possible to use them as surface moieties on chromatographic stationary phases. Such stationary phases can separate polar analytes in the hydrophilic interaction liquid chromatography (HILIC) mode. This special LC mode was used in separating a mixture of fructose, glucose, and mannose on ion exchange stationary phases as early as in the 1950s [5] and also was used in separation of saccharides and sugar alcohols on the cyclodextrin stationary phases in 1980s [4, 7, 8]. In 1990, the acronym HILIC was coined for the analysis of hydrophilic substances, such as proteins, peptides and nucleic acids [9]. HILIC is able to retain and separate polar and hydrophilic analytes, which often have insufficient retention and resolution in RPLC. Recently, HILIC has emerged as an increasingly popular chromatographic technique and has become a viable option to RPLC. FRULIC columns [4, 20, 114], as a type of native/derivatized cyclofructan 6 based stationary phases, appeared to have exceptionally broad applicability for HILIC separations, including nucleosides and nucleic acid base compounds, xanthenes, β-blockers, salicylic acid and its derivatives, amino acids, oligosaccharides, etc..

While native CF6 has limited capabilities as a chiral selector, Armstrong and co-workers have found that certain derivatives of cyclofructan, could be highly selective for different types of chiral molecules in HPLC, GC, and CE [65-67, 145, 251-260]. It appears that partial derivatization of the cyclofructan hydroxyl groups disrupts the molecular internal hydrogen bonding, therefore making the core of the molecule more accessible (Figure 7-1) [145]. In particular, aliphatic-derivatized CF6 with a low degree of

137

substitution, i.e. LARIHC CF6-P, showed baseline separation for above 90% of tested chiral primary amines, particularly, in the presence of organic solvents and even supercritical fluids [65, 145]. That is contrast to all known chiral crown ether CSPs that work exclusively with aqueous acidic solvents.
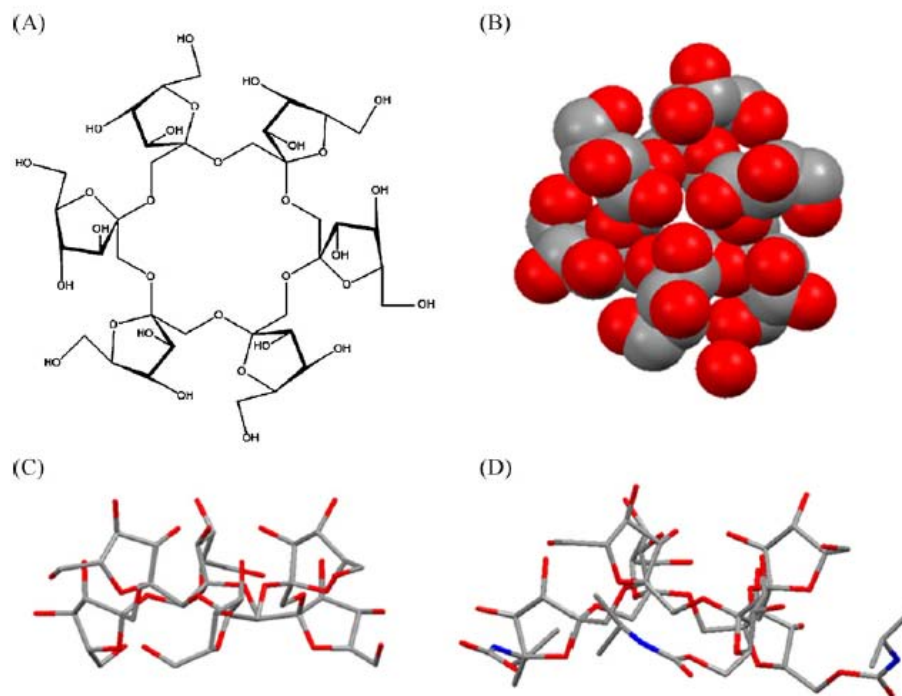
Figure 7-1 Crystal structure of CF6 and modeling structure of the isopropyl carbamated-CF6 (IP-CF6). (A) molecular structure of CF6; (B) crystal structure of CF6, spacefilling style (Hydrophilic side up); (C) crystal structure of CF6, capped stick style (side view); (D) modeling structure of isopropyl carbamated-CF6. For all structures, hydrogens are not shown. Color scheme: oxygen atoms, red; carbon atoms, grey; hydrogen atoms, white; nitrogen atoms, blue. [145] Copyright ©2010 with permission from Elsevier.

Since silica gel support is pH stable in the region of pH 3-7, it may be beneficial to develop CFs bonded to other supporting materials to create stationary phases with less pH sensitivity. Resins are macroreticular porous polymer adsorbents, which are widely used as polymeric media for recovery and separation of pharmaceuticals and their intermediates. They have the advantage of high adsorption capacity, i.e. they have been used for the separation and purification of antibiotics, including penicillin, cephalosporin and their derivatives. Resins have other favorable characteristics, such as high mechanical strength for industrial operations and chemical stability at higher or lower pH regions for recycled use of adsorption-elution-regeneration recovery systems. Generally, resins used as stationary phases, have broad application in ion-exchange chromatography (IEC) and size-exclusion chromatography (SEC). On the other hand, polymeric RPLC packing materials seem to provide excellent alternatives to the alkyl-bonded silica gels. Commercially available porous resins are copolymers of styrene crossed-linked divinyl benzene with diverse functional groups. However, few have been reported to be used as HILIC stationary phases or for chiral separations. In 1950s, resins were used to separate saccharides with hydro-organic mobile phases [5]. In 1982, Davankov developed chiral ligand exchange resins for enantiomeric separation of amino acids [261]. Slater and co-workers prepared porous polymer-based particulate stationary phases for UHPLC separation of peptides and proteins [262].

In the present work, CF6 was attached to a chloromethyl modified styrene divinyl benzene (MCI GEL™ CSP50/P10 CMS) using "click" chemistry. The CF6-CMS column was used for HILIC separations. Different types of polar compounds were used to evaluate the separation capability of the CF6-CMS column in the HILIC mode. The IP-CF6-CMS column was evaluated for its ability to achieve enantiomeric separations. The optimization of separation performance of these newly synthesized stationary phases

139

was investigated by examing the role of mobile phase composition, buffer pH, basic/acidic additives ratio and amounts, and column temperature. The stability and reproducibility of the IP-CF6-CMS column also were considered.

7.2 Experimental

7.2.1 Chemicals and materials

Cyclofructans were generously donated by AZYP, LLC, Arlington, TX, USA. Resin MCI GEL™ CSP50/P10 CMS was generously donated by Mitsubishi Chemical Corporation, Tokyo, Japan. Resins are porous spherical particles with 10 μm diameter. Anhydrous N,N-dimethylformamide (DMF), anhydrous pyridine, sodium azide, proparyglamine, copper(I) acetate, 2,6-lutidine, isopropyl isocyanate, ammonium acetate, triethtylamine, tributylamine, diethylamine, butylamine, ethanolamine, and acetic acid were purchased from Sigma-Aldrich (Milwaukee, WI). HPLC-grade methanol, acetonitrile, isopropanol and heptanes were purchased from EMD (Gibbstown, NJ) and used directly; ultra-pure water was prepared by a Milli-Q Water Prufication System (Millipore, Billerica, MA).

7.2.2 Instruments

Fourier-transform infrared (FT-IR) spectra were collected on IRPrestige-21 supplied by Shimadzu. Elemental analysis was performed by QTI, NJ. All the enantiomeric separations were performed on an Agilent 1100 HPLC series system equipped with a diode array detection (DAD) system (Agilent Technologies, Palo Alto, CA). Data acquisition and analysis were obtained from the Chemstation software version Rev. B.01.03 in Microsoft Windows XP environment. Separations were carried out at room temperature unless stated otherwise. The wavelengths of UV detection were set at

210 nm, 230 nm, 254 nm and 280 nm. The injection volume and flow rate were set as 5 µL and 1.0 mL/min, respectively. Each sample was analyzed in duplicate.

7.2.3 Synthesis of CF6-CMS and IP-CF6-CMS

The synthetic scheme for the bonding reaction of CF6 with MCI GEL™ CSP50/P10 CMS resin is depicted in Fig. 2. Tosylated CF6 (2) was obtained by reacting native CF6 with p-toluenesulfonyl chloride in anhydrous pyridine [263]. Treatment of tosylated CF6 (2) with an excess of sodium azide in water at 95 $^{\circ}$C for 15 hrs afforded azido-CF6 (3) [264]. Alkynyl functionalized resin (4) was prepared by reacting propargylamine with resin MCI GEL™ CSP50/P10 CMS in acetonitrile/10% NaOH solution (65/35, *v/v*). The "click" chemistry immobilization step was accomplished as follow: azide CF6 (3) was added to a suspension of alkynyl resin MCI GEL™ CSP50/P10 CMS (4) in methanol/acetonitrile (50/50, *v/v*) solvent mixture followed by the addition of Cu(I) acetate (0.025g, 10mmol%) in 2,6-lutidine in a single portion. The reaction mixture was heated and stirred for 2 days. The crude product CF6-CMS (5) was filtered, and later it was washed with 5% EDTA solution, water, methanol, acetonitrile, acetone, then dried in vacuo overnight. With addition of isopropyl isocyanate, a suspension of CF6-CMS (5) in anhydrous pyridine was heated and stirred for 7 hrs under Ar atmosphere and later washed with water methanol, acetonitrile and acetone, and finally dried in vacuo overnight to afford the chiral resin IP-CF6-CMS (6).

7.2.4 Preparation of CF6-CMS and IP-CF6-CMS columns

The HILIC stationary phase CF6-CMS and chiral stationary phase IP-CF6-CMS were slurry-packed into stainless-steel columns (250 mm×4.6 mm i.d.), respectively. Acetonitrile/1 M ammonium nitrate solution (96/4, *v/v*) was used as slurry solvent and 100% acetonitrile was used as propulsion solvent. The HPLC column packing system is composed of an air driven fluid pump (HASKEL, DSTV-122), an air compressor, a

pressure regulator, a low pressure gauge, two high pressure gauges, a slurry chamber, check valves, and several tubings.

7.2.5 Preparation of mobile phases

Ammonium acetate buffers were prepared using 20 mM aqueous ammonium acetate, which were adjusted by addition of glacial acetic acid to the desired pH. The mobile phase, comprised of ammonium acetate buffer and the appropriate amount of the organic modifier, was freshly prepared, filtered, and degassed under the vacuum. An equilibration of 1-2 hrs was allowed after a pH change in the mobile phase in order to obtain reproducible results. The mobile phase used in the HILIC mode contains a huge amount of poor hydrogen bonding solvent acetonitrile and a small amount of aqueous solution (water or ammonium acetate buffer). The mobile phase used in the reversed phase mode consist a huge amount of aqueous solution and a small amount of methanol. Heptane/ethanol/trifluoroacetic acid (Hep/EtOH/TFA) was the mobile phase used in the normal phase mode. Acetonitrile/methanol/triethylamine/acetic acid (ACN/MeOH/TEA/AA) was the mobile phase used in the polar organic mode.

7.3 Results and discussion

Native CF6 was bonded to resins to make HILIC stationary phases (CF6-CMS). In addition the IP-CF6-CMS resin column was developed and evaluated for its chromatographic chiral recognition properties.

7.3.1 Preparation and characterization of the CF6-CMS and IP-CF6-CMS stationary phases

Various approaches were investigated to bond native/derivatized CFs onto resins. To our knowledge, this is the first time "click" chemistry has been applied for the mild and selective immobilization of CFs onto functionalized styrene divinylbenzene via a 1,2,3-

triazole linker. The copper(I)-catalyzed (3+2) azide-alkyne cycloaddition, an element of "click chemistry", is a very efficient coupling reaction that provides an ideal reactivity profile for this purpose [265]. It has attracted burgeoning interest for surface modification in recent years. Broad applications of "click" chemistry have been summarized in several reviews [262, 266-268]. Some non-chiral stationary phases have been developed via click chemistry and tested in HPLC [269, 270]. The first application of "click" chemistry to the preparation of chiral stationary phases was the immobilization of a cinchona alkaloid derivative to silica surfaces [271]. Since both azide and alkynyl functional groups are relatively stable in many synthetic procedures, either group may be incorporated to the stationary phases or chiral selectors as desired. Thus, the solid support can include alkynyl functionality to later react with cyclofructan bearing azide groups or vice versa. In the case of the CF6-CMS stationary phase, the alkynyl derivative of the resin was used and coupled to an azide CF6 via a triazole ring (see Figure 7-2).
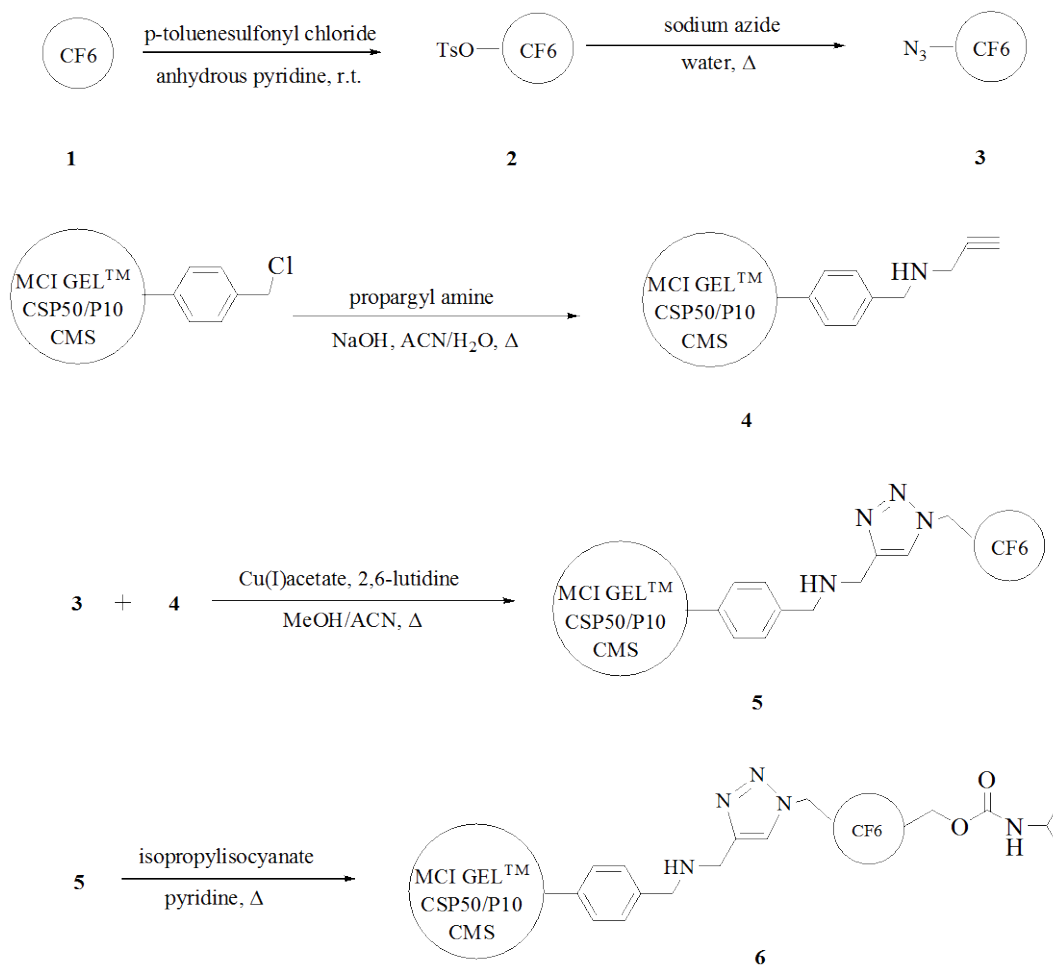
Figure 7-2 Synthetic scheme of CF6-CMS and IP-CF6-CMS.

There are two schemes to afford isopropyl carbamated CF6-CMS stationary phases. One is to react an azide substituted isopropyl carbamated CF6 with an alkynyl resin. Another one is to introduce isopropyl carbamate group directly to CF6-CMS resin with isopropyl isocyanate reagent. The IP-CF6-CMS was made by the second method, which is easily accomplished, as shown in Figure 7-2.

The alkynyl resin and CF6-CMS resin were characterized by FT-IR and elemental analysis. The acetylenic C-H stretch on alkynyl resin (2928 cm^{-1}) weakened

144

after the "click" step. The results of elemental analysis and the surface concentration are shown in Table 7-1. The nitrogen content of the alkynyl MCI GEL™ CSP50/P10 CMS is 1.35% and the nitrogen content of the CF6-CMS is 3.95%. The increase in nitrogen content demonstrated that CF6 was bonded to the alkynyl MCI GEL™ CSP50/P10 CMS resin successfully. According to the weight difference between the product and starting materials, the concentration of cyclofructan 6 on the resin is 0.16 mmol/g.

Table 7-1 Physical properties of modified MCI GEL™ CSP50/P10 CMS resins.

| resins | Particle size | Elemental analysis | | | CF6 loading |
	μm	C%	H%	N%	mmol/g
MCI GEL™ CSP50/P10 CMS	10	85.32	7.40	0.05	0
Alkenyl- MCI GEL™ CSP50/P10 CMS	10	85.92	7.67	1.35	0
CF6-CMS	10	77.32	7.53	3.90	0.16
IP-CF6-CMS	10	79.23	7.29	4.36	0.16

7.3.2 Achiral compound screening on the CF6-CMS column

The performance of the CF6-CMS column has been evaluated by separating different types of polar mixtures in the HILIC mode. It should be noted that these resin particles are 10 μm in diameter as compared to 5 μm diameter silica gel particles in typical analytical column. As shown in Figure 7-3(A), the CF6-CMS column has potential to separate nucleosides and nucleic acid base compounds in the HILIC mode. The adjacent peaks of adenosine, cytidine, cytosine, and guanosine were baseline separated on the CF6-CMS column. Thymidine, thymine and uracil showed partial separations on the CF6-CMS column. This is due to poor column efficiency and short retention time. Uridine and adenosine co-eluted using a optimized mobile phase of acetonitrile/20 mM ammonium acetate buffer, pH=4.1. This column performed well in separating different cyclofructans, see Figure 7-3B. CF6, CF7 and CF8 were baseline separated with a

mobile phase of acetonitrile/water (70/30, *v/v*). This indicates the possibility of using CF6-CMS columns to purify the crude cyclofructan fermentation product in the future.
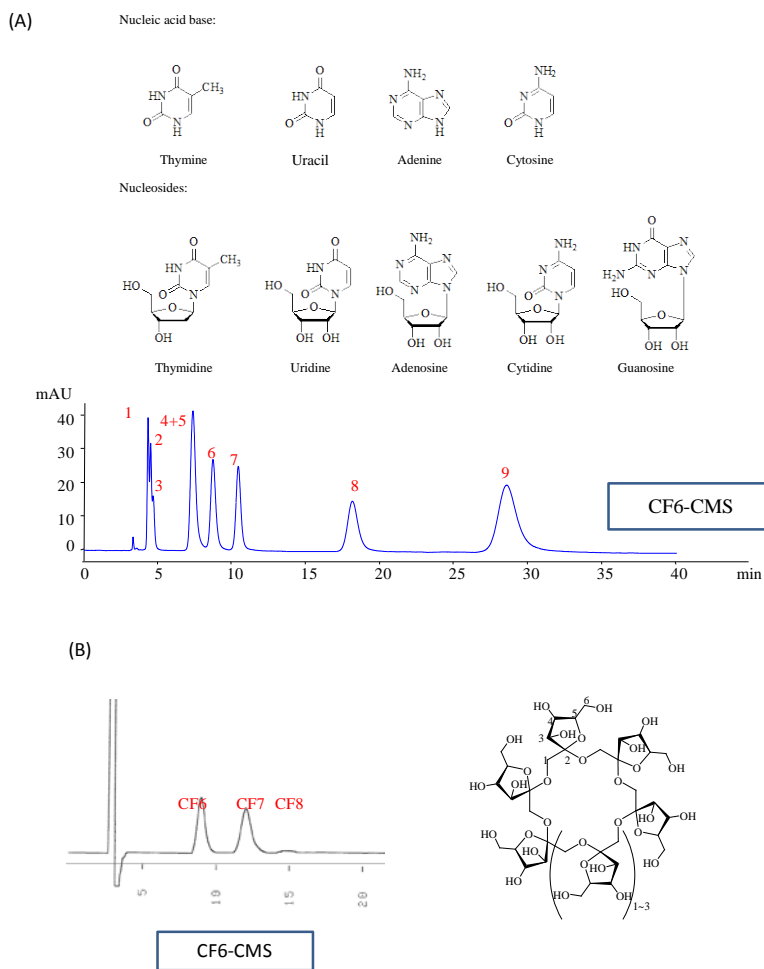
Figure 7-3 Separation of polar mixtures on the CF6-CMS column (0.46×25 cm). (A) Separation of nucleo compounds with a mobile phase of acetonitrile/20 mM ammonium acetate, pH=4.1, 92/8 (v/v); flow rate: 1.0 mL/min; UV detection: 254 nm. Compounds: (1) thymine; (2) uracil; (3) thymidine; (4) uridine; (5) adenine; (6) adenosine; (7) cytosine; (8) cytidine; (9) guanosine. (B) Separation of cyclofructan mixture with a mobile phase of acetonitrile/water 75/25 (v/v); Flow rate: 1.0 mL/min; RI detection.

7.3.3 Chiral compound screening on the IP-CF6-CMS column

To investigate the enantioselectivity of the IP-CF6-CMS column, a wide range of chiral compounds from neutral to basic as well as a few acidic compounds were screened. Separations were carried out in the polar organic mode as well as the normal phase mode. Representative chromatograms of racemates separated on the IP-CF6-CMS column are shown in Figure 7-4. (1S,2S/1R,2R)-*trans*-1-amino-2-indanol was separated in the polar organic mode with α = 1.24 and R_s = 1.4 and (1R,2R/1S,2S)-N-*p*-tosyl-1,2-diphenylethylenediamine was separated in the normal phase mode with α = 1.41 and R_s = 1.4.
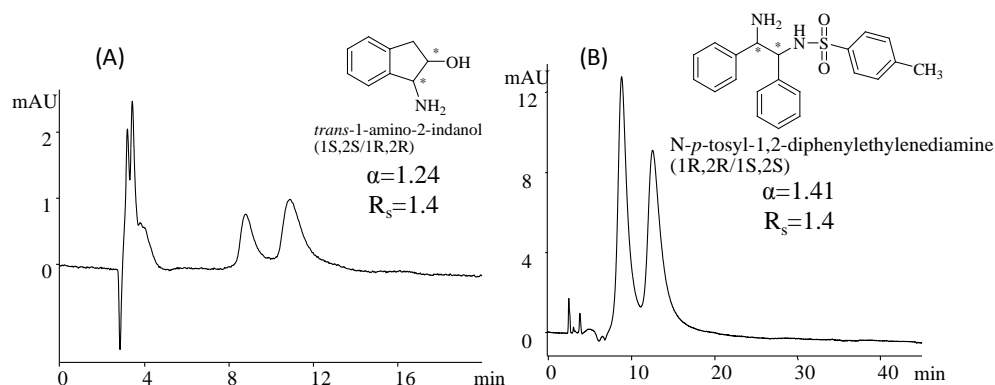
Figure 7-4 Selective enantiomeric separations on the IP-CF6-CMS column. (A) enantiomeric sepration of (1S,2S/1R,2R)-trans-1-amino-2-indanol with a mobile phase of acetonitrile/methanol/triethylamine/acetic acid 70/30/0.2/0.5 (*v/v/v/v*), flow rate: 1.0 mL/min, UV detection: 280 nm. (B) enatniomeric separation of (1R,2R/1S,2S)-N-*p*-tosyl-1,2-diphenylethylenediamine with a mobile phase of heptanes/ethanol/trifluoroacetic acid 70/30/0.1 (v/v/v), flow rate: 1.0 mL/min, UV detection: 254 nm.

A total of 37 chiral compounds listed in Table 7-2 were completely or partially separated on the IP-CF6-CMS column with optimized conditions. The chromatographic data include retention factor (k_1), selectivity (α), and resolution (R_s). If racemates were separated under a variety of mobile phase conditions, the best combination of high resolution and short retention was chosen. When optimizing enantioseparations, the polar organic mode was tested first for all analytes. If insufficient retention with poor resolution was obtained, the normal phase mode was then examined. The selectivity of the same racemates on the IP-CF6-CMS column is comparable to that on the of LARIHC CF6-P silica gel based column [145]. Slightly lower enantioselectivity data were obtained on the IP-CF6-CMS column than on the LARIHC CF6-P column in the polar organic mode. In contrast, higher enantioselectivity data were obtained on the IP-CF6-CMS column than on the LARIHC CF6-P column in the normal phase mode when using the same mobile phase condition. The IP-CF6-CMS stationary phase is based on styrene divinylbenzene polymer as supporting materials and consists of a 1,2,3-triazole linker. 1,2,3-triazole has its advantageous properties of high chemical stability (generally inert to severe hydrolytic oxidizing and reducing conditions, even at high temperatures), strong dipole moment (4.8-5.6 Debye) [272], aromatic character and hydrogen bond accepting ability [272]. This unique structure enhances π-π interactions and dipolar interactions with the analyte. This might be the reason for the improved selectivity in the normal phase mode on the IP-CF6-CMS column. However, the resolution obtained on the IP-CF6-CMS column was not as good as on the LARIHC CF6-P column. This was mainly attributed to poor column efficiency from larger particle sizes. Compared to silica gel, IP-CF6-CMS used supporting materials has bigger particle sizes (10 μm) and bigger pore sizes (170 Å), the former of which results in lower efficiencies and resolutions as well.

Table 7-2 Enantiomeric separations on the IP-CF6-CMS column.

No.	Compound	Structure	k_1	R_s	α	Mobile phase
1	trans-1-Amino-2-indanol (1S,2S/1R,2R)		1.72	1.90	1.24	70A30M0.2TEA0.5AA
2	cis-1-Amino-2-indanol (1S,2R/1R,2S)		1.22	1.0	1.12	70A30M0.2TEA0.5AA
3	1-Aminoindan		1.36	0.8	1.12	65A35M0.2TEA0.5AA
4	1,2-Diphenylethylamine		0.25	1.0	1.22	80A20M0.2TEA0.5AA
5	2-Amino-1-(4-nitrophenyl)-1,3-propanediol (1R,2R/1S,2S)		3.66	0.6	1.09	75A25M0.2TEA0.5AA
6	alpha-(1-Aminoethyl)-4-hydroxybenzyl alcohol hydrochloride (1R,2R/1S,2S)		1.57	0.5	1.08	65A35M0.2TEA0.5AA
7	Norephedrine hydrochloride (1R,2S/1S,2R)		5.94	1.3	1.15	70A30M0.2TEA0.5AA
8	Normetanephrine		4.39	1.0	1.15	70A30M0.2TEA0.5AA
9	Norepinephrine L-bitartrate hydrate		4.41	0.55	1.11	65A35M0.2TEA0.5AA
10	Norephedrine (1R,2S/1S,2R)		1.55	0.39	1.05	65A35M0.2TEA0.5AA
11	4-Chlorophenylalaninol		1.90	0.68	1.09	65A35M0.2TEA0.5AA

Table 7-2—*Continued*
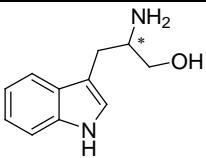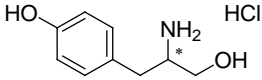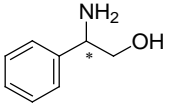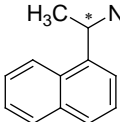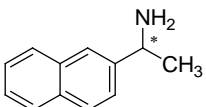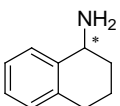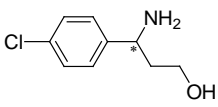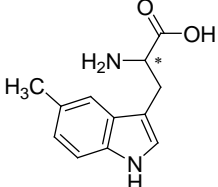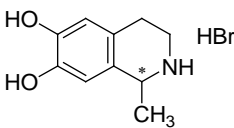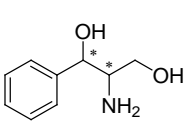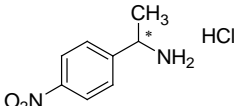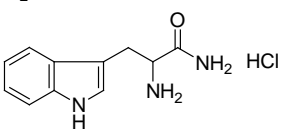
12	Tryptophanol		1.70	0.74	1.11	65A35M0.2TEA0.5A A
13	Tyrosinol hydrochloride		1.60.	0.47	1.09	65A35M0.2TEA0.5A A
14	2-Phenylglycinol		1.00	0.20	1.02	65A35M0.2TEA0.5A A
15	1-(1-Naphthyl)ethyla mine		1.24	0.95	1.11	65A35M0.2TEA0.5A A
16	1-(2-Naphthyl)ethyla mine		1.30	0.48	1.05	65A35M0.2TEA0.5A A
17	1,2,3,4-Tetrahydro-1-naphthylamine		0.86	0.89	1.10	65A35M0.2TEA0.5A A
18	3-(4-Chlorophenyl) alaninol		1.89	0.63	1.10	70A30M0.2TEA0.5A A
19	5-Methyl-tryptophan		4.54	0.6	1.2	65A35M0.2TEA0.5A A
20	1-Methyl-6,7-dihydroxy-1,2,3,4-tetrahydroisoqui noline hydrobromide		1.77	0.2	1.02	65A35M0.2TEA0.5A A
21	2-Amino-1-phenyl-1,3-propanediol (1R,2R/1S,2S)		1.88	0.2	1.02	70A30M0.2TEA0.5A A
22	α-Methyl-4-nitrobenzylamin e hydrochloride		1.71	0.2	1.02	65A35M0.2TEA0.5A A
23	Tryptophanamid e hydrochloride		1.16	0.2	1.02	65A35M0.2TEA0.5A A

Table 7-2—*Continued*
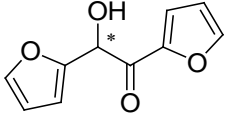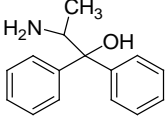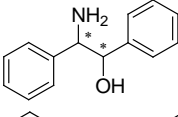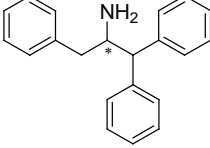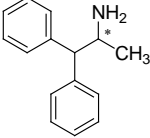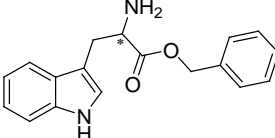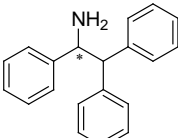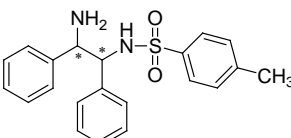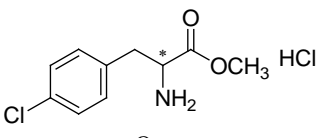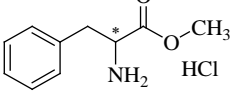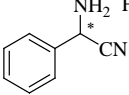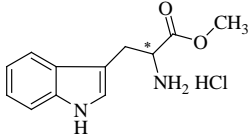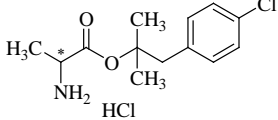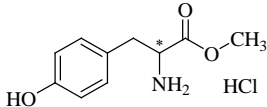
24	Furoin		0.17	0.2	1.32	65A35M0.2TEA0.5AA
25	2-Amino-1,1-diphenyl-1-propanol		1.63	0.2	1.06	70H30E0.1TFA
26	2-Amino-1,2-diphenylethanol (1R,2S/1S,2R)		2.73	1.2	1.41	70H30E0.1TFA
27	1-Benzyl-2,2-diphenylethylamine		0.80	0.2	1.05	70H30E0.1TFA
28	1,1-Diphenyl-2-aminopropane		1.30	0.7	1.15	70H30E0.1TFA
29	Tryptophan benzyl ester		6.28	1.0	1.21	70H30E0.1TFA
30	1,2,2-Triphenylethylamine		1.06	1.0	1.22	70H30E0.1TFA
31	N-p-Tosyl-1,2-diphenylethylenediamine (1R,2R/1S,2S)		2.54	1.4	1.41	70H30E0.1TFA
32	4-Chloro-DL-phenylalanine methyl ester hydrochloride		4.14	0.6	1.14	70H30E0.1TFA
33	4-Chloro-DL-phenylalanine methyl ester hydrochloride		3.79	0.59	1.14	70H30E0.1TFA
34	2-Phenylglycinonitrile hydrochloride		4.54	0.58	1.10	70H30E0.1TFA

151

Table 7-2—*Continued*

35	DL-Tryptophan methyl ester hydrochloride		5.74	0.62	1.17	70H30E0.1TFA
36	Alaproclate hydrochloride		3.14	0.3	1.05	70H30E0.1TFA
37	DL-Tyrosine methyl ester hydrochloride		6.40	0.63	1.17	70H30E0.1TFA

7.3.4 Effect of mobile phase parameters on enantiomeric separations on the IP-CF6-CMS column

7.3.4.1 Chromatographic mode

Different chromatographic modes were used for separating DL-tryptophanol on the IP-CF6-CMS column (Figure 7-5). Enantiomeric separations were obtained in the polar organic mode and the normal phase mode rather than in the reversed phase mode and HILIC mode. The most efficient separations were obtained in the polar organic mode on the IP-CF6-CMS column. This is consistent with the separation strategy on the silica gel based LARIHC CF6-P column, which showed high enantioselectivity in the presence of organic solvents and supercritical fluids [65, 145].
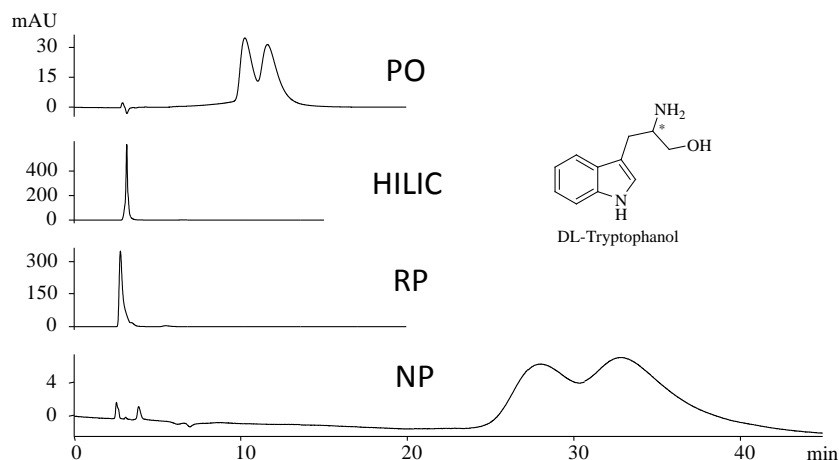
Figure 7-5 Different chromatographic modes were used in the enantiomeric separation of DL-tryptophanol on the IP-CF6-CMS column with (A) PO: the polar organic mode with a mobile phase of acetonitrile/methanol/triethylamine/acetic acid 70/30/0.2/0.5 (*v/v/v/v*); (B) HILIC: the HILIC mode with a mobile phase of acetonitrile/20mM ammonium acetate, pH=4.1, 80/20 (v/v); (C) RP: the reversed phase mode with a mobile phase of acetonitrile/20mM ammonium acetate, pH=4.1, 10/90 (*v/v*); (D) NP: the normal phase mode with a mobile phase of heptanes/ethanol/trifluoroacetic acid, 70/30/0.1 (*v/v/v*). Flow rate: 1.0 mL/min, UV detection: 254 nm.

Acetonitrile, THF, dioxane and ethyl acetate were tested as organic modifiers in the polar organic mode in order to achieve better separations. Among these four modifiers, the worst enantioselectivity and resolution were observed using dioxane, while the lowest efficiency and the poorest peak symmetry were obtained with ethyl acetate as the modifier. In most cases, the use of acetonitrile as a modifier produced the best resolution and most efficient peaks. This trend is true for most primary amine-containing compounds. It should be noted that acetonitrile has the lowest viscosity of all solvents

tested. In all subsequent studies, the mobile phase system composed of acetonitrile/methanol was utilized to separate all other primary amine containing analytes.

7.3.4.2 Effect of additives

In order to evaluate the effects of different basic additives in the polar organic mode on the separation of enantiomers, different types of additives were investigated and the results are shown in Figure 7-6. Triethylamine, tributylamine, and diethylamine combined with acetic acid were all beneficial and improved the enantiomeric separation of DL-tryptophanol in the polar organic mode on the IP-CF6-CMS column. The combination of triethylamine/acetic acid provided the best resolution.
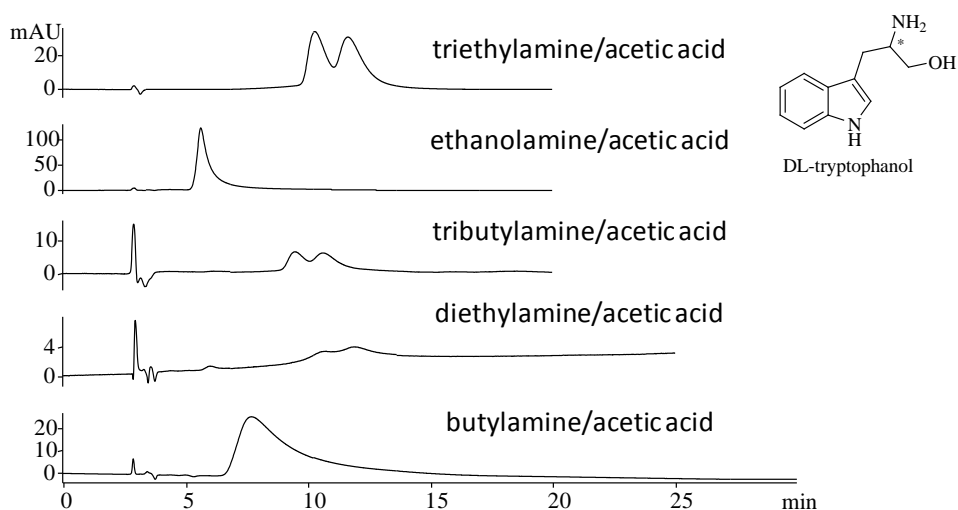

Figure 7-6 Different basic additives were used in the enantiomeric separation of DL-tryptophanol on the IP-CF6-CMS column in the polar organic mode. Mobile phase: acetonitrile/methanol/basic additive/acidic additive 70/30/0.2/0.5 (*v/v/v/v*), flow rate: 1.0 mL/min, UV detection: 254 nm.

The ratio of basic/acidic additives was investigated in the region of 2/1 – 2/8 by volume. This was carried out by varying the acetic acid concentrations from 0.1% - 0.8%,

154

while fixing the triethylamine to 0.2% in the mobile phase of acetonitrile/methanol (70/30, *v/v*), see Figure 7-7. The retention of most analytes increased with increasing acetic acid content up to 0.5%, except for DL-tryptophanol. The retention factors of all analytes then decrease when the acetic acid is greater than 0.5%. Selectivity and resolution were both accentuated with the acetic acid concentration from 0.1% to 0.5% and then they only changed slightly when the acetic acid is higher than 0.5%. It was determined that the addition of 0.2% triethylamine/0.5% acetic acid usually results in the highest selectivity and best resolution.
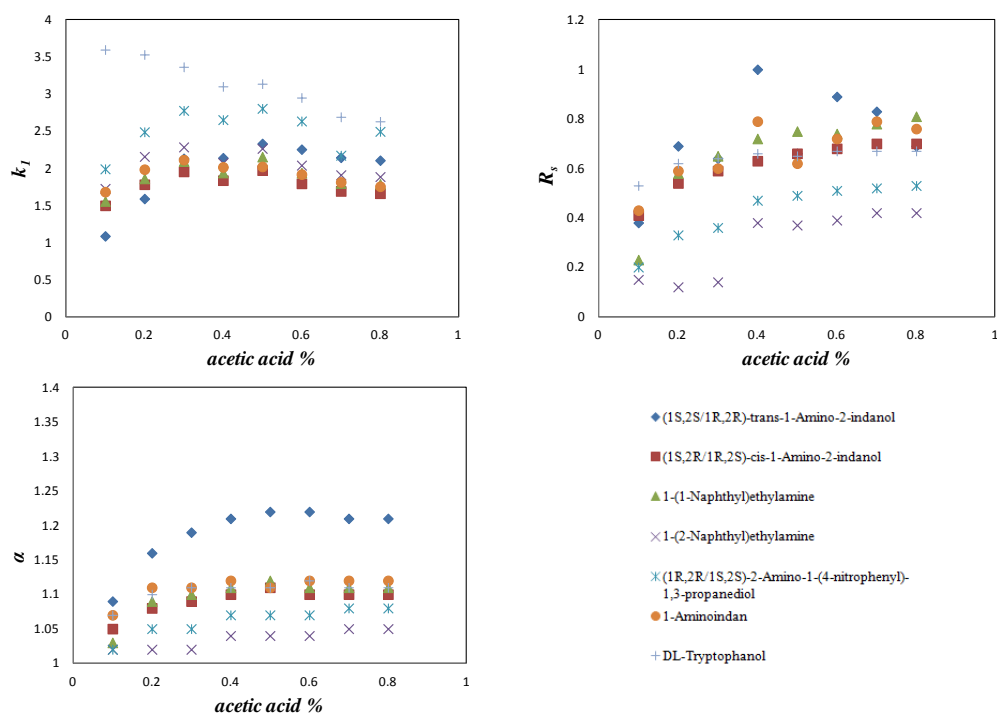
Figure 7-7 The effect of basic/acidic additives ratio on the enantiomeric separations on the IP-CF6-CMS column. Mobile phase: acetonitrile/methanol, 70/30 (*v/v*), with 0.2% triethylamine, flow rate: 1.0 mL/min, UV detection: 254 nm.

Figure 7-8 shows the effect of basic/acidic additive strength for a given ratio (2/5) on the enantiomeric separations on the IP-CF6-CMS column. This was investigated by varying the triethylamine concentration from 0.02% to 2%, while fixing the ratio of triethylamine/acetic acid to 2/5 in the mobile phase of acetonitrile/methanol (70/30, *v/v*). The retention factors of most analytes increase with increasing triethylamine% from 0.02% to 0.2%, except for DL-tryptophanol. When the amount of triethylamine in the mobile phase is greater than 0.2%, the retention factor of all analytes displayed similar trends. Selectivity improves in the region of 0.02% - 0.2% and changes only slightly above 0.2%. Resolution showed a similar trend. Thus, the optimized starting condition was found to be 0.2% triethylamine/0.5% acetic acid as additives in the polar organic mode.
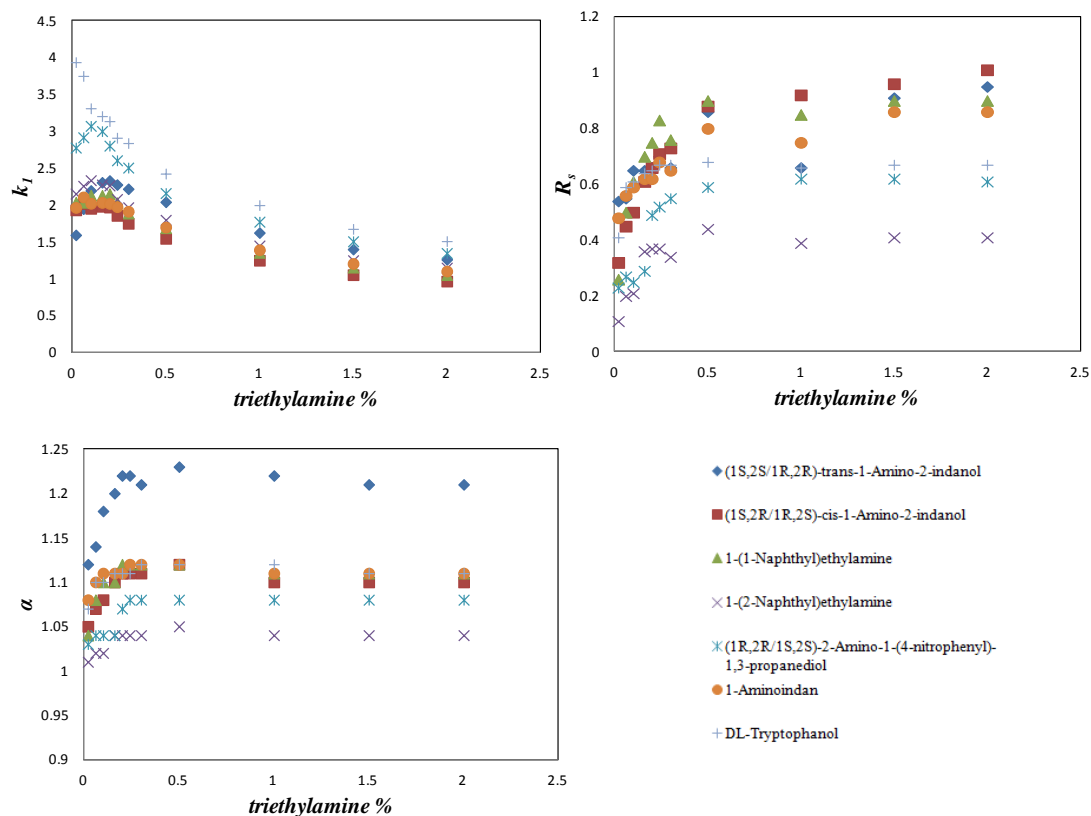
Figure 7-8 The effect of basic acidic additives amounts on the enantiomeric separations on the IP-CF6-CMS column. Mobile phase: acetonitrile/methanol 70/30 (*v/v*) with different amount of triethylamine/acetic acid with fixed ratio 2/5, flow rate: 1.0 mL/min, UV detection: 254 nm.

7. 3.5 Column temperature effect

The column temperature effect on enantiomeric separations is illustrated in Table 7-3, at three specific temperatures (5 ^{o}C, 25 ^{o}C and 45 ^{o}C). With decreasing column temperatures, the 1-(1-naphthyl)-ethylamine has a greater retention factor on the IP-CF6-CMS column. The retention factor is 2.74 at 5 ^{o}C and decreased to 1.53 at 45 ^{o}C. It is also demonstrated that decreasing the column temperature from 45 ^{o}C to 5 ^{o}C can

effectively increase selectivity from 1.06 to 1.28 and improve the resolution from 0.2 to

1.0. Therefore, optimization of enantiomeric separations can also be achieved by

decreasing the column temperature.

Table 7-3 Column temperature effect on the enantiomeric separation of 1-(1-naphthyl)-

ethylamine on the IP-CF6-CMS column.

Column Temperature (^{o}C)	k_1	α	R_s
5	2.74	1.28	1.0
25	1.95	1.15	0.6
45	1.53	1.06	0.2

Mobile phase: acetonitrile/methanol/triethylamine/acetic acid 70/30/0.2/0.5, flow rate: 1.0 mL/min, UV detection: 254 nm.

Based on these empirical studies, optimization of enantioseparations using the

polar organic mobile phases on the IP-CF6-CMS column has been carried out as follows:

the mobile phase composed of acetonitrile/methanol/triethylamine/acetic acid

70/30/0.2/0.5 was utilized as the starting condition. Subsequent optimization of individual

compounds can be achieved easily by altering the acetonitrile percentage and

occasionally decreasing the column temperature.

3.6 Column stability and reproducibility

Column stability and reproducibility are critical to demonstrate the ruggedness of

a new chiral stationary phase. After more than 1000 injections, the column still gave good

selectivity and similar retention for the same analytes. There was no significant

deterioration observed for the column after six months of use. 1-(1-naphthyl)-ethylamine

was used as a model compound for evaluation of the column separation stability and

reproducibility. A total of 30 injections of 1-(1-naphthyl)-ethylamine were performed for

three consecutive days on the IP-CF6-CMS column. The detailed reproducibility data

shown in Table 7-4 revealed that the intra-day RSD for the retention factor was 1.33-1.80%

and the inter-day RSD was 2.56%. The reproducibility of selectivity is good with intra-day and inter-day RSDs lower than 0.46% and 0.53%, respectively. The intra-day RSD for the resolution was 3.44-4.37% and inter-day RSD is 4.36%. Compared with other parameters, the RSD for the resolution was slightly high, but it is still considered satisfactory for practical applications. Therefore, the results clearly demonstrated the good separation stability and reproducibility of the optimized IP-CF6-CMS column.

Table 7-4 Intra-day and inter-day reproducibility of retention factor, selectivity and resolusion for 1-(1-naphthyl)-ethylamine on the IP-CF6-CMS column.

Day	Total injection	Average k_1 (RSD, %)	Average α (RSD, %)	Average R_s (RSD, %)
1	10	2.10 (1.80)	1.11 (0.46)	0.71 (3.60)
2	10	2.09 (1.57)	1.11 (0.46)	0.68 (4.37)
3	10	2.00 (1.33)	1.11 (0.44)	0.67 (3.44)
overall	30	2.06 (2.56)	1.11 (0.53)	0.69 (4.36)

Mobile phase: acetonitrile/methanol/triethylamine/acetic acid 70/30/0.2/0.5, flow rate: 1.0 mL/min, UV detection: 254 nm.

7.4 Conclusions

A native cyclofructan 6 based stationary phases (CF6-CMS) was made by immobilizing functionalized 4-azido-β-cyclofructan 6 to chloromethyl modified styrene divinylbenzene (MCI GEL™ CSP50/P10 CMS) via a 1,2,3-triazole linker. This stationary phase was used for the HILIC separation of different types of polar compounds. Another novel stationary phase IP-CF6-CMS was obtained by further introduction of isopropyl carbamate group onto the CF6-CMS stationary phase. It was used in enantiomeric separations in HPLC. Under the optimum mobile phase condition, 37 different types of enantiomeric compounds showed selectivity on the IP-CF6-CMS column. The starting mobile phase condition for enantiomeric separations on the IP-CF6-CMS column was found to be acetonitrile/methanol/triethylamine/acetic acid 70/30/0.2/0.5. The separations can then be optimized by varying the mobile phase composition and adjustment of

159

additives. Lower column temperatures also enhance enantiomeric separations. The selectivity for the same analytes on the IP-CF6-CMS column is somewhat comparable with that on the silica gel based LARIHC-CF6 column, although efficiencies are lower. These results indicate the potential of resin based cyclofructan columns for HILIC and/or chiral separations in process chemistry. Finally, the column demonstrated good stability and reproducibility of retention factor and selectivity using 1-(1-naphthyl)-ethylamine as the model analyte to investigate the intra-day and inter-day separation results.

Chapter 8

General summary

8.1 Part one (Chapters 2-4)

Two types of new HILIC stationary phases were discussed. One was based on native cyclofructan 6 bound to silica gel, and the other one was a zwitterionic stationary phase based on 3-P,P-diphenylphosphonium-propylsulfonate attached to silica gel. Their performance in the HILIC mode can provide increased retention, improved selectivity and resolution for multiple classes of polar compounds, which are difficult to retain and separate in RP-HPLC. They also showed advantages over commercially available HILIC stationary phases (e.g., the ZIC-HILIC and SiO_2 columns) for many HILIC separations. Their exceptional separation capability was demonstrated by resolution of a variety of polar analytes, including nucleic acid bases, nucleosides, xanthines, β-blockers, salicylic acid and its derivatives, water soluble vitamins, and carbohydrates in the HILIC mode. The retention behavior in the HILIC mode was investigated by varying factors such as the organic modifier, the mobile phase composition, the buffer concentration and the buffer pH. It was confirmed that aprotic solvents, such as acetonitrile and tetrahydrofuran, are the preferred organic modifiers in HILIC separations. Thermodynamic studies of these HILIC stationary phases suggested that the hydrated layer on the surface of the stationary phase (especially for zwitterionic stationary phases) could have a temperature dependent composition and stationary phase volume. Additionally, these columns are stable, have good efficiency and reproducibility, and are versatile alternatives to commercially available HILIC columns (e.g. the ZIC-HILIC and bare SiO_2 columns).

8.2 Part two (Chapters 5-6)

Appropriately derivatized cyclofructans were found to be highly selective for different types of chiral molecules in HPLC, GC, and CE. Aliphatic-derivatized CF6 with a low degree of substitution, i.e. LARIHC CF6-P, has shown baseline separation for more than 90% of tested chiral primary amines, particularly, in the presence of organic solvents and notably even in supercritical fluids. This dissertation describes development of aromatic-derivatized cyclofructan based chiral stationary phases. R-naphthylethyl-carbamate cyclofructan 6 (RN-CF6) and dimethylphenyl-carbamate cyclofructan 7 (DMP-CF7) stationary phases were successfully synthesized. The RN-CF6 and DMP-CF7 stationary phases are the two best aromatic-functionalized cyclofructan chiral stationary phases. They are complementary to the isopropyl-carbamate cyclofructan 6 stationary phase (the LARIHC CF6-P column) in the separation of various enantimeric compounds, including acidic, basic, neutral organic compounds, and metal complexes.

The enantiomeric purity of chiral molecules is important not only in the final products from the pharmaceutical, biotechnology and agrochemical industries, but also in asymmetric syntheses during manufacturing. Enantiomeric impurities can directly affect the reaction selectivity and product purity. Forty six commercially available chiral compounds were evaluated for enantiomeric impurities. The majority of tested reagents were determined to have enantiomeric contaminants less than 1%, and only one of them was found to contain optical impurity levels of exceeding 10%. The LARIHC CF6-P and Chirobiotic V2 chiral stationary phase was found to be the most effective for separation of these kinds of small molecules at low concentrations. These results provide importanct evaluations of these enantiomers, and identify when further purification is required.

162

8.3 Part three (Chapter 7)

This dissertation also discussed development and application of new stationary phases based on polymeric resins rather than on silica gel solid supports. A resin based HILIC stationary phase (CF6-CMS) was successfully prepared by immobilizing functionalized 4-azido-β-cyclofructan 6 on chloromethyl modified styrene divinylbenzene (MCI GEL™ CSP50/P10 CMS) via a 1,2,3-triazole linker. This stationary phase performed well in separating different types of polar compounds in the HILIC mode. Resin based chiral stationary phase IP-CF6-CMS was obtained by further introduction of isopropyl-carbamate group onto the CF6-CMS stationary phase. This chiral stationary phase appears to have potential for enantiomeric separations. Under the optimum mobile phase conditions, 37 different types of enantiomeric compounds showed selectivity on the IP-CF6-CMS column. The selectivity for the same analytes on the IP-CF6-CMS column is somewhat comparable with that on the silica gel based LARIHC-CF6 column, although efficiencies are modestly lower. The column showed good stability and reproducibility of retention factors and selectivity factors based on 1-(1-naphthyl)-ethylamine as the model analyte for investigating the intra-day and inter-day separation results. There was no detectable deterioration of the column after extensive use (~1,000 injections in six months).

Appendix A

PUBLICATION INFORMATION OF CHAPTERS 2-7

Chapter 2: A manuscript published in Journal of Chromatography A. Haixiao Qiu,Lucie Loukotková,Ping Sun,Eva Tesařová,Zuzana Bosáková,Daniel W. Armstrong, 2011, 1218, 270-279. Copyright ©2011 with permission from Elsevie.

Chapter 3: A manuscript published in Journal of Chromatography A. Haixiao Qiu,Eranda Wanigasekara,Ying Zhang,Tran Tran,Daniel W. Armstrong, 2011, 1218, 8075-8082. Copyright ©2011 with permission from Elsevie.

Chapter 4: A manuscript published in Journal of Chromatography A. Haixiao Qiu, Daniel W. Armstrong, Alain Berthod, 2013, 1272, 81-89. Copyright ©2013 with permission from Elsevie.

Chapter 5: A manuscript published in Analyst. Ping Sun, Chunlei Wang, Nilusha Lasanthi Thilakarathna Padivitage, Yasith S. Nanayakkara, Sirantha Perera, Haixiao Qiu, Ying Zhang and   Daniel W. Armstrong, 2011, 136, 787-800. Copyright ©2011 with permission from Royal Society of Chemistry.

Chapter 6: A manuscript accepted in Tetrahedron: Asymmetry. Haixiao Qiu, Nilusha L. T. Padivitage, Lillian A. Frink and Daniel W. Armstrong

Chapter 7: A manuscript accepted in Journal of Liquid Chromatography & Related Technologies. Haixiao Qiu; Mayumi Kiyono-Shimobe; Daniel W. Armstrong

References

[1] F. Gerber, M. Krummen, H. Potgeter, A. Roth, C. Siffrin, C. Spoendlin, J. Chromatogr. A 1036 (2004) 127.

[2] K. Miyabe, G. Guiochon, Adv. Chromatogr. 40 (2000) 1.

[3] P. Hemstroem, K. Irgum, J. Sep. Sci. 29 (2006) 1784.

[4] C. Wang, C. Jiang, D.W. Armstrong, J. Sep. Sci. 31 (2008) 1980.

[5] O. Samuelson, E. Sjostrom, Sven. Kem. Tidskr. 64 (1952) 305.

[6] J.C. Linden, C.L. Lawhead, J. Chromatogr. 105 (1975) 125.

[7] D.W. Armstrong, H.L. Jin, J. Chromatogr. 462 (1989) 219.

[8] H.L. Jin, A.M. Stalcup, D.W. Armstrong, J. Liq. Chromatogr. 11 (1988) 3295.

[9] A.J. Alpert, J. Chromatogr. 499 (1990) 177.

[10] T. Yoshida, J. Biochem. Biophys. Methods 60 (2004) 265.

[11] T. Ikegami, K. Tomomatsu, H. Takubo, K. Horie, N. Tanaka, J. Chromatogr. A 1184 (2008) 474.

[12] B. Herbreteau, Analusis 20 (1992) 355.

[13] Z.L. Nikolov, P.J. Reilly, J. Chromatogr. 325 (1985) 287.

[14] L.A.T. Verhaar, B.F.M. Kuster, J. Chromatogr. 234 (1982) 57.

[15] F. Gritti, Y.V. Kazakevich, G. Guiochon, J. Chromatogr. A 1169 (2007) 111.

[16] B. Buszewski, M. Jezierska, M. Welniak, R. Kaliszan, J. Chromatogr. A 845 (1999) 433.

[17] D.V. McCalley, U.D. Neue, J. Chromatogr. A 1192 (2008) 225.

[18] A.J. Alpert, Anal. Chem. 80 (2008) 62.

[19] M. D'Amboise, D. Noel, T. Hanai, Carbohydr. Res. 79 (1980) 1.

[20] H. Qiu, L. Loukotkova, P. Sun, E. Tesarova, Z. Bosakova, D.W. Armstrong, J. Chromatogr. A 1218 (2011) 270.

[21] D.W. Armstrong, H.L. Jin, Chirality 1 (1989) 27.

[22] K.E. Bij, C. Horvath, W.R. Melander, A. Nahum, J. Chromatogr. 203 (1981) 65.

[23] M. Benincasa, G.P. Cartoni, F. Coccioli, R. Rizzo, L.P.T.M. Zevenhuizen, J. Chromatogr. 393 (1987) 263.

[24] A. Nahum, C. Horvath, J. Chromatogr. 203 (1981) 53.

[25] B. Buszewski, M. Jezierska-Switala, S. Kowalska, J. Chromatogr. B: Anal. Technol. Biomed. Life Sci. 792 (2003) 279.

[26] H.P. Nguyen, K.A. Schug, J. Sep. Sci. 31 (2008) 1465.

[27] P.J. Boersema, N. Divecha, A.J.R. Heck, S. Mohammed, J. Proteome Res. 6 (2007) 937.

[28] M. Gilar, P. Olivova, A.E. Daly, J.C. Gebler, Anal. Chem. 77 (2005) 6426.

[29] P. Dugo, N. Fawzy, F. Cichello, F. Cacciola, P. Donato, L. Mondello, J. Chromatogr. A 1278 (2013) 46.

[30] A.J. Alpert, M. Shukla, A.K. Shukla, L.R. Zieske, S.W. Yuen, M.A.J. Ferguson, A. Mehlert, M. Pauly, R. Orlando, J. Chromatogr. A 676 (1994) 191.

[31] S.C. Churms, J. Chromatogr. A 720 (1996) 75.

[32] A.R. Oyler, B.L. Armstrong, J.Y. Cha, M.X. Zhou, Q. Yang, R.I. Robinson, R. Dunphy, D.J. Burinsky, J. Chromatogr. , A 724 (1996) 378.

[33] Z. Hao, C. Lu, B. Xiao, N. Weng, B. Parker, M. Knapp, C. Ho, J. Chromatogr. A 1147 (2007) 165.

[34] R. Li, J. Huang, J. Chromatogr. A 1041 (2004) 163.

[35] M.A. Strege, S. Stevenson, S.M. Lawrence, Anal. Chem. 72 (2000) 4629.

[36] J. Clayden, W.J. Moran, P.J. Edwards, S.R. LaPlante, Angew. Chem. , Int. Ed. 48 (2009) 6398.

[37] T.J. Ward, K.D. Ward, Anal. Chem. 84 (2012) 626.

[38] T.J. Ward, K.D. Ward, Anal. Chem. 82 (2010) 4712.

[39] Y. Okamoto, T. Ikai, Chem. Soc. Rev. 37 (2008) 2593.

[40] M. Eichelbaum, A.S. Gross, Adv. Drug Res. 28 (1996) 1.

[41] R.R. Shah, J.M. Midgley, S.K. Branch, Adverse Drug React. Toxicol. Rev. 17 (1998) 145.

[42] S. Fabro, R.L. Smith, R.T. Williams, Nature 215 (1967) 296.

[43] B.J. Davies, J.K. Coller, A.A. Somogyi, R.W. Milne, B.C. Sallustio, Drug Metab. Dispos. 35 (2007) 128.

[44] B.J. Davies, M.K. Herbert, J.A. Culbert, S.M. Pyke, J.K. Coller, A.A. Somogyi, R.W. Milne, B.C. Sallustio, J. Chromatogr. B: Anal. Technol. Biomed. Life Sci. 832 (2006) 114.

[45] G. Blaschke, H.P. Kraft, K. Fickentscher, F. Koehler, Arzneim. -Forsch. 29 (1979) 1640.

[46] Anonymous, Chirality 4 (1992) 338.

[47] D.W. Armstrong, B. Zhang, Anal. Chem. 73 (2001) 557A.

[48] B.A. Olsen, J. Chromatogr. A 913 (2001) 113.

[49] E.C. Conrad, G.J. Fallick, Brew. Dig. 49 (1974) 72.

[50] J.K. Palmer, Anal. Lett. 8 (1975) 215.

[51] R. Schwarzenbach, J. Chromatogr. 117 (1976) 206.

[52] C. Brons, C. Olieman, J. Chromatogr. 259 (1983) 79.

[53] S.M. Han, Biomed. Chromatogr. 11 (1997) 259.

[54] W.Z. Shou, N. Weng, J. Chromatogr. B: Anal. Technol. Biomed. Life Sci. 825 (2005) 186.

[55] Y. Guo, S. Gaiki, J. Chromatogr. A 1074 (2005) 71.

[56] J.J. Pesek, M.T. Matyska, J. Sep. Sci. 28 (2005) 1845.

[57] T. Yoshida, Anal. Chem. 69 (1997) 3038.

[58] A. Berthod, S.S.C. Chang, J.P.S. Kullman, D.W. Armstrong, Talanta 47 (1998) 1001.

[59] N.S. Quiming, N.L. Denola, Y. Saito, A.P. Catabay, K. Jinno, Chromatographia 67 (2008) 507.

[60] T.K. Chambers, J.S. Fritz, J. Chromatogr. A 797 (1998) 139.

[61] J. Havlicek, O. Samuelson, Anal. Chem. 47 (1975) 1854.

[62] W. Jiang, K. Irgum, Anal. Chem. 71 (1999) 333.

[63] M. Kawamura, T. Uchiyama, T. Kuramoto, Y. Tamura, K. Mizutani, Carbohydr. Res. 192 (1989) 83.

[64] M. Kawamura, T. Uchiyama, Carbohydr. Res. 260 (1994) 297.

[65] P. Sun, C. Wang, Z.S. Breitbach, Y. Zhang, D.W. Armstrong, Anal. Chem. 81 (2009) 10215.

[66] C. Jiang, M. Tong, Z.S. Breitbach, D.W. Armstrong, Electrophoresis 30 (2009) 3897.

[67] Y. Zhang, Z.S. Breitbach, C. Wang, D.W. Armstrong, Analyst 135 (2010) 1076.

[68] T. Kida, Y. Inoue, W. Zhang, Y. Nakatsuji, I. Ikeda, Bull. Chem. Soc. Jpn. 71 (1998) 1201.

[69] S. Kushibe, R. Sashida, Y. Morimoto, Biosci. , Biotechnol. , Biochem. 58 (1994) 1136.

[70] S. Immel, G.E. Schmitt, F.W. Lichtenthaler, Carbohydr Res 313 (1998) 91.

[71] T. Kanai, N. Ueki, T. Kawaguchi, Y. Teranishi, H. Atomi, C. Tomorbaatar, M. Ueda, A. Tanaka, Appl. Environ. Microbiol. 63 (1997) 4956.

[72] G. Marrubini, B.E.C. Mendoza, G. Massolini, J. Sep. Sci. 33 (2010) 803.

[73] A. dos Santos Pereira, A.J. Giron, E. Admasu, P. Sandra, J. Sep. Sci. 33 (2010) 834.

[74] G. Jin, Z. Guo, F. Zhang, X. Xue, Y. Jin, X. Liang, Talanta 76 (2008) 522.

[75] J. Wu, W. Bicker, W. Lindner, J. Sep. Sci. 31 (2008) 1492.

[76] F. Gritti, A. dos Santos Pereira, P. Sandra, G. Guiochon, J. Chromatogr. A 1217 (2010) 683.

[77] W. Li, Y. Li, D.T. Francisco, W. Naidong, Biomed. Chromatogr. 19 (2005) 385.

[78] Y. Guo, S. Srinivasan, S. Gaiki, Chromatographia 66 (2007) 223.

[79] Y. Liu, S. Urgaonkar, J.G. Verkade, D.W. Armstrong, J. Chromatogr. A 1079 (2005) 146.

[80] P.J. Simms, R.M. Haines, K.B. Hicks, J. Chromatogr. 648 (1993) 131.

[81] D. Schumacher, L.W. Kroh, Food Chem. 54 (1995) 353.

[82] L. Dong, J. Huang, Chromatographia 65 (2007) 519.

[83] B. Chauve, D. Guillarme, P. Cleon, J. Veuthey, J. Sep. Sci. 33 (2010) 752.

[84] U. Domanska, A. Pobudkowska, A. Pelczarska, M. Winiarska-Tusznio, P. Gierycz, J. Chem. Thermodyn. 42 (2010) 1465.

[85] Z. Hao, B. Xiao, N. Weng, J. Sep. Sci. 31 (2008) 1449.

[86] W. Jiang, K. Irgum, Anal. Chem. 73 (2001) 1993.

[87] W. Jiang, G. Fischer, Y. Girmay, K. Irgum, J. Chromatogr. A 1127 (2006) 82.

[88] P.N. Nesterenko, P.R. Haddad, Anal. Sci. 16 (2000) 565.

[89] W. Hu, H. Haraguchi, Anal. Chem. 66 (1994) 765.

[90] W. Hu, T. Takeuchi, H. Haraguchi, Anal. Chem. 65 (1993) 2204.

[91] H. Kitano, T. Mori, Y. Takeuchi, S. Tada, M. Gemmei-Ide, Y. Yokoyama, M. Tanaka, Macromol. Biosci. 5 (2005) 314.

[92] C. Viklund, A. Sjoegren, K. Irgum, I. Nes, Anal. Chem. 73 (2001) 444.

[93] W. Bicker, J.Y. Wu, H. Yeman, K. Albert, W. Lindner, J. Chromatogr. A 1218 (2011) 882.

[94] W. Chung, S. Tso, S. Sze, J. Chromatogr. Sci. 45 (2007) 104.

[95] S. Vikingsson, R. Kronstrand, M. Josefsson, J. Chromatogr. A 1187 (2008) 46.

[96] J. Pesek, M.T. Matyska, LCGC North Am. 25 (2007) 480.

[97] T. Zhou, C.A. Lucy, J. Chromatogr. A 1217 (2010) 82.

[98] D.S. Bell, A.D. Jones, J. Chromatogr. A 1073 (2005) 99.

[99] Z. Guo, Y. Jin, T. Liang, Y. Liu, Q. Xu, X. Liang, A. Lei, J. Chromatogr. A 1216 (2009) 257.

[100] L.G. Gagliardi, C.B. Castells, C. Rafols, M. Roses, E. Bosch, Anal Chem 79 (2007) 3180.

[101] D.V. McCalley, J. Chromatogr. A 1171 (2007) 46.

[102] M. Liu, E.X. Chen, R. Ji, D. Semin, J. Chromatogr. A 1188 (2008) 255.

[103] D. Sykora, E. Tesarova, D.W. Armstrong, LCGC North Am. 20 (2002) 974, 976.

[104] Y. Takegawa, K. Deguchi, H. Ito, T. Keira, H. Nakagawa, S. Nishimura, J. Sep. Sci. 29 (2006) 2533.

[105] T. Okada, J.M. Patil, Langmuir 14 (1998) 6241.

[106] M. Verzele, F. Van Damme, J. Chromatogr. 362 (1986) 23.

[107] H. Hyakutake, T. Hanai, J. Chromatogr. 108 (1975) 385.

[108] S.M. Han, D.W. Armstrong, J. Chromatogr. 389 (1987) 256.

[109] M.T.W. Hearn, B. Grego, J. Chromatogr. 218 (1981) 497.

[110] Y. Guo, S. Gaiki, J. Chromatogr. A 1218 (2011) 5920.

[111] B. Dejaegher, Y. Vander Heyden, J. Sep. Sci. 33 (2010) 698.

[112] N.P. Dinh, T. Jonsson, K. Irgum, J. Chromatogr. A 1218 (2011) 5880.

[113] P. Jandera, J. Sep. Sci. 31 (2008) 1421.

[114] N.L.T. Padivitage, D.W. Armstrong, J. Sep. Sci. 34 (2011) 1636.

[115] H. Qiu, E. Wanigasekara, Y. Zhang, T. Tran, D.W. Armstrong, J. Chromatogr. A 1218 (2011) 8075.

[116] K.B. Sentell, J.G. Dorsey, J. Liq. Chromatogr. 11 (1988) 1875.

[117] W. Melander, D.E. Campbell, C. Horvath, J. Chromatogr. 158 (1978) 215.

[118] L.A. Cole, J.G. Dorsey, Anal. Chem. 64 (1992) 1317.

[119] R. Chirita, C. West, S. Zubrzycki, A. Finaru, C. Elfakir, J. Chromatogr. A 1218 (2011) 5939.

[120] T.L. Chester, J.W. Coym, J. Chromatogr. A 1003 (2003) 101.

[121] T. Takamuku, Y. Noguchi, M. Matsugami, H. Iwase, T. Otomo, M. Nagao, J. Mol. Liq. 136 (2007) 147.

[122] A.M. Stalcup, Annu. Rev. Anal. Chem. 3 (2010) 341.

[123] D.W. Armstrong, J.R. Faulkner Jr., S.M. Han, J. Chromatogr. 452 (1988) 323.

[124] D.W. Armstrong, A.M. Stalcup, M.L. Hilton, J.D. Duncan, J.R. Faulkner Jr., S.C. Chang, Anal. Chem. 62 (1990) 1610.

[125] D.W. Armstrong, M. Hilton, L. Coffin, Lc-Gc 9 (1991) 646, 648.

[126] D.W. Armstrong, C.D. Chang, S.H. Lee, J. Chromatogr. 539 (1991) 83.

[127] T. Hargitai, Y. Kaida, Y. Okamoto, J. Chromatogr. 628 (1993) 11.

[128] A.M. Stalcup, S.C. Chang, D.W. Armstrong, J. Chromatogr. 540 (1991) 113.

[129] Q. Zhong, L. He, T.E. Beesley, W.S. Trahanovsky, P. Sun, C. Wang, D.W. Armstrong, Chromatographia 64 (2006) 147.

[130] Y. Okamoto, R. Aburatani, T. Fukumoto, K. Hatada, Chem. Lett.(1987) 1857.

[131] Y. Okamoto, Y. Kaida, J. Chromatogr. A 666 (1994) 403.

[132] Y. Okamoto, E. Yashima, Angew. Chem. , Int. Ed. 37 (1998) 1021.

[133] Y. Okamoto, M. Kawashima, K. Hatada, J. Am. Chem. Soc. 106 (1984) 5357.

[134] C. Czerwenka, M. Laemmerhofer, N.M. Maier, K. Rissanen, W. Lindner, Anal. Chem. 74 (2002) 5658.

[135] K. Gyimesi-Forras, K. Akasaka, M. Laemmerhofer, N.M. Maier, T. Fujita, M. Watanabe, N. Harada, W. Lindner, Chirality 17 (2005) S134.

[136] K. Gyimesi-Forras, A. Leitner, K. Akasaka, W. Lindner, J. Chromatogr. A 1083 (2005) 80.

[137] C.V. Hoffmann, R. Pell, M. Laemmerhofer, W. Lindner, Anal. Chem. 80 (2008) 8780.

[138] K.H. Krawinkler, N.M. Maier, E. Sajovic, W. Lindner, J. Chromatogr. A 1053 (2004) 119.

[139] M. Lammerhofer, P. Franco, W. Lindner, J. Sep. Sci. 29 (2006) 1486.

[140] A. Mandl, L. Nicoletti, M. Lammerhofer, W. Lindner, J. Chromatogr. A 858 (1999) 1.

[141] Y. Okamoto, H. Sakamoto, K. Hatada, M. Irie, Chem. Lett.(1986) 983.

[142] M. Kawamura, T. Uchiyama, Denpun Kagaku 39 (1992) 109.

[143] H. Mori, M. Nishioka, F. Nanjo, Jpn. Kokai Tokkyo Koho 2004-255007; 2004-255007 (2006) 10.

[144] H. Mori, M. Nishioka, F. Nanjo, Jpn. Kokai Tokkyo Koho 2004-255009; 2004-255009 (2006) 13.

[145] P. Sun, D.W. Armstrong, J. Chromatogr. A 1217 (2010) 4904.

[146] M. Sawada, T. Tanaka, Y. Takai, T. Hanafusa, K. Hirotsu, T. Higuchi, M. Kawamura, T. Uchiyama, Chem. Lett.(1990) 2011.

[147] M. Sawada, T. Tanaka, Y. Takai, T. Hanafusa, T. Taniguchi, M. Kawamura, T. Uchiyama, Carbohydr. Res. 217 (1991) 7.

[148] C. Wang, Z.S. Breitbach, D.W. Armstrong, Sep. Sci. Technol. 45 (2010) 447.

[149] P. Sun, A. Krishnan, A. Yadav, S. Singh, F.M. MacDonnell, D.W. Armstrong, Inorg. Chem. 46 (2007) 10312.

[150] M. Hilton, D.W. Armstrong, J. Liq. Chromatogr. 14 (1991) 9.

[151] M.H. Hyun, Anonymous Section Title: Organic Analytical Chemistry. 2007, p. 275.

[152] M.H. Hyun, S.C. Han, B.H. Lipshutz, Y. Shin, C.J. Welch, J. Chromatogr. A 959 (2002) 75.

[153] M. Ho Hyun, J. Sung Jin, W. Lee, J. Chromatogr. A 822 (1998) 155.

[154] B.S. Kersten, J. Liq. Chromatogr. 17 (1994) 33.

[155] A.L. Jenkins, W.A. Hedgepeth, Chirality 17 (2005) S24.

[156] D.W. Armstrong, J.T. Lee, L.W. Chang, Tetrahedron: Asymmetry 9 (1998) 2043.

[157] D.W. Armstrong, L. He, T. Yu, J.T. Lee, Y. Liu, Tetrahedron: Asymmetry 10 (1999) 37.

[158] J. Zukowski, Chirality 10 (1998) 362.

[159] K. Huang, Z.S. Breitbach, D.W. Armstrong, Tetrahedron: Asymmetry 17 (2006) 2821.

[160] D.W. Armstrong, W. DeMond, J. Chromatogr. Sci. 22 (1984) 411.

[161] A.M. Stalcup, S.C. Chang, D.W. Armstrong, J. Pitha, J. Chromatogr. 513 (1990) 181.

[162] D.W. Armstrong, Y. Liu, K.H. Ekborgott, Chirality 7 (1995) 474.

[163] T.L. Xiao, E. Tesarova, J.L. Anderson, M. Egger, D.W. Armstrong, J. Sep. Sci. 29 (2006) 429.

[164] D.W. Armstrong, Y. Tang, S. Chen, Y. Zhou, C. Bagwill, J. Chen, Anal. Chem. 66 (1994) 1473.

[165] Z. Bosakova, E. Curinova, E. Tesarova, J. Chromatogr. A 1088 (2005) 94.

[166] W.Y. Li, H.L. Jin, D.W. Armstrong, J. Chromatogr. 509 (1990) 303.

[167] A. Berthod, W. Li, D.W. Armstrong, Anal. Chem. 64 (1992) 873.

[168] E. Zeeck, J.D. Hardege, A. Willig, R. Krebber, W.A. Koenig, Naturwissenschaften 79 (1992) 182.

[169] N. Marion, S. Diez-Gonzalez, S.P. Nolan, Angew. Chem. , Int. Ed. 46 (2007) 2988.

[170] M.S. Kerr, T. Rovis, J. Am. Chem. Soc. 126 (2004) 8876.

[171] M. He, J.R. Struble, J.W. Bode, J. Am. Chem. Soc. 128 (2006) 8418.

[172] M. He, G.J. Uc, J.W. Bode, J. Am. Chem. Soc. 128 (2006) 15088.

[173] P. Chiang, J. Kaeobamrung, J.W. Bode, J. Am. Chem. Soc. 129 (2007) 3520.

[174] B. Bartels, G. Helmchen, Chem. Commun. (1999) 741.

[175] J. Bao, W.D. Wulff, J.B. Dominy, M.J. Fumo, E.B. Grant, A.C. Rob, M.C. Whitcomb, S. Yeung, R.L. Ostrander, A.L. Rheingold, J. Am. Chem. Soc. 118 (1996) 3392.

[176] Y. Zhang, S. Yeung, H. Wu, D.P. Heller, C. Wu, W.D. Wulff, Org. Lett. 5 (2003) 1813.

[177] S. Yu, C. Rabalakos, W.D. Mitchell, W.D. Wulff, Org. Lett. 7 (2005) 367.

[178] J.C. Antilla, W.D. Wulff, Angew. Chem. , Int. Ed. 39 (2000) 4518.

[179] J.C. Antilla, W.D. Wulff, J. Am. Chem. Soc. 121 (1999) 5099.

[180] C. Loncaric, W.D. Wulff, Org. Lett. 3 (2001) 3675.

[181] A.P. Patwardhan, Z. Lu, V.R. Pulgam, W.D. Wulff, Org. Lett. 7 (2005) 2201.

[182] A.P. Patwardhan, V.R. Pulgam, Y. Zhang, W.D. Wulff, Angew. Chem. , Int. Ed. 44 (2005) 6169.

[183] S. Xue, S. Yu, Y. Deng, W.D. Wulff, Angew. Chem. , Int. Ed. 40 (2001) 2271.

[184] G.B. Rowland, H. Zhang, E.B. Rowland, S. Chennamadhavuni, Y. Wang, J.C. Antilla, J. Am. Chem. Soc. 127 (2005) 15696.

[185] K. Endo, S. Yakeishi, D. Hamada, T. Shibata, Chem. Lett. 42 (2013) 547.

[186] P. Suresh, S. Srimurugan, R.T. Dere, R.V. Ragavan, V.S. Gopinath, Tetrahedron: Asymmetry 24 (2013) 669.

[187] K. Endo, S. Yakeishi, D. Hamada, T. Shibata, Chem. Lett. 42 (2013) 547.

[188] P. Suresh, S. Srimurugan, R.T. Dere, R.V. Ragavan, V.S. Gopinath, Tetrahedron: Asymmetry 24 (2013) 669.

[189] U. Gerlach, T. Haubenreich, S. Huenig, Chem. Ber. 127 (1994) 1969.

[190] D.J. Dixon, R.D. Richardson, Synlett(2006) 81.

[191] T. Kull, R. Peters, Adv. Synth. Catal. 349 (2007) 1647.

[192] D. Tian, B. Liu, Q. Gan, H. Li, D.J. Darensbourg, ACS Catal. 2 (2012) 2029.

[193] S. Wang, M. Wang, D. Wang, J. Zhu, Org. Lett. 9 (2007) 3615.

[194] M. Bandini, A. Garelli, M. Rovinetti, S. Tommasi, A. Umani-Ronchi, Chirality 17 (2005) 522.

[195] S.S. Kim, D.H. Song, Eur. J. Org. Chem.(2005) 1777.

[196] G.M. Sammis, H. Danjo, E.N. Jacobsen, J. Am. Chem. Soc. 126 (2004) 9928.

[197] G.M. Sammis, H. Danjo, E.N. Jacobsen, J. Am. Chem. Soc. 126 (2004) 9928.

[198] M. Bandini, M. Fagioli, P. Melchiorre, A. Melloni, A. Umani-Ronchi, Tetrahedron Lett. 44 (2003) 5843.

[199] B.M. Trost, M.L. Crawley, Chem. Rev. 103 (2003) 2921.

[200] B.M. Trost, D.R. Fandrick, Aldrichimica Acta 40 (2007) 59.

[201] B.M. Trost, O.R. Thiel, H. Tsui, J. Am. Chem. Soc. 124 (2002) 11616.

[202] B.M. Trost, D.L. Van Vranken, Chem. Rev. (Washington, D. C.) 96 (1996) 395.

[203] M.T. Reetz, X. Li, J. Am. Chem. Soc. 128 (2006) 1044.

[204] J.W.A. Kinnaird, P.Y. Ng, K. Kubota, X. Wang, J.L. Leighton, J. Am. Chem. Soc. 124 (2002) 7920.

[205] R. Berger, K. Duff, J.L. Leighton, J. Am. Chem. Soc. 126 (2004) 5686.

[206] K. Kubota, J.L. Leighton, Angew. Chem. , Int. Ed. 42 (2003) 946.

[207] R. Berger, P.M.A. Rabbat, J.L. Leighton, J. Am. Chem. Soc. 125 (2003) 9596.

[208] T. Kusumi, H. Takahashi, P. Xu, T. Fukushima, Y. Asakawa, T. Hashimoto, Y. Kan, Y. Inouye, Tetrahedron Lett. 35 (1994) 4397.

[209] A. Wilsily, F. Tramutola, N.A. Owston, G.C. Fu, J. Am. Chem. Soc. 134 (2012) 5794.

[210] P.M. Lundin, G.C. Fu, J. Am. Chem. Soc. 132 (2010) 11027.

[211] B. Saito, G.C. Fu, J. Am. Chem. Soc. 130 (2008) 6694.

[212] D.J. Bailey, D. O'hagan, M. Tavasli, Tetrahedron: Asymmetry 8 (1997) 149.

[213] E.J. Corey, R.K. Bakshi, Tetrahedron Lett. 31 (1990) 611.

[214] E.J. Corey, J.O. Link, Tetrahedron Lett. 33 (1992) 3431.

[215] E.J. Corey, J.O. Link, J. Am. Chem. Soc. 114 (1992) 1906.

[216] T. Sakai, F. Yan, S. Kashino, K. Uneyama, Tetrahedron 52 (1996) 233.

[217] L. Schwink, P. Knochel, Tetrahedron Lett. 37 (1996) 25.

[218] K.A. Parker, M.W. Ledeboer, J. Org. Chem. 61 (1996) 3214.

[219] R.T. Stemmler, Synlett(2007) 997.

[220] D.H. Ryu, E.J. Corey, J. Am. Chem. Soc. 125 (2003) 6388.

[221] S. Mukherjee, E.J. Corey, Org. Lett. 12 (2010) 632.

[222] M. Fontes, X. Verdaguer, L. Sola, M.A. Pericas, A. Riera, J. Org. Chem. 69 (2004) 2532.

[223] M. Fontes, X. Verdaguer, L. Sola, A. Vidal-Ferran, K.S. Reddy, A. Riera, M.A. Pericas, Org. Lett. 4 (2002) 2381.

[224] J. Vazquez, M.A. Pericas, F. Maseras, A. Lledos, J. Org. Chem. 65 (2000) 7303.

[225] G. Schilling, GIT Labor-Fachz. 49 (2005) 600.

[226] A. Preetz, H. Drexler, C. Fischer, Z. Dai, A. Boerner, W. Baumann, A. Spannenberg, R. Thede, D. Heller, Chem. - Eur. J. 14 (2008) 1445.

[227] S. Luehr, J. Holz, O. Zayas, V. Wendisch, A. Boerner, Tetrahedron: Asymmetry 23 (2012) 1301.

[228] C. Gonzalez-Rodriguez, S.R. Parsons, A.L. Thompson, M.C. Willis, Chem. - Eur. J. 16 (2010) 10950.

[229] D.P. Steinhuebel, S.W. Krska, A. Alorati, J.M. Baxter, K. Belyk, B. Bishop, M. Palucki, Y. Sun, I.W. Davies, Org. Lett. 12 (2010) 4201.

[230] N.W. Boaz, S.D. Debenham, E.B. Mackenzie, S.E. Large, Org. Lett. 4 (2002) 2421.

[231] N.W. Boaz, S.E. Large, J.A. Ponasik Jr., M.K. Moore, T. Barnette, W.D. Nottingham, Org. Process Res. Dev. 9 (2005) 472.

[232] N.W. Boaz, E.B. Mackenzie, S.D. Debenham, S.E. Large, J.A. Ponasik Jr, J. Org. Chem. 70 (2005) 1872.

[233] A.K. Misra, A.K. Mehrotra, R.D. Srivastava, A.N. Nandy, Wear 26 (1973) 229.

[234] A. Holy, H. Dvorakova, M. Masojidkova, Collect. Czech. Chem. Commun. 60 (1995) 1390.

[235] S. Siedler, S. Bringer, M. Bott, Appl. Microbiol. Biotechnol. 92 (2011) 929.

[236] G. Wang, N. Yin, E. Negishi, Chem. - Eur. J. 17 (2011) 4118.

[237] K.R. Anderson, S.L.G. Atkinson, T. Fujiwara, M.E. Giles, T. Matsumoto, E. Merifield, J.T. Singleton, T. Saito, T. Sotoguchi, J.A. Tornos, E.L. Way, Org. Process Res. Dev. 14 (2010) 58.

[238] T. Osawa, Y. Hayashi, A. Ozawa, T. Harada, O. Takayasu, J. Mol. Catal. A: Chem. 169 (2001) 289.

[239] B. Chatelet, L. Joucla, J. Dutasta, A. Martinez, K.C. Szeto, V. Dufaud, J. Am. Chem. Soc. 135 (2013) 5348.

[240] A. Trifonov, F. Ferri, J. Collin, J. Organomet. Chem. 582 (1999) 211.

[241] T. Iizawa, A. Goto, T. Nishikubo, Bull. Chem. Soc. Jpn. 62 (1989) 597.

[242] D.C. Behenna, B.M. Stoltz, J. Am. Chem. Soc. 126 (2004) 15044.

[243] P.C.B. Page, G.A. Rassias, D. Barros, A. Ardakani, D. Bethell, E. Merifield, Synlett(2002) 580.

[244] P.C.B. Page, G.A. Rassias, D. Bethell, M.B. Schilling, J. Org. Chem. 63 (1998) 2774.

[245] P.C.B. Page, G.A. Rassias, D. Barros, A. Ardakani, D. Bethell, E. Merifield, Synlett(2002) 580.

[246] P.C.B. Page, G.A. Rassias, D. Bethell, M.B. Schilling, J. Org. Chem. 63 (1998) 2774.

[247] P.V. Ramachandran, M.V. Rangaishenvi, B. Singaram, C.T. Goralski, H.C. Brown, J. Org. Chem. 61 (1996) 341.

[248] P. Chen, C.G. Caldwell, W. Ashton, J.K. Wu, H. He, K.A. Lyons, N.A. Thornberry, A.E. Weber, Bioorg. Med. Chem. Lett. 21 (2011) 1880.

[249] X. Zheng, C. Day, R. Gollamudi, Chirality 7 (1995) 90.

[250] B. Sezen, D. Sames, J. Am. Chem. Soc. 126 (2004) 13244.

[251] P. Sun, C. Wang, N.L.T. Padivitage, Y.S. Nanayakkara, S. Perera, H. Qiu, Y. Zhang, D.W. Armstrong, Analyst 136 (2011) 787.

[252] Y. Zhang, D.W. Armstrong, Analyst 136 (2011) 2931.

[253] A. Aranyi, A. Bagi, I. Ilisz, Z. Pataj, F. Fueloep, D.W. Armstrong, A. Peter, J. Sep. Sci. 35 (2012) 617.

[254] D.W. Armstrong, S. Ping, Z.S. Breitbach, C. Wang, PCT Int. Appl. 2010-US38981; 2009-187868P (2010) 91.

[255] T. Gondova, J. Petrovaj, P. Kutschy, D.W. Armstrong, J. Chromatogr. A 1272 (2013) 100.

[256] K. Kalikova, L. Janeckova, D.W. Armstrong, E. Tesarova, J. Chromatogr. A 1218 (2011) 1393.

[257] C. Morrison, Anonymous Section Title: Organic Analytical Chemistry. 2012, p. 333.

[258] S. Perera, Y. Na, T. Doundoulakis, V.J. Ngo, Q. Feng, Z.S. Breitbach, C.J. Lovely, D.W. Armstrong, Chirality 25 (2013) 133.

[259] J. Vozka, K. Kalikova, L. Janeckova, D.W. Armstrong, E. Tesarova, Anal. Lett. 45 (2012) 2344.

[260] J. Vozka, K. Kalikova, C. Roussel, D.W. Armstrong, E. Tesarova, J Sep Sci(2013) .

[261] V.A. Davankov, Pure Appl. Chem. 54 (1982) 2159.

[262] M. Slater, M. Snauko, F. Svec, J.M.J. Frechet, Anal. Chem. 78 (2006) 4969.

[263] T.D. Inch, G.J. Lewis, R.P. Peel, Carbohyd. Res. 19 (1971) 29.

[264] W. Tang, S. Ng, Nat. Protoc. 3 (2008) 691.

[265] H.C. Kolb, M.G. Finn, K.B. Sharpless, Angew. Chem. , Int. Ed. 40 (2001) 2004.

[266] B. Gerard, J. Ryan, A.B. Beeler, J.A. Porco Jr, Tetrahedron 62 (2006) 6405.

[267] J.P. Collman, N.K. Devaraj, E.D. Chidsey Christopher, Langmuir 20 (2004) 1051.

[268] S. Prakash, T.M. Long, J.C. Selby, J.S. Moore, M.A. Shannon, Anal. Chem. 79 (2007) 1661.

[269] Y. Liu, Z. Guo, Y. Jin, X. Xue, Q. Xu, F. Zhang, X. Liang, J. Chromatogr. , A 1206 (2008) 153.

[270] Y. Zhang, Z. Guo, J. Ye, Q. Xu, X. Liang, A. Lei, J. Chromatogr. , A 1191 (2008) 188.

[271] K.M. Kacprzak, N.M. Maier, W. Lindner, Tetrahedron Lett. 47 (2006) 8721.

[272] J.E. Hein, V.V. Fokin, Chem. Soc. Rev. 39 (2010) 1302.

Biographical Information

Haixiao Qiu obtained her Bachelor of Science degree in pharmaceutical engineering from East China University of Science and Technology in 2005 and earned her Master of Science degree in applied chemistry in 2008 from the same college. She then chose to further her doctorate education by joining Dr. Armstrong's research group at the University of Texas at Arlington in 2008. Her research focused on development of new stationary phases, evaluation of new stationary phases in achiral and/or chiral separations, and method development in separation science.